Aus dem Institut für Neuropathologie
der Medizinischen Fakultät Charité – Universitätsmedizin Berlin

DISSERTATION

Influence of IL-12 / IL-23 signaling on Alzheimer's disease β-amyloid pathology

zur Erlangung des akademischen Grades
Doctor of Philosophy (PhD)

vorgelegt der Medizinischen Fakultät
Charité – Universitätsmedizin Berlin

von

Juliane Obst

aus Coswig (Anhalt)

Datum der Promotion: 10.03.2017

Table of contents

Abstract

Alzheimer's disease (AD) is a progressive neurodegenerative disorder which displays an inflammatory component characterized by the presence of pro-inflammatory cytokines. Previously, the hetero-dimeric cytokines interleukin- (IL-) 12 and IL-23 have been found to be up-regulated by brain-intrinsic microglia cells in Alzheimer's disease *APPPS1* mice, while the genetic deficiency or pharmacological blockade of p40, the common essential subunit of both IL-12 and IL-23, resulted in a strong reduction of amyloid-β (Aβ) plaque burden. Based on these findings, this thesis aimed to investigate possible mechanisms that lead to the observed modulation of Aβ pathology, to identify downstream effector cells of p40 signaling and to evaluate whether pharmacological blockade affects Aβ pathology and cognitive function in two AD-like mouse models with established disease phenotype. As a potential mechanism of Aβ modulation, the production of Aβ by amyloid precursor protein (APP) processing was found to be unaltered in the absence of p40. In contrast, microglial phagocytosis activity as a possible Aβ clearance mechanism was improved upon p40 deficiency in AD-prone *APPPS1* brain slices. While microglia constitute the cell type producing p40 in the context of AD, accumulating evidence points towards astrocytes being the cells responding to p40 and facilitating downstream effector function. Astrocytes were found to be expressing the common intracellular downstream mediator of both IL-12 and IL-23 signaling, namely STAT4, in the diseased brain and proved to be able to express IL-12 receptor subunits *in vitro*. Pharmacological blockade of p40 signaling using anti-p40 antibodies was not sufficient to reduce Aβ pathology in aged AD-like *APP23* mice, whereas aged *APPPS1* mice demonstrated reduced soluble Aβ levels and improved cognitive function after anti-p40 treatment. These findings suggest that reducing p40 by anti-p40 antibodies appears to be a novel preventive or therapeutic strategy to combat AD pathology in prospective clinical trials.

Zusammenfassung

Die Alzheimersche Krankheit ist eine fortschreitende neurodegenerative Erkrankung, die durch entzündliche Prozesse und die Anwesenheit proinflammatorischer Zytokine gekennzeichnet ist. In früheren Studien wurde eine Hochregulation der Zytokine Interleukin- (IL-) 12 und IL-23 durch die ortsständigen Mikrogliazellen im Gehirn von *APPPS1* Mäusen, einem Tiermodell der Alzheimer Pathologie, gezeigt. Darüber hinaus wurde dargelegt, dass die genetische Defizienz oder pharmakologische Inhibition von p40, der gemeinsamen Untereinheit von IL-12 und IL-23, zu einer ausgeprägten Reduktion der Amyloid-β (Aβ) Plaque-Last im Gehirn von *APPPS1* Mäusen führt. Basierend auf die genannten Ergebnisse zielt diese Arbeit darauf aus, mögliche Mechanismen zu untersuchen, die zu der beobachteten Modulation der Aβ Pathologie führen könnten, die Zellen im Gehirn zu definieren, die als Zielzellen von p40 nachgeschaltete Effekte bewirken, sowie zu bewerten, ob pharmakologische Inhibition von p40 die Aβ Pathologie sowie kognitive Funktionen in zwei Mausmodellen der Alzheimer Erkrankung mit bestehendem Krankheits-Phänotyp beeinflusst. Als möglicher Mechanismus der Aβ Modulation wurde die Produktion von Aβ durch Prozessierung des Amyloid-Vorläuferproteins (APP) untersucht, die keine Veränderung in Abwesenheit von p40 zeigte. Im Gegensatz dazu war die Phagozytose-Aktivität der Mikrogliazellen als potenzieller Mechanismus der Aβ-Beseitigung in Gehirnschnitten von *APPPS1*-Tieren in der Abwesenheit von p40 erhöht. Während Mikroglia den Zelltyp darstellen, der p40 im Alzheimer-Kontext produziert, mehren sich Hinweise, die zeigen, dass Astrozyten der Zelltyp im Gehirn ist, der auf p40 reagiert und nachgeschaltete Effektor-Funktionen ausübt. So produzieren Astrozyten den gemeinsamen intrazellulären Mediator von IL-12 und IL-23, STAT4, im Gehirn von Alzheimer-Mäusen und waren fähig, IL-12-Rezeptoruntereinheiten *in vitro* zu exprimieren. Pharmakologische Inhibition des p40-Signalweges mithilfe von neutralisierenden Antikörpern wies zwar keinen Effekt auf die Aβ Pathologie im Alzheimer-Mausmodell *APP23* auf, jedoch zeigten *APPPS1*-Tiere eine Reduktion von löslichem Aβ im Gehirn sowie eine Verbesserung der kognitiven Leistungen nach der Behandlung mit p40-neutralisierenden Antikörpern. Diese Ergebnisse unterstützen anti-p40 Antikörper als neue präventive oder therapeutische Strategie gegen die Alzheimer Krankheit in zukünftigen klinischen Studien anzuwenden.

1. Introduction

1.1 Alzheimer's disease

Alzheimer's disease (AD) is a chronic progressive neurodegenerative disorder and the most common form of dementia, affecting 35 million people worldwide[1]. The highest risk factor to develop AD is advancing age. The incidence for AD increases exponentially over the age of 65, with up to 38 % people being affected at the age of 85 and older[2]. It is estimated that the prevalence rate of AD doubles every 5 years after the age of 65 and that, due to steadily increasing life expectancy in first world countries, the total number of cases will approximately triplicate by 2040[3]. Hence, AD represents a major health concern in the aging population and an enormous cost burden for the public health system in the future. To date, no effective treatment is available to attenuate or even reverse the progression of the disease, which emphasizes the importance of further research on the pathophysiological mechanisms underlying the disease and the development of novel treatment strategies to target AD.

1.1.1 Clinical symptoms and diagnosis of Alzheimer's disease

Clinical manifestations of AD typically include progressive memory impairments and cognitive deficits. The first symptoms appear as mild memory loss and the inability to remember recent information, a stage referred to as mild cognitive impairment (MCI). Though the progression of the disease differs between individuals, initial memory problems slowly worsen over time, with a gradual decline in cognitive and functional abilities. Along with memory loss, individuals develop deficits in judgement, language and abstract thinking. At later stages of AD, other neuropsychologic symptoms occur, such as depression, sleep disturbances, hallucinations and personality changes. In the advanced state of the disease, individuals are unable to perform basic daily activities like bathing, eating and dressing and lose their ability to communicate[4].

Clinical diagnosis of AD requires a detailed assessment of medical and family history of the patient together with clinical, neurological and psychiatric examination[5]. Neuropsychological testing, using the mini-mental state examination (MMSE) and

others, helps to determine the exact state of cognitive impairment. Structural neuroimaging techniques like CT (computed tomography) and MRI (magnetic resonance imaging) are mainly utilized to exclude other causes of dementia, such as brain tumor, subdural hematoma and cerebrovascular disease, and enable to evaluate cortical and hippocampal atrophy, a consequence of AD-associated neurodegeneration[6]. In addition, functional imaging techniques are also used for diagnosis and might be useful to distinguish between AD and other types of dementia[5]. Fluorodeoxyglucose positron emission tomography (FDG-PET) measures glucose metabolism and has shown good accuracy in differentiating Alzheimer's disease patients from both normal control individuals and patients with non-AD dementias[7,8]. Other promising functional imaging techniques include PET with Aβ ligands (Pittsburgh compound B-PIB) and single-photon emission CT (SPECT)[9]. Although a combination of different diagnostic tools enables to diagnose symptomatic AD cases with high accuracy, diagnosis at earliest stages of AD is problematic and depends on the discovery of specific, reliable biomarkers. Multiple studies have implicated $A\beta_{42}$, total tau (t-tau) and phosphorylated tau (p-tau) as potential cerebrospinal fluid (CSF) biomarkers, showing that AD patients can be distinguished from age-matched healthy controls by increased levels of t-tau and p-tau and decreased levels of $A\beta_{42}$ in the CSF. These studies demonstrate a predictive value of more than 80 % for the identification of incipient AD in patients with MCI when a combination of all biomarkers is considered[10–13]. Nowadays, due to steadily improving diagnostic techniques and criteria, and the detection and characterization of specific biomarkers, a reliable diagnosis of AD in the living patient is possible with a high accuracy. Histopathological examination of the brain tissue *post mortem* is usually carried out to confirm the diagnosis[9].

1.1.2 Pathophysiological alterations in Alzheimer's disease

Brains of AD patients typically show a symmetric pattern of cerebral atrophy, primarily in the medial temporal lobe, including the entorhinal cortex and the hippocampus[5], brain regions involved in learning and memory formation. As a result of this cortical thinning, the lateral ventricles can appear dilated and enlarged. Cerebral atrophy is due to the degeneration of neurons and synaptic loss, leading to pronounced cerebral shrinkage (Figure 1 a). At the microscopic level, AD is characterized by the presence of extracellular and intracellular accumulations of misfolded proteins in the affected cortical

brain regions. Extracellular depositions of amyloid-β (Aβ) peptide in senile plaques and intraneuronal neurofibrillary tangles (NFT) composed of hyperphosphorylated tau protein are the main pathological hallmarks of AD[14,15] (Figure 1 b, c). Further histopathological features are astrogliosis and microgliosis around Aβ plaques and NFT, as well as cerebral amyloid angiopathy (CAA) and granulovacuolar degeneration in hippocampal pyramidal neurons[16].
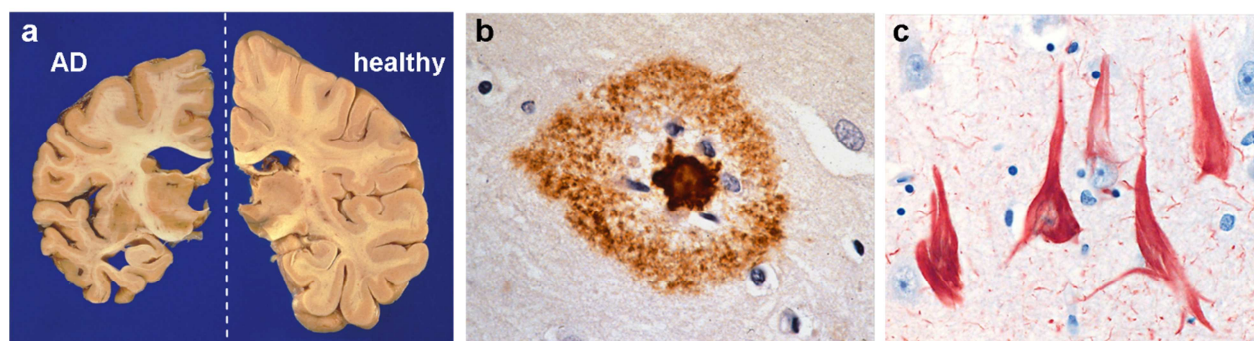
Figure 1: Neuropathological alterations in the human AD brain.
(a) Cross sections from an AD brain (left) and a healthy brain (right). Pathological hallmarks of AD are the deposition of Aβ in senile plaques (b) and hyperphosphorylated tau protein in neurofibrillary tangles (NFT, c). Source: Courtesy of Department of Neuropathology, Charité – Universitätsmedizin Berlin.

Aβ plaques vary in appearance, and two main subtypes are distinguished. While diffuse plaques mainly consist of non-fibrillar Aβ, neuritic dense-core plaques contain Aβ that is mostly in the form of amyloid fibrils and thus can be stained by amyloid dyes such as Thioflavin S and Congo red. Dense-core plaques typically contain dystrophic neurites and are surrounded by activated microglia and astrocytes[17].The major constituent of the amyloid plaques is a 4 kDa peptide called Aβ which can range from 36-43 amino acids in length, with $A\beta_{40}$ and $A\beta_{42}$ peptides being the most prevalent species. Aβ is the product of regulated intramembrane proteolysis of the Amyloid Precursor Protein (APP). APP is a type I transmembrane protein that is cleaved by three different enzymes: α-secretase and β-secretase in the extracellular domain and γ-secretase in the transmembrane region. In the amyloidogenic pathway, Aβ is generated from the sequential proteolytic cleavage of APP, first by a β-secretase called BACE-1 (β-site APP cleaving enzyme 1), releasing a soluble ectodomain fragment (sAPP-β) and a membrane-associated C-terminal fragment (CTFβ), followed by a presenilin-containing γ-secretase complex leading to the generation of Aβ. Alternatively, in a competing non-amyloidogenic pathway, α-secretase can cleave APP within the Aβ domain to preclude Aβ generation (Figure 2)[18,19].
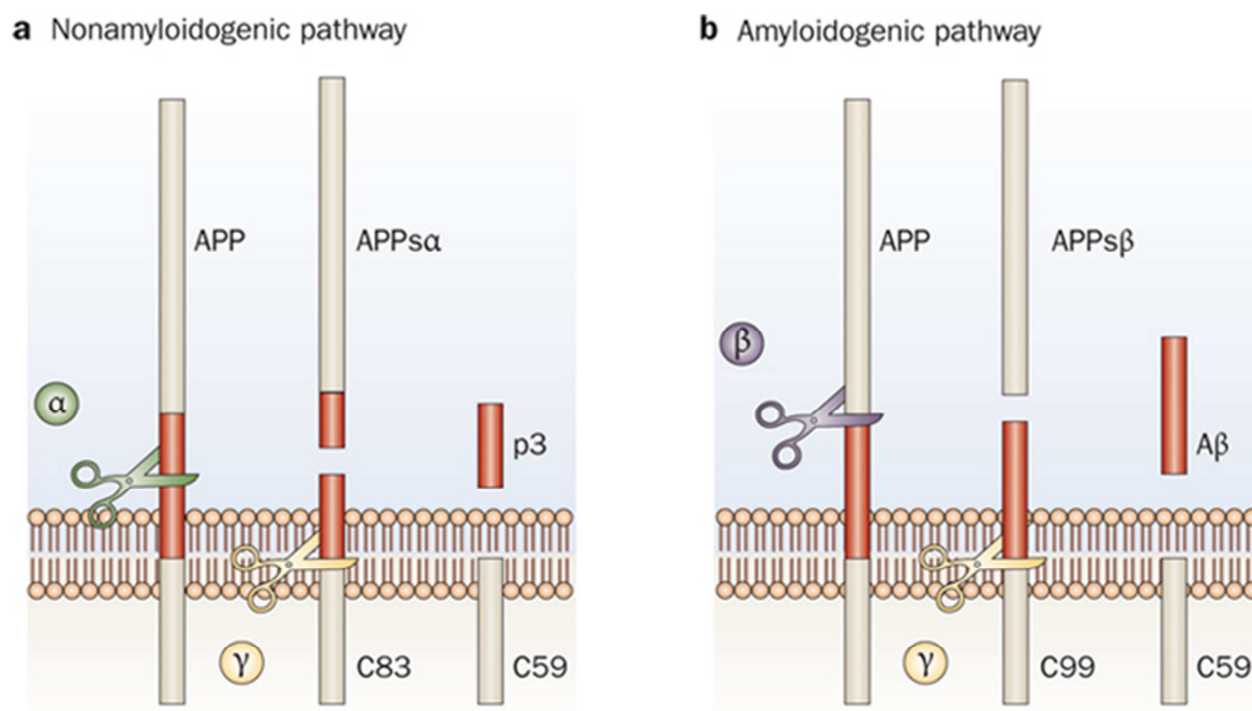
Figure 2: Processing of APP by secretases.
APP can be processed by the (a) non-amyloidogenic pathway, mediated by α- and γ-secretase, or by the (b) amyloidogenic pathway, mediated by β- and γ-secretase cleavage. In the non-amyloidogenic pathway, α-secretase first cleaves APP within the Aβ domain which results in the release of APPsα. Further processing by γ-secretase leads to the release of the p3 fragment. In the amyloidogenic pathway, APP is first cleaved by β-secretase at the amino terminus, releasing the APPsβ ectodomain. The carboxy-terminal domain is then cleaved by γ-secretase which results in the release of Aβ. Adapted by permission from Macmillan Publishers Ltd: B. De Strooper et.al, *Nature Reviews. Neurology,* 2010, 6*,* 99-107[19], copyright © 2010, Nature Publishing Group.

Aβ peptides are steadily produced under physiological conditions and can be detected in human biological fluids such as CSF and plasma[20]. However, an imbalance in Aβ production, aggregation and clearance[21] can lead to an accumulation of Aβ in various forms such as monomers, oligomers, insoluble fibrils, and finally plaques, with $Aβ_{42}$ being the peptide most prone to aggregation. Initially, it was assumed that Aβ plaques mediate neurotoxicity, however recent studies propose that oligomeric species are the more damaging form of Aβ[22–24]. This is in accordance with the observation that in contrast to Aβ deposits, levels of soluble Aβ species in human brain are a strong correlate of synaptic damage[25]. Even though extensive research is conducted and despite increasing knowledge of underlying mechanisms, the etiology of AD remains largely unknown. According to the amyloid cascade hypothesis, the accumulation of toxic Aβ species in the brain is the primary event driving AD pathogenesis by causing oxidative damage, neuroinflammation and the formation of NFT, which ultimately leads to synaptic failure, neurodegeneration and dementia[26] (Figure 3).
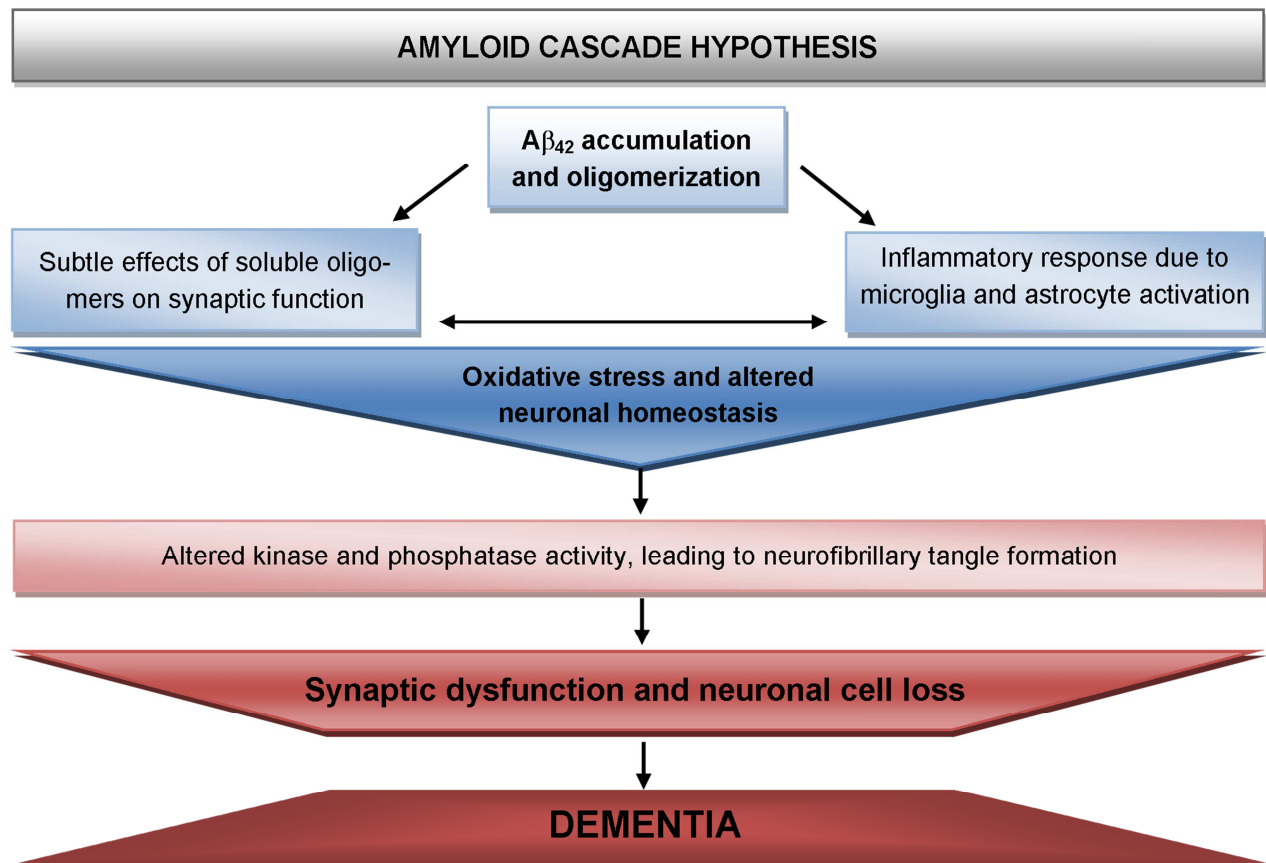
Figure 3: The amyloid cascade hypothesis of AD pathology.
According to the amyloid cascade hypothesis, Aβ accumulation and oligomerization leads via several mechanisms to neuronal cell loss and dementia. Modified from: J. Hardy and D. Selkoe et.al. *Science*, 2002[26]. Reprinted with permission from AAAS.

This hypothesis, after being established more than 10 years ago, is still widely accepted and is supported by a recent model that relates disease stage to AD biomarkers, and which demonstrated that Aβ biomarkers become abnormal first, before tau-mediated neuronal injury, neurodegenerative biomarkers and cognitive symptoms appear[27].

1.1.3   Genetic factors and transgenic mouse models of Alzheimer's disease

Most cases of AD develop at an age above 60 years and are termed late-onset AD (LOAD) or "sporadic" AD. However a minority of cases (about 5 %) account for familial AD (FAD), which appear much earlier in life and are thus referred to as early-onset AD. The basis for the early type of AD are rare mutations in one of three genes encoding for APP, presenilin 1 (PS1) or presenilin 2 (PS2). PS1 and PS2 are the catalytically active components of the γ-secretase complex and facilitate Aβ generation by cleavage of APP. Nearly all of the mutations are inherited in an autosomal dominant manner and

lead to an increase in the ratio of $A\beta_{42}$ to $A\beta_{40}$[28]. For LOAD, the risk of developing AD is assumed to be determined by genetic variants combined with lifestyle and environmental factors. The apolipoprotein ε4 allele (ApoE ε4) is a well-established genetic risk factor for LOAD and is estimated to increase risk of approximately 4-fold when inherited in one copy[29], while the ε2 allele was found to be protective[30]. ApoE is involved in lipoprotein metabolism and transport, and though its exact role in AD pathogenesis is not clear, it is believed to influence the conformation and the clearance of cerebral $A\beta$[31]. Over the past several years genome-wide association studies (GWAS) have identified a number of genes with single nucleotide polymorphisms (SNP) associated with increased risk of AD. These include susceptibility genes involved in lipid metabolism (*CLU, APOE* and *ABCA7*), innate immunity (*CLU, CR1, ABCA7, CD33, EPHA1* and *TREM2*) and cellular signaling (*PICALM, BIN1, CD33, CD2AP* and *TREM2*)[32]. However most of these variants confer only small effects on risk in a small proportion of individuals and their specific role in the occurrence and progression of LOAD needs to be determined.

Based on mutations associated with early-onset AD transgenic mouse models have been developed that mimic certain aspects of the disease and are widely used to study the pathogenesis of AD *in vivo*. Mice overexpressing mutated human *APP* develop cerebral amyloidosis similar to $A\beta$ deposits found in the human brain. $A\beta$ plaque deposition in these mice is age-dependent and accompanied by gliosis and dystrophic neurites. Hyperphosphorylated tau also occurs in *APP* transgenic mice, however they do not develop NFT and marked neuronal loss, major hallmarks of AD pathology in humans[33]. In addition, most of these models exhibit cognitive deficits in the form of memory impairment[34]. Co-expression of mutated *APP* with *PS1* mutations strongly accelerates plaque deposition, due to increased production of $A\beta_{42}$ which is more prone to aggregate[35]. In *APPPS1* mice, both $A\beta_{40}$ and $A\beta_{42}$ levels are elevated due to mutated *APP* expression, while the *PS1* mutation additionally drives $A\beta_{42}$ production that leads to early cerebral amyloidosis including diffuse and dense-core plaques beginning at 6 – 8 weeks of age[36]. In contrast, cerebral amyloidosis in the *APP23* model is mainly driven by $A\beta_{40}$ production and occurs later starting at 6 months of age[37]. Both mouse models of cerebral amyloidosis develop hyperphosphorylated tau and cognitive impairment, however a major limitation of these models is the lack of NFT and substantial neuronal loss. In order to circumvent this fact, transgenic mice have been generated that also

mirror tau abnormalities which are frequently observed in human AD pathology. An example is the 3xTg AD model which, in addition to *APP* and *PS1* mutations, harbors a mutation in the *tau* gene, leading to the development of NFTs in this model[38]. These mice are especially useful to study the relationship between tau and Aβ pathology. Although mouse models harboring mutations in disease-causing genes only represent certain aspects of AD pathology and never reproduce the full spectrum of the human disease, they are an extremely useful tool to study basic mechanisms and disease processes of AD pathogenesis *in vivo*. Despite their limitations they are most valuable in deciphering the complexity of the disease and can contribute to the development of novel diagnostic and therapeutic approaches[39].

1.1.4 Therapy of Alzheimer's disease

Current therapeutic strategies are limited to mainly symptomatic treatment without targeting the initial cause of AD, since no disease-modifying drug is available to reverse or stop the course of the disease. The first drugs developed for symptomatic therapy were acetylcholinesterase inhibitors, which aim at balancing disturbances in neurotransmitter homeostasis[40]. Clinical trials showed that the effect of these drugs on cognitive function is moderate, and that they temporarily improve some of the symptoms in mild-to-moderate AD[41]. Apart from acetylcholinesterase inhibitors, N-methyl-D-aspartate (NMDA) receptor antagonists are a further symptomatic therapeutic option for treatment of moderate-to-severe AD, which aims at protecting neurons from excitotoxicity[40].

Novel disease-modifying approaches are currently in the stage of clinical testing and focus mainly on targeting Aβ pathology. This is based on the widely accepted hypothesis that Aβ deposition is the central pathogenic event in AD. Active (vaccination) and passive (humanized monoclonal antibodies) Aβ immunotherapy aims at clearing cerebral Aβ and has been shown to be effective in decreasing Aβ pathology and improving cognition in mouse studies[42,43]. Though pre-clinical data were promising, first clinical trials using whole-length, pre-aggregated Aβ$_{1-42}$ revealed serious side-effects after active immunization, as 6% of immunized patients developed symptoms of aseptic meningoencephalitis[44]. Hence, recent active immunization strategies focus on the development of new modified vaccines, which are currently in clinical testing. These

second-generation active immunization strategies were designed to more specifically target pathological forms of Aβ and may decrease chances of autoimmune toxicity[45]. One prominent example is the vaccine CAD106 (Novartis Pharmaceuticals), which is designed to target only a B-cell epitope, the small amino-terminal Aβ fragment (Aβ$_{1-6}$), in this case along with an adjuvant carrier that is derived from multiple copies of the coat protein of bacteriophage Qβ[46]. Furthermore, AC Immune has initiated Phase I / IIa trials with their product, ACI-24, which works by generating a humoral immune response to Aβ in a primarily β sheet conformation. The design is based on previous work by this group in an AD-like mouse model, where a tetra-palmitoylated amyloid 1–15 peptide that exists primarily in a β sheet conformation was used as an immunogen[45,47,48]. Clinical trials using passive immunotherapy have been shown to be ineffective in improving cognition in mild-to-moderate AD patients, which suggested that an earlier intervention is needed for effective passive immunization approaches. Currently, several clinical trials are conducted, which include asymptomatic individuals carrying high-risk mutations[49,50]. Besides immunotherapy promising therapeutic approaches target the generation and the aggregation of Aβ. Modifying Aβ production by either inhibiting amyloidogenic BACE1 cleavage, activating α-secretase processing or targeting γ-secretase function to decrease Aβ$_{42}$ levels, is an attractive therapeutic strategy, and several enzyme-specific inhibitors or activators are currently tested in clinical trials[51]. Strategies to prevent or reverse Aβ aggregation by inhibiting Aβ-Aβ interactions and fibrillization could have a potential therapeutic benefit. Examples for potential compounds are glycosaminoglycan analogues that bind to soluble Aβ peptides and prevent Aβ plaque formation[52], zinc-and copper-chelating compounds which dissolve amyloid deposits[53], and scyllo-inositols which directly bind to Aβ oligomers and promote the dissociation of Aβ aggregates[54]. Apart from Aβ-centered approaches, another therapeutic strategy is to target tau phosphorylation and aggregation. Therefore, inhibitors of kinases involved in tau phosphorylation and drugs interfering with tau aggregation have been developed and are currently evaluated in clinical studies[55,56]. Another interesting therapeutic approach is to modulate inflammation, which is a major characteristic of AD and mainly mediated by microglia, the brain's intrinsic immune cells (also see chapter 1.2). Although first clinical trials using non-selective non-steroidal anti-inflammatory drugs (NSAIDs) or selective cyclooxygenase 2 (COX2) inhibitors in the treatment or prevention of AD have not been successful, targeting specific immune pathways implicated in AD might be more beneficial. One attractive immune target is

tumor necrosis factor (TNF)-α, a microglia-derived pro-inflammatory cytokine. Etanercept is a potent anti-TNF fusion protein approved by the Food and Drug Administration (FDA) which is broadly used for treatment of rheumatoid arthritis and other chronic inflammatory diseases[57]. Perispinal administration of etanercept rapidly improved cognitive functions of AD patients[58], however, etanercept is yet to be tested in larger-scale double-blind, randomized, placebo-controlled trials. Other possible immune targets could be, for example, CD33 and TREM2 (also see chapter 1.2), CD36, complement receptor 1 (CR1) and transforming growth factor (TGF)-β, which were all implicated in AD-associated inflammation, but are still in the stage of pre-clinical assessment[59]. Despite extensive research the initial causes for AD are still largely unknown and thus cannot be targeted by specific therapeutic approaches. A better understanding of underlying mechanisms involved in the pathogenic processes in AD is necessary to develop novel strategies to combat the disease.

1.2 Innate immune response in Alzheimer's disease

AD is characterized by an inflammatory component, composed of reactive microglia and astrocytes in the vicinity of Aβ plaques in the human brain and in AD mouse models[60,61]. Microglia are the brain's intrinsic myeloid cells and phagocytes. In the healthy CNS they have a ramified morphology, with a small soma and fine cellular processes. This condition was termed the "resting" state, although microglia constantly survey the surrounding tissue for pathogenic disturbances under physiological conditions[62]. Upon pathogenic insult, microglia undergo major morphological and functional changes which originally have been defined as "microglia activation"[63]. This term was partially based on the fact that microglia in close proximity to Aβ plaques express increased levels of MHC class II, which indicates the activated state of these cells close to pathological deposits[64]. In response to Aβ, reactive microglia secrete a number of inflammatory mediators and growth factors, such as Interleukin (IL)-1β, IL-6, TNF-α, chemokines like macrophage inflammatory protein (MIP)1α and macrophage chemotactic protein (MCP)-1, macrophage-colony stimulating factor (M-CSF) and complement proteins[65,66], but also anti-inflammatory cytokines such as IL-4, IL-10, IL-13, and TGF-β[67].

Whether "microglial activation" and subsequent chronic inflammation due to Aβ deposition in the AD brain is beneficial or detrimental in the pathogenesis of the disease is still under debate. However, recent findings obtained in murine models and *in vitro* studies indicate, that microglia reactivity in early stages of amyloid deposition seems to be beneficial to prevent plaque formation and to promote removal of existing Aβ deposits, while microglia-mediated inflammation in later stages of AD appears to be rather detrimental[68]. This is due to the dysfunctional state of human microglia observed during the late course of the disease, which is characterized by reduced phagocytic capacity, reduced motility and altered cytokine production, an irreversible state which is termed "microglia senescence" [69,68].

The significant impact of microglia-mediated inflammation on AD pathology has been emphasized by the recent discovery of disease-causing mutations in microglia-associated genes. A variant in the gene encoding the triggering receptor expressed on myeloid cells 2 (TREM2) which is predicted to result in a R47H substitution was found to be highly associated with increased risk to develop Alzheimer's disease[70,71]. In addition, the TREM2 adaptor protein TYROBP / DAP12 has been identified as a key regulator associated with LOAD[72]. Another microglial protein, the immunoglobulin-like cell surface protein CD33, has been implicated as a risk factor in LOAD[73]. CD33 was found to be increased in microglia cells of human AD brains and the deficiency of CD33 reduced insoluble $A\beta_{42}$ levels and amyloid plaque burden in AD mice, which is most likely due to increased cellular uptake and clearance of Aβ by microglia[74].

Early epidemiological studies targeting inflammation in AD indicated that the incidence or severity of AD was reduced in individuals who were treated with NSAIDs[75,76]. While several clinical trials have failed to show a beneficial effect of anti-inflammatory agents in AD patients[77,78], a re-evaluation of the data demonstrated that treatment initiation in asymptomatic individuals results in lower AD incidence[79], indicating that early intervention with anti-inflammatory agents might be valuable. In addition, rather than inhibiting inflammation in general, intervention in specific immune pathways might be a more promising approach. Previous studies targeting individual pathways associated with inflammation shed more light on the contribution of different immune mediators on AD pathology. *APPPS1* mice deficient in the NLRP3 inflammasome show rescued spatial memory, synaptic plasticity and a reduction in Aβ load when compared with age-matched *APPPS1* mice. These changes were associated with an increase in microglial

phagocytic activity and increased expression of anti-inflammatory markers[80]. Another study reports that the genetic deletion of the tumor necrosis factor type 1 death receptor (TNFR1) facilitates a reduction in Aβ deposition and prevents learning and memory deficits in *APP23* mice by influencing APP processing[81]. Recently, two independent research groups demonstrated the effect of the anti-inflammatory cytokine IL-10 on AD pathology. While an overexpression of IL-10 in APP transgenic mice exacerbated Aβ deposition[82], IL-10 deficiency decreased Aβ pathology, by altering microglia-mediated Aβ clearance[83]. Further investigation of the role of specific immune pathways in Aβ pathology could help to decipher mechanisms by which innate immunity affects progression of AD pathogenesis.

1.3   IL-12 and IL-23 family of cytokines

IL-12 and IL-23 are pro-inflammatory cytokines which are mainly produced by antigen-presenting cells like macrophages and dendritic cells upon pathogenic insult and play a key role in initial host defense against intracellular microbial infection[84–87]. Though both cytokines share many structural features and molecular partners, their physiological effects are overlapping to some extent, but are not redundant. During the last decade it became clear that these two cytokines have distinct roles in the regulation of T cells during infection and autoimmunity. It is well established that IL-12 induces interferon-γ (IFNγ) in T cells and natural killer (NK) cells[88] and promotes the differentiation of naive CD4^{+} T cells into mature T helper 1 (Th1) effector cells[89,90]. Secretion of IL-12-induced IFNγ by cells of the adaptive immune system in turn acts on monocytes and dendritic cells which are primed for further IL-12 production[91,92]. Hence, IL-12 plays an important role in coordinating innate resistance and adaptive cell-mediated immunity[93].

IL-23 seems to be less efficient than IL-12 at inducing IFN-γ production and Th1-cell differentiation. Unlike IL-12, it does not act on naive CD4^{+} T cells, but is particularly efficient at inducing the proliferation of mouse memory T cells[94]. IL-23 plays a key role in TH17 development by stabilizing IL-17 expression and the TH17 phenotype, but does not directly promote differentiation of TH17 cells[95], owing to the absence of IL-23 receptor (IL-23R) on naive T cells[96]. IL-23R signaling in effector and memory T cells further enhances *Il23r* expression, which facilitates a positive feedback loop with IL-23

driving the expansion and differentiation of proliferating T cells[97,98]. Data on brain endogenous IL-12 and IL-23 are sparse. However, expression of a functional IL-12 receptor and the induction of bioactive IL-12 production upon IL-12 stimulation were shown by microglia isolated from pre-natal human brains[99]. Primary murine microglia have been shown to express a functional IL-23 receptor[100] and are able to up-regulate IL-12 and IL-12 receptor subunits on gene expression and protein level after pro-inflammatory stimuli *in vitro*[101,102]. In addition, expression of a functional IL-12 receptor and its implication in an antiviral response in cultured neurons has been postulated[103]. However, the physiological role of brain-derived IL-12 or IL-23 is unclear.

IL-12 and IL-23 are heterodimeric cytokines that share many structural similarities (Figure 4). They both contain a common subunit called p40 (also known as *Il12b*), which can pair with either p35 (*Il12a*) to form the biologically active heterodimer IL-12, or with p19 (*Il23a*) to form the functional IL-23 cytokine. One receptor chain, IL-12Rβ1, is also used by both cytokines. The IL-12- specific receptor subunit is called IL-12Rβ2, the unique receptor subunit of IL-23 is IL-23R. Co-expression of both respective receptor subunits is required for the generation of high-affinity IL-12- or IL-23-binding sites, and the IL-12Rβ2 and IL-23R subunits function as the signal-transducing component of the high-affinity receptor complex[104]. Binding of IL-12 and IL-23 to their respective receptors activates the Janus kinase (JAK)–STAT (signal transducer and activator of transcription) pathway of signal transduction[104]. Signal transduction through the receptors induces tyrosine phosphorylation primarily of the Janus kinases JAK2 and TYK2, which then phosphorylate and activate the STAT proteins. The STATs are then capable of homo- or hetero-dimerization and translocation to the nucleus where they modulate gene expression[105]. IL-12 and IL-23 activate the same JAK-STAT signaling molecules, but induce different DNA-binding STAT dimers. While STAT1, STAT3, and STAT4 have all been reported to be activated by IL-12, STAT4 appears to be mediating the specific cellular effects in IL-12 signaling, since STAT4-deficient mice have an identical phenotype to mice that are deficient for IL-12p40, showing impaired IFN-γ production and Th1 polarization[105,106]. In contrast, IL-23 activates STAT4 to a lesser extent than IL-12, and induces STAT3, suggesting that possibly a STAT3 / STAT4 heterodimer mediates intracellular signal transduction[107].
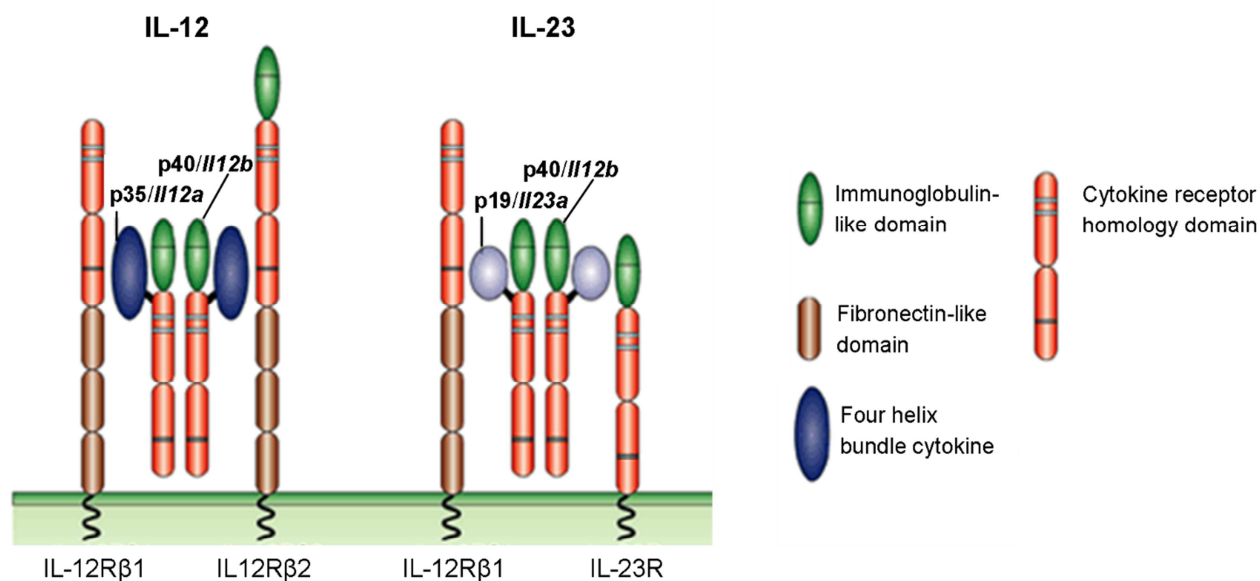
Figure 4: Structure of IL-12, IL-23 and their receptors.
IL-12 is a heterodimer formed by a 35 kDa light chain (known as p35 or *Il12a*) and a 40 kDa heavy chain (known as p40 or *Il12b*). The IL-12 receptor is composed of two chains, IL-12Rβ1 and IL-12Rβ2. The heterodimeric cytokine IL-23 shares the p40 subunit with IL-12, the second chain is a 19 kDa light chain (called p19 or *Il23a*). IL-12 and IL-23 also share the receptor subunit IL-12Rβ1, the IL-23R chain complements the IL-23 receptor. Adapted by permission from Macmillan Publishers Ltd: G. Trinchieri, *Nature Reviews. Immunology*, 2003, 3, 133-46[108]; copyright © 2003, Nature Publishing Group.

IL-12 and IL-23 have been implicated in a number of inflammatory diseases, such as psoriasis, Crohn's disease and multiple sclerosis[109–111]. Monoclonal antibodies against the p40 subunit have been used in clinical trials for the treatment of Crohn's disease[112], multiple sclerosis[113], and have been proven to be efficient at ameliorating plaque type psoriasis[114,115]. Due to the use of p40 neutralizing antibodies and p40-deficient mouse models, the effect on psoriasis and multiple sclerosis was initially accounted to Th1 responses mediated by IL-12. However, the generation of specific IL-23-deficient models made it more and more clear that the pathogenic potential is primarily mediated by IL-23-induced Th17 responses in these diseases[116–118].

1.4   Manipulation of the IL-12 and IL-23 pathway in AD – previous findings

Alzheimer's disease is characterized by an inflammatory component, mediated by microglia, the brain's intrinsic immune cells. They are reported to be a major source of inflammatory mediators in many CNS disorders, including Alzheimer's disease[119,120]. However, studies of expression patterns of pro-inflammatory cytokines and their impact

on disease progression are rare. To investigate the role of specific immune pathways in the pathogenesis of AD, previous data in the laboratory of Prof. Heppner demonstrated that the common subunit of IL-12 and IL-23, namely p40, is specifically up-regulated by brain-derived microglia cells in AD-prone *APPPS1* mice compared to wildtype (wt) control mice[121]. Quantitative PCR analysis of FACS-sorted microglia versus other brain cells confirmed this finding, showing a strong increase in *Il23a* and *Il12b* by microglia, while *Il12a* was slightly increased in the non-microglia cell population in the AD context. The up-regulation of IL-12 and IL-23 components in AD mice suggested a possible role of these cytokines in AD pathology.

To investigate the impact of IL-12 and/or IL-23 on AD pathology, mice deficient in *Il12a* (lacking the IL-12-specific subunit), *Il23a* (deficient in the IL-23-specific subunit) and *Il12b* (lacking the common subunit p40) were crossed to *APPPS1* mice, and Aβ plaque burden was analyzed at 120 days of age, a time-point when this mouse model shows robust cerebral amyloidosis. *APPPS1* mice which lack either of the IL-12 or IL-23 subunits showed a significant decrease in cerebral plaque burden compared to *APPPS1* control mice (Figure 5 a, b). This effect was most pronounced in the mice that lacked the common subunit p40. In addition, *APPPS1xIl12b$^{-/-}$* mice at a later time-point (250 days of age) also revealed a substantial reduction in Aβ plaque burden compared to *APPPS1* control mice (Figure 5c).
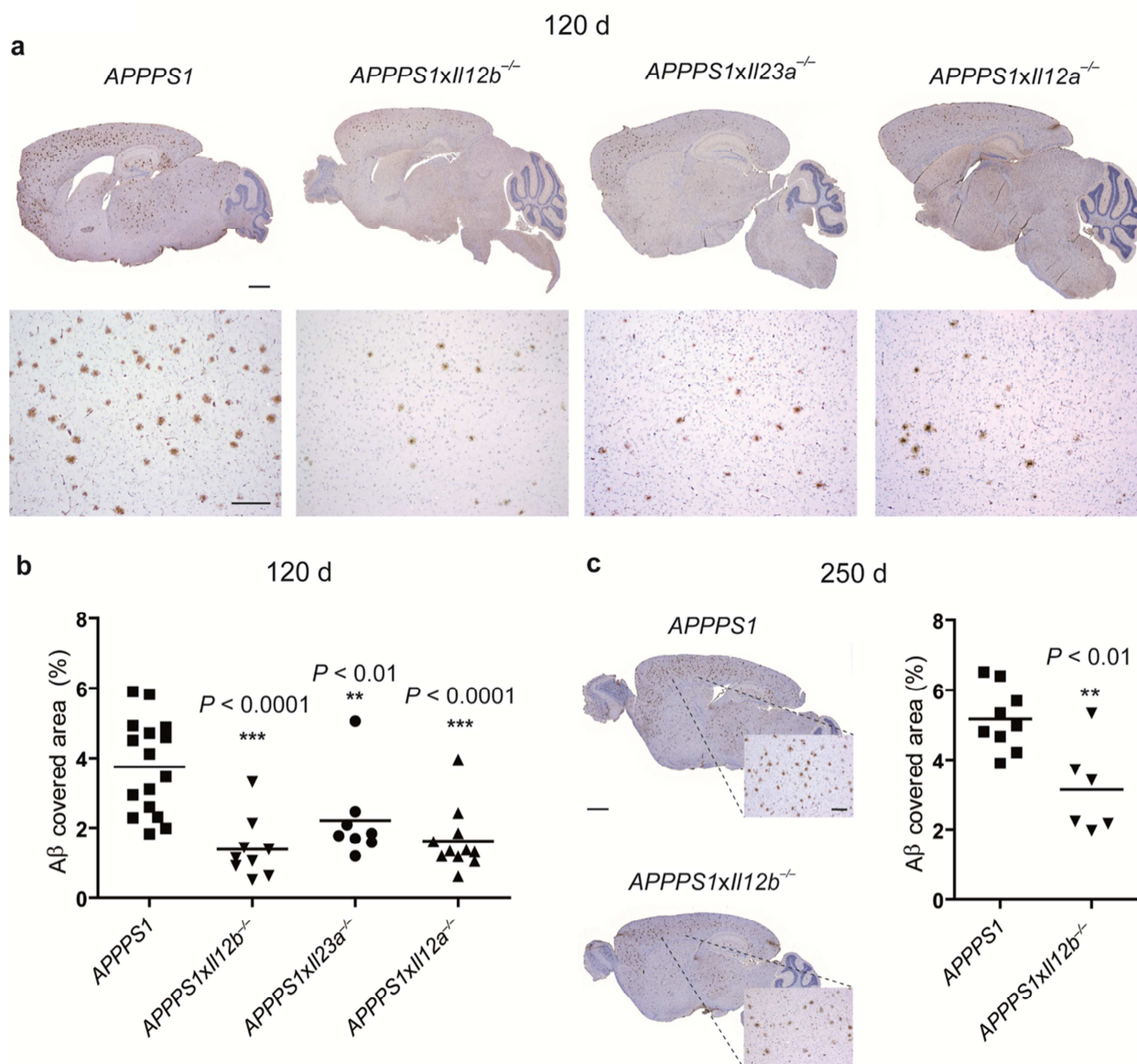
Figure 5: Genetic deletion of IL-12 and/or IL-23 subunits reduces Aβ burden in *APPPS1* mice.
(a) Aβ burden in cytokine-deficient *APPPS1* mice was assessed by immunohistochemical staining using the β-amyloid reactive antibody 4G8 (upper row: low magnification pictures, scalebar 500 µm; lower row: higher magnification images used for morphometric quantification, scalebar 200 µm). (b) Morphometric analysis of β-amyloid covered area in *APPPS1* mice lacking the IL-12 and/or IL-23 subunits p40 (*Il12b*$^{-/-}$), p19 (*Il23a*$^{-/-}$) or p35 (*Il12a*$^{-/-}$) at 120 d of age, compared to control Alzheimer's *APPPS1* mice with functional IL-12 and/or IL-23 signaling. (c) Analysis of β-amyloid plaque load at 250 d of age in *APPPS1* mice compared to *APPPS1*x*Il12b*$^{-/-}$ mice (left: low magnification picture, scalebar 500 µm; insert: high magnification image used for morphometric quantification, scale bar 200 µm; right: morphometric quantification of *APPPS1* and *APPPS1*x*Il12b*$^{-/-}$ mice. Adapted from Vom Berg et.al. *Nature Medicine*, 2012[121].

To dissect the site of p40 action in *APPPS1* mice, bone marrow chimeric mice lacking p40 in the radio-resistant (i.e. the CNS) or radio-sensitive, hematopoietic compartment were generated. *APPPS1*x*Il12b*$^{-/-}$ recipients receiving *Il12b*$^{-/-}$ bone marrow (*Il12b*$^{-/-}$ →*APPPS1*x*Il12b*$^{-/-}$) retained the reduced plaque load (Figure 6 a), indicating that

irradiation and reconstitution *per se* did not affect cerebral amyloidosis. *Il12b*$^{+/+}$ →*APPPS1*x*Il12b*$^{-/-}$ mice, which exhibit a loss of the *Il12b* alleles in the radio-resistant microglial compartment, displayed a reduction in Aβ plaque load and thus phenocopied unmanipulated *APPPS1*x*Il12b*$^{-/-}$ mice. Importantly, *Il12b*$^{-/-}$→*APPPS1*x*Il12b*$^{+/+}$ chimeric mice showed no decrease in Aβ plaque load when compared to the baseline control. This demonstrates that p40 expression by CNS-resident cells modulates Aβ plaque load in Alzheimer's *APPPS1* mice.

To determine the IL-12 / IL-23 responsive cellular compartment mediating the reduction of amyloid plaques in *APPPS1* mice, additional bone marrow chimeric mice were created lacking the IL-12Rβ1 receptor (*Il12rb1*$^{-/-}$). Consistent with a role of IL-12 / IL-23 signaling in modulating amyloid formation, the selective absence of the common receptor subunit in CNS-resident cells of chimeric mice resulted in a drastic reduction of Aβ plaque burden (Figure 6 b).

In order to translate these findings into a clinically relevant context, p40 signaling was blocked in *APPPS1* mice by intraperitoneally injecting a neutralizing p40-specific antibody. Notably, morphometric analyses of the Aβ burden of *APPPS1* mice taken at 120 d revealed a profound and statistically significant overall reduction of Aβ burden by 31% exclusively in the anti-p40 antibody treatment group (Figure 6 c, d).

The genetic and pharmacological data presented in this study[121] demonstrate that the pro-inflammatory cytokines IL-12 and IL-23 play a major role in the pathogenesis of Aβ deposition and that the deletion or pharmacological blockade of these pathways ameliorate Aβ pathology in an Alzheimer's disease mouse model. Interestingly, analyzing p40 levels in the cerebrospinal fluid (CSF) of patients with AD compared to healthy controls revealed a significant linear correlation between p40 levels and the cognitive status of the subjects assessed by the mini-mental score evaluation (MMSE)[121]. This validates the relevance of these results in a mouse model of AD for human subjects.
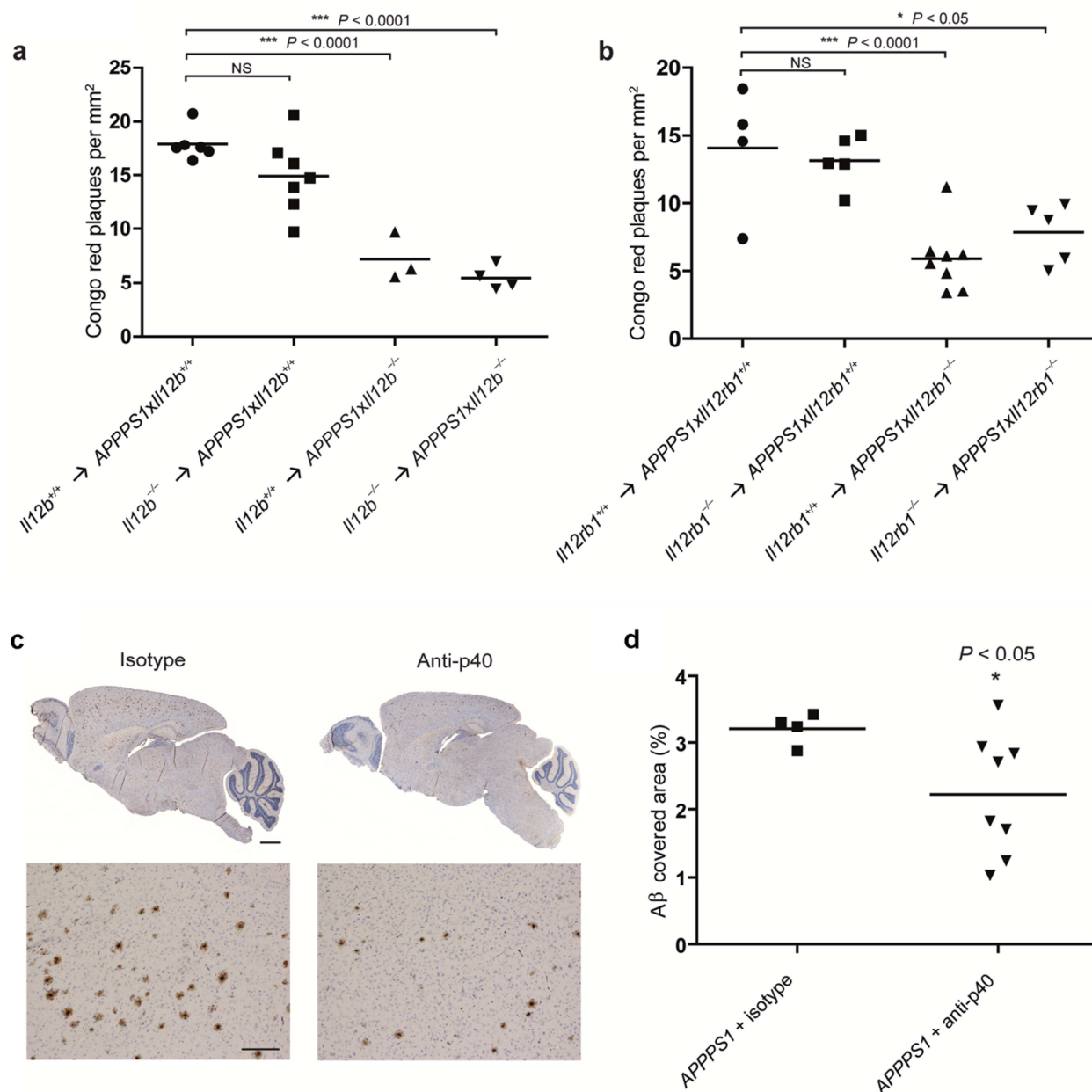
Figure 6: Deficiency of IL-12 / IL-23 signaling in the radioresistant compartment or peripheral p40-antibody treatment is sufficient to reduce Aβ plaque load in *APPPS1* mice.

The number of Congo red-positive plaques was assessed stereomorphometrically at 120 d of age, either 11 weeks after reconstitution (a and b), or 13 weeks after commencing antibody treatment (c and d). (a) *APPPS1* or *APPPS1xIl12b*$^{-/-}$ mice were lethally irradiated at 6 weeks of age and reconstituted with bone marrow isolated from C57BL/6 mice (wt) or *Il12b*$^{-/-}$ mice of the same age (n = 3–7 animals per group). (b) *APPPS1* or *APPPS1xIl12rb1*$^{-/-}$ mice were lethally irradiated at 6 weeks of age and reconstituted with bone marrow from C57BL/6 mice or *Il12rb1*$^{-/-}$ mice (n = 4–8 animals per group). (c and d) *APPPS1* mice were treated with anti-p40 antibodies (n = 8) or isotype control antibodies (n = 4), twice a week starting at 4 weeks until 120 d of age. (c) Representative overview and high magnification images of plaque burden in antibody-treated animals (4G8 staining; scale bars as in Fig. 5). (d) Morphometric analysis of Aβ covered area in antibody-treated mice. Each symbol represents the mean of the morphometrically assessed Aβ plaque load or number of Congo red-positive plaques of one mouse. Adapted from Vom Berg et.al. *Nature Medicine*, 2012[121].

2.   Scientific aims

Previous findings showed that subunits of the pro-inflammatory cytokines IL-12 and IL-23 are up-regulated in brains of AD-prone *APPPS1* mice and that the genetic deletion or pharmacological blockade of these immune pathways suffices to dramatically reduce Aβ plaque deposition[121]. Based on these findings, the first aim of this thesis was to elucidate mechanistic aspects of Aβ modulation mediated by IL-12 and IL-23. Possible mechanisms by which the lack of IL-12 and IL-23 could facilitate the observed reduction in Aβ burden include changes in Aβ production, Aβ aggregation and/or Aβ clearance. Secondly, it was aimed to define cellular players and signaling pathways involved in mediating the observed effects on Aβ pathology. As a third aim, it was sought to substantiate the possibility to use pharmacological reduction of p40, the common subunit of IL-12 and IL-23, to impact disease pathology which would further validate p40 as potential target for interventional treatment of AD.

Mechanisms of Aβ modulation by IL-12 and IL-23

The absence of IL-12 and IL-23 has been shown to alter Aβ homeostasis during AD pathogenesis. To address whether the production of Aβ is affected by the absence of these cytokines, Aβ levels were assessed in brains of young *APPPS1* and *APPPS1* mice deficient in p40 before onset of plaque deposition. A modulatory effect of IL-12 and IL-23 on steady-state Aβ levels during an early disease stage would provide hints towards altered Aβ production in the absence of p40 and would explain the changed Aβ phenotype observed at later stages. To further address whether the production of Aβ is changed upon p40 deficiency, the amount of soluble APPβ in the brain of young mice as an indicator of amyloidogenic APP processing was evaluated.

Apart from an effect on Aβ production, the lack of IL-12 and IL-23 could affect Aβ clearance mechanisms, resulting in a higher degree of clearance of Aβ from the brain. Clearance of Aβ is facilitated mainly by either transcytosis across the blood–brain barrier into the vascular lumen, extracellular proteolytic degradation by enzymes or cellular uptake and degradation of Aβ. To determine whether p40 signaling affects Aβ efflux from the brain to the peripheral blood stream, peripheral Aβ levels were measured. In addition, the effect of p40 deficiency on microglial phagocytosis was investigated to address mechanisms by which IL-12 and IL-23 could affect cell-

mediated Aβ clearance. Furthermore, the impact of the lack of p40 on the expression of pro- and anti-inflammatory mediators was analyzed on gene expression and protein level to evaluate the inflammatory profile in the brain. An alteration of inflammatory markers could provide hints towards altered functional capacities of brain-intrinsic cell types involved in p40 signaling.

Cellular localization of IL-12 and IL-23 components in the AD context

IL-12 and IL-23 typically participate in cell-mediated immunity by binding to their receptor complex located on the respective target cells. To determine whether Aβ modulating effects by IL-12 and IL-23 require the presence of their receptor, Aβ pathology was analyzed in mice deficient in the common receptor subunit. Altered Aβ load upon receptor-deficiency similar to that observed in the absence of p40 would indicate that receptor-mediated downstream signaling facilitated by p40-binding target cells is responsible for the Aβ-modulating effects.

To gain further insight into the role of IL-12 and IL-23 pathways in the AD context, it is necessary to identify potential target cells of p40 signaling which mediate downstream Aβ-modulatory effects. It was demonstrated that microglia are the cellular source of p40 in the CNS, while non-myeloid cells, possibly astrocytes, express the receptor of IL-12 and IL-23[121]. Based on this observation, it is hypothesized that astrocytes are the direct target cells of p40 and responsible for mediating downstream signaling. To address whether this is true, the cellular localization of STAT4 as the main downstream mediator of IL-12 and IL-23 signaling was investigated to identify downstream effector cells in the brain. In addition, the expression pattern of IL-12 and IL-12 receptor subunits in primary microglia and astrocytes after stimulation was examined *in vitro*, to determine the general capacity of the glia cells to produce IL-12-related components.

Pharmacological reduction of p40 as a therapeutic strategy in AD

Since the efficiency of p40-blocking antibodies in reducing Aβ plaque burden when applied early during the disease course was demonstrated[121], suggesting IL-12 and IL-23 pathways as novel therapeutic targets in AD, it was aimed in this thesis to find out whether the pharmacological blockade of IL-12 and IL-23 by p40-neutralizing antibodies affected cognitive outcome and Aβ pathogenesis in *APPPS1* mice with established AD pathology. Analysis of Aβ plaque burden after long-term p40 inhibition would provide information on the effect of anti-p40 antibodies on an established Aβ plaque phenotype,

which would emphasize a possible therapeutic effect during advanced disease stages. A positive effect on behavioral deficits and Aβ pathology upon p40 inhibition would recommend IL-12 and IL-23 as novel druggable targets for interventional or prophylactic treatment approaches in prospective clinical trials. To further validate the effect of p40-blocking antibodies on Aβ pathology and cognitive function, p40-neutralizing treatment was repeated in a different model of cerebral amyloidosis, the *APP23* mice.

3. Methodology

3.1 *In vivo* manipulations

3.1.1 Animals

As animal models for Alzheimer's disease, transgenic, heterozygous $APPPS1^{+/-}$ mice (Tg(Thy1-APPKM670/671NL, Thy1-PS1L166P)21) and $APP23^{+/-}$ mice (Tg(Thy1-APPKM670/671NL)23), termed *APPPS1* and *APP23* throughout this thesis, and age matched littermate controls (termed wt throughout this thesis) were used. *APPPS1* mice harbor the Swedish amyloid precursor protein (APP) mutation KM670/671NL in conjunction with the presenilin 1 mutation L166P. The Swedish APP mutation is located within the β-secretase cutting site which shifts Aβ production towards the amyloidogenic pathway. The presenilin mutation shifts the $A\beta_{40}$ / $A\beta_{42}$ ratio towards $A\beta_{42}$ without increasing the total amount of $A\beta^{[36]}$. *APP23* mice overexpress human APP_{751} containing the KM670/671NL Swedish double mutation under the control of the neuron-specific mouse Thy-1 promoter[37]. *APPPS1* and *APP23* mice were crossed to $Il12b^{-/-}$ mice, lacking p40, the common subunit of IL-12 and IL-23[122]. *APPPS1* mice were also crossed to $Il12rb1^{-/-}$ mice, deficient in IL12Rβ1, the essential receptor subunit of IL-12 and IL-23 mediated signaling[123]. Both $Il12b^{-/-}$ and $Il12rb1^{-/-}$ mice were kindly provided by B. Becher (Institute of Experimental Immunology, University of Zurich, Switzerland). Equal amounts of female and male mice were analyzed. Mice were group housed under specific pathogen–free conditions on a 12 h light/dark cycle, and food and water were provided to the mice *ad libidum*. All animal experiments were performed in accordance to the national animal protection guidelines approved by the regional offices for health and social services in Berlin (LaGeSo).

3.1.2 Genotyping of experimental animals

Polymerase chain reaction (PCR) was used to determine the genotype of transgenic *APPPS1* and *APP23* mice, $Il12b^{-/-}$ and $Il12rb1^{-/-}$ mice. Mouse ear or tail biopsies served as templates for DNA preparation, which were incubated in 300 µl tail lysis buffer (10 mM Tris(hydroxymethyl)-aminomethan (Tris) hydrochlorid (Merck; pH = 9), 50 mM

potassium chloride (KCl), 0.5 % Nonidet P-40, 0.5 % Tween20) containing 0.1 mg/ml proteinase K (in 10 mM Tris (pH = 7.5); Roche) overnight at 55 °C on a shaker. To inactivate the proteinase K, samples were incubated at 95 °C for 5 min and subsequently centrifuged at 13.000x rpm for 10 min. The supernatant was directly used as template for PCR reaction. All amplifications were performed in a total reaction volume of 20 µl, containing 1 - 2 µl template DNA, 375 nM of each sequence specific primer (listed in Table 1), and diluted RED Mastermix (Invitek). The PCR reaction was performed in a Thermocycler PCR machine, with the respective cycle conditions for each mouse line as depicted in Table 2.

Table 1: Oligonucleotides used for genotyping

Primer	Sequence 5'-3'	$T_{Annealing}$ (°C)
APP CT 5'	GAA TTC CGA CAT GAC TCA GG	58
APP CT 3'	GTT CTG CTG CTG CAT CTT GGA CA	58
p40 5'	TTCAGCAGTGACAAATCCCAC	61
p40 wt 3'	TGGGAAGAGACAGCCAGCTAC	61
p40 ko 3'	CTACCCGCTTCCATTGCTC	61
IL12Rb1 wt 5'	CAG GGT TTC CAA GAC AGA CT	58
IL12Rb1 wt 3'	GTT GAC CTT GGA CAG CAC AG	58
IL12Rb1 ko 5'	CTT GGG TGG AGA GGC TAT TC	64
IL12Rb1 ko 3'	AGG TGA GAT GAC AGG AGA TC	64

Table 2: PCR profiles used for genotyping

PCR	APP CT			p40			IL12Rb1		
Initial denaturation	94°C	2 min	1 x	94°C	4 min	1 x	94°C	3 min	1 x
Denaturation	94°C	30 sec		94°C	45 sec		94°C	35 sec	
Annealing	58°C	30 sec		61°C	45 sec		64°C	45 sec	
Elongation	72°C	30 sec	35 x	72°C	40 sec	35 x	72°C	45 sec	12 x
Denaturation							94°C	35 sec	
Annealing							58°C	30 sec	
Elongation	-			-			72°C	45 sec	25 x
Final elongation	72°C	5 min	1 x	72°C	5 min	1 x	72°C	2 min	1 x

Afterwards the PCR samples were separated on a 1.5 % (w/v) agarose gel (1 x TAE, 0.5 µg/ml ethidium bromide) at 120 V for 30 minutes.

3.1.3 Intraperitoneal application of anti-p40 antibody

A single bolus intraperitoneal (i.p.) injection of 0.5 mg of anti-mouse p40 antibody (clone C17.8, rat IgG2a, BioXcell Inc.) or isotype control (clone 2A3, rat IgG2a, BioXcell Inc.) to *APP23* mice at 365 days of age was followed by biweekly i.p. injections of 0.25 mg for 3 months until behavioral testing (450 days of age). Afterwards mice were sacrificed, brains sampled for histological and biochemical analysis and plasma for flow cytometric analysis of blood immune cells (Figure 7, Table 3).
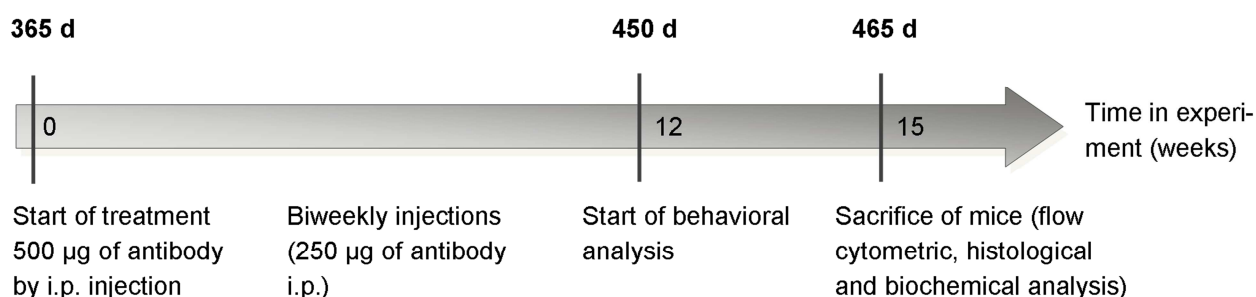
Figure 7: Experimental setup of i.p. application of anti-p40 antibody to aged *APP23* mice.
Treatment of *APP23* mice was started at 365 days of age, with a single i.p. injection of 500 μg anti-p40 antibody or isotype control, followed by biweekly injections of 250 μg of antibody until the start of behavioral tests at 450 days of age. After behavioral assessment, animals were sacrificed for histological, biochemical and flow cytometric analysis.

Table 3: Experimental groups of i.p. application of anti-p40 antibody to aged *APP23* mice

Genotype	Treatment	Number (n)
APP23$^{+/-}$	isotype	15
APP23$^{+/-}$	anti-p40	17

3.1.4 Intracerebroventricular application of anti-p40 antibody

Anti-mouse p40 antibody (clone C17.8, rat IgG2a, BioXcell Inc.) or isotype control (clone 2A3, rat IgG2a, BioXcell Inc.) were directly delivered into the brain using Alzet® mini-osmotic pumps (model 2004, flow rate 0.25 μl/ h, 4 weeks delivery). 24 hours prior to implantation, pumps were filled with 500 μg of anti-p40 antibody or isotype control antibody dissolved in phosphate buffered saline (PBS) and primed at 37°C, according to manufacturer's protocol. Transgenic *APPPS1* mice and littermate controls (190 days of age, Table 4) were anesthetized with isoflurane and received Rimadyl (Carprofen, 5 mg/ kg) by subcutaneous injection for pain relief. A midline incision in the neck was done

and a subcutaneous pocket in the back was prepared using blunt scissors. The pump reservoir was then implanted into the pocket. The pump was connected to a brain infusion cannula (Brain Infusion Kit III 1 - 3 mm, Charles River, Germany) using a catheter tube. The coordinates for implantation of the cannula into the lateral ventricle of the brain from bregma were AP: +0.1 mm, ML: +1.0 mm and DV: -2.5 mm. After surgery, mice received Paracetamol (Ben-u-Ron) in the drinking water for 3 days. The pump duration is 4 weeks, after which the pump reservoir was removed and exchanged by a new one, which was reconnected to the tubing without disturbance of the brain infusion cannula. Treatment continued for another 4 weeks during which mice were behaviorally tested within the last 2 weeks of treatment. Afterwards, mice were sacrificed and brains sampled for histological and biochemical analysis (Figure 8).

Figure 8: Experimental setup of icv application of anti-p40 antibody to aged *APPPS1* mice.
Anti-p40 antibody or isotype control antibody was constitutively applied directly into the brain for 2 months using Alzet mini-osmotic pumps. Pumps filled with 500 µg of antibody were implanted into wt or *APPPS1* mice at 190 days of age. Four weeks later pump reservoir was replaced with a newly filled pump. Two weeks later mice underwent behavioral tests, before being sacrificed for histological and biochemical analysis at 250 days of age.

Table 4: Experimental groups of icv application of anti-p40 antibody or isotype control

Genotype	Treatment	Number (n)
APPPS1$^{-/-}$	isotype	11
APPPS1$^{-/-}$	anti-p40	20
APPPS1$^{+/-}$	isotype	18
APPPS1$^{+/-}$	anti-p40	14

3.1.5 Behavioral assessment of aged *APPPS1* and *APP23* mice

Following antibody treatment of *APPPS1* and *APP23* mice, mice underwent different behavior tests to determine cognitive performance. The following behavior tests were used.

3.1.5.1 Open field test

A standard plastic open field testing arena (50 x 50 cm) was used for testing general locomotor activity. Experiments were conducted in a sound-attenuated testing chamber with the illumination set at 30 lux. Mice were allowed to acclimate to the testing area for at least 30 minutes prior to testing. Each animal was allowed to explore freely for 5 minutes and activity was recorded with an overhead camera using an automated system (Viewer III Version 3.0.1.205, Biobserve, St. Augustin, Germany). Animals were returned to their home cage at the conclusion of the trial.

3.1.5.2 Novel object recognition

The Novel object recognition task was conducted in the open field arena (50 x 50 cm) at low lighting (30 lux) with two different kinds of objects. During habituation (day 1), the animals were allowed to explore an empty arena for 5 minutes. 24 hours after habituation, the animals were exposed to the familiar arena with two identical objects placed at an equal distance and allowed to explore for 5 minutes. On the 3rd day, one of the familiar objects was exchanged for a different, novel object and the mice were allowed to explore the open field in the presence of the familiar and novel objects for 5 minutes. The time spent exploring each object and the number of visits to each object were recorded using an automated system (Viewer III Version 3.0.1.205, Biobserve, St. Augustin, Germany).

3.1.5.3 Barnes maze

An elevated Barnes maze apparatus (TSE Systems GmbH, Bad Homburg, Germany; diameter 920 mm) containing 19 empty holes and one hole with a hidden escape chamber was used for testing spatial learning and memory. Animals were trained on the Barnes maze task for 4 days prior to testing. Each animal received 4 trials per day, spaced at 15 minute intervals for each of the 4 days in order to learn the task. Extra-maze cues were placed around the room and remained consistent throughout the training and testing phase. During training, mice were placed onto the center of the maze in a covered 'start box' for 10 seconds. Afterwards, the chamber was removed and the animals were allowed to freely explore for 3 minutes per trial. Bright lights (75 - 85 lux) and a loud clicking noise were used to motivate the animals to locate the escape

box (on training days only). The number of errors (nose-pokes into incorrect holes) and latency to reach the target (hole with escape box) were scored. If the animal did not locate the escape hole within 3 minutes, it was gently guided and placed into the escape chamber for 1 minute. At the conclusion of the trial, animals were returned to their home cage. To test short-term spatial memory, one 90 second trial was conducted on day 5 wherein the escape box was removed. The animal was allowed to freely explore for 90 seconds and the number of nose pokes in the target hole, number of errors and time to reach the correct hole (latency to target) were measured. Behavior was recorded using an overhead camera and automated software system (Viewer III Version 3.0.1.205, Biobserve, St. Augustin, Germany).

3.1.5.4 Morris water maze

A round water basin of 1.20 m in diameter containing a rescue platform 2 cm below the surface of the water was used for testing. Extra-maze cues were placed around the room to allow orientation. Animals were placed carefully in the basin and trained to locate the target platform on 4 consecutive days with 4 trials each day. If the mice did not locate the target within the 90 seconds trial, they were gently guided to the platform and allowed to sit there for 30 seconds. 24 hours after the last training the short term retention test trial was conducted to assess spatial memory. The target platform was removed from the basin and the time the animals needed to reach the target position (latency to target), as well as the number of crossings within 60 seconds were measured. Behavior was recorded using an overhead camera and automated software system (Viewer III Version 3.0.1.205, Biobserve, St. Augustin, Germany).

3.1.6 Brain tissue sampling

Animals were euthanized and transcardially perfused with 1x PBS. Brains were carefully removed and one hemisphere was fixed in 4% paraformaldehyde (PFA) for 2 days followed by immersion in 30% sucrose for at least 1 day for subsequent immunohistochemical analysis. The other hemisphere was gently snap-frozen in a 2-methylbutane (Merck) bath placed in liquid nitrogen and stored at -80°C until further use. For cell isolation procedure, the whole brain was placed in HBSS on ice.

3.2 Histological and stereomorphological analysis

3.2.1 Preparation of free floating sections

Brain sections were prepared by embedding PFA-fixed brain tissue in tissue tec (Richard-Allan Scientific™ Neg-50™ Frozen Section medium, Thermo Scientific) and freezing down to -22 °C placed on a metal plate. Frozen tissue was cut as serial coronal, 40 µm thick sections using a cryostat (HM560, Microm) and stored free floating in cryoprotectant solution (30% ethylenglycol, 20% glycerol, 50 mM sodium phosphate buffer, pH 7.4) at 4°C.

3.2.2 Immunohistochemistry and immunofluorescence

Cerebral free floating sections were used for immunohistological labeling of Aβ deposits (mouse anti-human Aβ antibody 4G8) and microglia (Iba-1). Also, double labeling of Signal Transducer and Activator of Transcription 4 (STAT4) with astrocytes (glial fibrillary acidic protein (GFAP)), microglia (CD68) or neurons (NeuN) was conducted (antibodies listed in Table 5). Sections were rinsed 3 times in 1x PBS and incubated in blocking buffer (1x PBS containing 0,3 % Triton X-100 (TX) and 10 % normal goat serum (NGS)) for 1 h at RT. Primary antibodies were diluted in 1x PBS/ 0.3 % TX/ 5 % NGS and incubated over night at 4°C. After rinsing the sections three times with 1x PBS to wash off excessive primary antibodies, they were incubated with species specific peroxidase coupled or fluorescently labelled secondary antibodies (Table 5). Secondary antibodies were diluted in 1x PBS/ 0.3 % TX/ 5 % NGS and sections were incubated for 1 h on a shaker at RT. After rinsing the sections three times with 1x PBS, stainings using peroxidase coupled secondary antibodies were developed with liquid 3,3'-Diaminobenzidin (DAB; Dako, K3647) and counterstained with matured hematoxylin. Dehydration in an ascending alcohol series, including the steps 70 %, 80 %, 96 % and 100 % ethanol was carried out, followed by two times rinsing in 98 % xylene for 1 min, before slides were covered using Roti®-Histokitt II mounting medium.

Table 5: Antibodies used for immunohistochemistry and immunofluorescence stainings

Primary antibody	Host	Dilution	Company	Secondary antibody	Host	Dilution	Company
4G8	mouse	1:1000	Covance	POD anti-mouse IgG	goat	1:300	Dianova
Iba-1	rabbit	1:500	Wako	POD anti-rabbit IgG	goat	1:300	Dianova
Stat4	rabbit	1:100	Santa Cruz	Alexa Fluor® 568 Anti-rabbit IgG	donkey	1:300	Dianova
CD68	rat	1:200	AbD Serotec	Alexa Fluor® 488 Anti-rat IgG	donkey	1:300	Dianova
GFAP	chicken	1:1000	Abcam	Alexa Fluor® 488 Anti-chicken IgG	donkey	1:300	Dianova
NeuN	mouse	1:2000	Chemicon	Alexa Fluor® 488 Anti-mouse IgG	donkey	1:300	Dianova

Immunohistological stainings using fluorescent secondary antibodies were mounted after rinsing with 1x PBS (3x) and counterstained with 4′,6-Diamidin-2-phenylindol (DAPI) containing aqueous mounting medium (Fluoroshiled Mounting Medium with DAPI, abcam®). Until further microscopic analyses, sections stained with fluorescent secondary antibodies were stored light protected at 4 °C.

3.2.3 Congo red staining

Cerebral free floating sections were mounted on glass slides and counterstained with matured hematoxilin. Sections were then incubated in stock solution I (0.5 M NaCl in 80 % ethanol, 1 % NaOH) for 20 minutes and in stock solution II (8.6 mM Congo red in stock solution I, 1 % NaOH) for 45 minutes. After rinsing the sections twice in absolute ethanol, they were incubated in xylene for 1 minute and then covered using Roti®-Histokitt II mounting medium.

3.2.4 Quantitative analysis of Aβ plaque burden and microglia number

Quantitative analyses of Aβ plaque load and microglia number in cerebral sections were done using the Stereo Investigator system including an Olympus microscope BX53, the QImaging camera COLOR 12 BIT and a stage controller MAC 6000. For analyses the Stereo Investigator 64-bit software (MBF Bioscience) was used. Cortical Aβ plaque burden as assessed by 4G8 or Congo red staining was quantified with the Area Fraction Fractionator method of the Stereo Investigator software, analyzing 10 systematically

randomly sampled sections throughout the cortex. Area covered by Aβ was quantified by setting the counting frame to 90x90 µm, the scan grid size to 300x500 µm and the Cavallieri grid spacing to 10 µm. Microglia number as assessed by Iba-1 staining was determined using the optical fractionator technique of the Stereo Investigator software (settings: counting frame 120x90, grid size: 400x500, Cavallieri grid spacing 10 µm).

3.3 Biochemical and molecular analysis

3.3.1 Protein extraction from frozen brain hemispheres

Frozen brain tissue was homogenized according to a 4-step extraction method as described in published protocols[124] with slight modifications. In brief, hemispheres were homogenized consecutively in 1.) Tris buffered saline (TBS buffer) (20 mM Tris, 137 mM NaCl, pH = 7.6), 2.) TX buffer (TBS buffer containing 1 % Triton X-100), 3.) SDS buffer (2 % SDS in ddH_2O) and 4.) FA (70 % formic acid in ddH_2O). Immediately before use protease inhibitors (Roche, 1 tablet per 10 ml) were added to all buffers. Initial homogenization occurred mechanically by consecutive passing the solution through a 2 ml syringe and cannulas with decreasing diameter (G 23, G 27 and G 30). Brain extracts were incubated 30 min on ice (except FA homogenate, which was incubated at RT) and centrifuged at 100.000x g for 1 h at 4 °C. The supernatant was collected, aliquoted, snap frozen in liquid nitrogen and stored at -80 °C until further use, the remaining pellet was re-suspended in subsequent buffers. Protein concentrations of each fraction were determined using the Quantipro BCA Protein Assay Kit (Pierce) according to the manufacturer's protocol using the Photometer Tecan Infinite® 200M (Tecan).

3.3.2 Protein quantification in brain homogenates and plasma

$Aβ_{40}$ and $Aβ_{42}$ concentrations in brain extracts were determined with an electrochemiluminescence linked immunosorbent assay system using the MSD 96-Well MULTI-SPOT® Human (6E10) Abeta Triplex Assay (Meso Scale Discovery) according to manufacturer's instructions. In brief, samples were diluted to fit the standard curve (Aβ peptide 3-plex) and after blocking the MSD plate with 1% Blocker A Solution, 25 µl

detection antibody solution and 25 µl sample or calibrator were added and incubated for 2 hours. After washing the plate, reading buffer was added to the wells and the plate was analyzed on a MS6000 machine. To analyze Aβ amounts in the plasma, the MSD 96-Well MULTI-SPOT® Human/Rodent (4G8) Abeta Triplex Ultra-Sensitive Assay (MSD) was used. Aβ detection was conducted according to manufacturer´s protocol, as described above for the MULTI-SPOT® Human (6E10) Abeta Triplex Assay. Soluble APPβ levels in brain homogenates were analyzed using the MSD 96-Well MULTI-SPOT® sw sAPPbeta Kit (MSD), according to manufacturer's protocol. Inflammatory markers in brain extracts were determined using the MSD V-PLEX Plus Proinflammatory Panel 1 (mouse) Kit (MSD), according to manufacturer's instructions.

3.3.3 Western blot

For detection of anti-p40 antibody in i.p. treated *APP23* mice, brain TBS-extracts and plasma samples were run on 10-20 % Tricine gradient polyacrylamide gels (Novex, San Diego, CA) for approximately 1 hour at 120 V, according to manufacturer's instructions. Proteins were subsequently electroblotted on nitrocellulose membranes (Hybond, Amersham Biosciences) for 1 h at 100 V. After blocking the membranes with 5% milk in wash-buffer (PBS-Tween20 0.1%) for 1h at RT, an HRP-conjugated anti-rat IgG antibody (1:1000, GE healthcare) was incubated over night at 4°C. Following three 10-minute washes, immunoreactive bands were visualized using the Amersham ECL immunoblotting detection system (GE healthcare).

3.3.4 Enzyme-linked immunosorbent assay (ELISA)

TNFα and IL-12 / IL-23 total p40 ELISAs (eBioscience) were performed according to manufacturer's instructions. 50 µl of cell culture supernatant or brain homogenate were analyzed in duplicate wells, with samples diluted to fit the standard curve. Absorption was read at 450 nm and 570 nm (for wavelength correction) on a microplate reader (Infinite® 200M, Tecan) and analyzed using the Magellan Software (Tecan).

3.3.5   RNA isolation and quantitative RT-PCR

RNA isolation from primary glia cells and isolated CD11b$^+$ and CD11b$^-$ brain cells was performed using the peqGOLD TriFastTMFL reagenz (peqlab) according to manufactor's protocol. For synthesis of cDNA the QuantiTect$^®$ Reverse Transcription Kit (Qiagen) was used, according to manufacturer's protocol. For qRT-PCR, TaqMan$^®$ Gene Expression Assays for respective genes and the TaqMan$^®$ Fast Universal PCR Master Mix (Invitrogen) were used, with 1 – 3 µl cDNA (pre-diluted 1:10). The plate was read using a Realtime-PCR 7900 HT FAST machine and data were analyzed with the delta-delta C$_t$ method.

3.4   Isolation of CD11b$^+$ brain cells

Isolation of CD11b$^+$ cells from brain tissue was performed using the Neural Tissue Dissociation Kit (P) (Miltenyi Biotech) and the magnetic cell sorting (MACS) technique using CD11b labelled magnetic MicroBeads (Miltenyi Biotech). The procedure was carried out according to manufacturer's protocol. In brief, brain without cerebellum and olfactory bulbs was kept in ice-cold HBSS and manually minced with a scalpel. The tissue was then enzymatically digested by incubation with the buffers provided in the Neural Tissue Dissociation Kit (P) at 37°C and dissociated using the gentleMACS Dissociator (Miltenyi Biotech). The brain homogenate was passed through a 70 µm pre-separation filter and washed thoroughly several times to obtain a single cell suspension with minimal cell loss. Cells were then centrifuged at 1000x rpm for 10 min and resuspended in MACS buffer (PBS, pH 7.2, 0.5 % bovine serum albumin (BSA)). To label the cell suspension for magnetic cell sorting, 40 µl of CD11b MicroBeads per brain were added and incubated for 20 minutes at 4°C. The cell suspension was washed, centrifuged and resuspended in 1 ml MACS buffer. Cells were then transferred to a LS column (Miltenyi Biotech) placed in the MidiMACS magnetic separation unit (Miltenyi Biotec). The column was washed three times with MACS buffer and then separated from the magnet and flushed to collect cells labelled with CD11b MicroBeads. Following MACS isolation, CD11b$^+$ cells were subjected to FACS sorting as described in chapter 3.7.3.

3.5 Phagocytosis assay in adult brain slices

3.5.1 Preparation of adult brain slices

Preparation of acute cortical brain slices from 90 day old *Il12b$^{+/+}$*, *Il12b$^{-/-}$*, *APPPS1xIl12b$^{+/+}$* and *APPPS1xIl12b$^{-/-}$* mice followed previously described protocols[125]. In brief, mice were decapitated, brains were carefully removed and washed in artificial CSF (aCSF), containing: 134 mM NaCl, 2.5 mM KCl, 1.3 mM $MgCl_2$, 2 mM $CaCl_2$, 1.25 mM K_2HPO_4, 26 mM $NaHCO_3$, 10 mM D-glucose, pH 7.4, which was saturated with carbogen (95 % O_2, 5 % CO_2). Coronal cortical slices at 130 µm thickness were prepared at 4°C using a vibratome and were then kept in aCSF at RT for 2 hours until phagocytosis experiment.

3.5.2 Phagocytosis experiment in adult brain slices

Phagocytosis assay in acute brain slices was carried out as previously described[125]. Yellowgreen fluorescent Fluoresbrite carboxylated microspheres (2 µm diameter, Polysciences Europe GmbH, Eppelheim, Germany) were coated with fetal calf serum (FCS) by shaking at 1000x rpm for 30 min at RT. Microspheres were centrifuged at 3000x rpm for 5 minutes and then washed twice in HBSS followed by a centrifugation step at 3000x rpm for 5 minutes. They were resuspended in HBSS and applied on acute brain slices at 8.4x 10^6 microspheres per well. Slices were incubated for 1 hour at 37°C. Afterwards they were washed twice with 1x PBS on an orbital shaker for 15 minutes and then fixed with 4% PFA for 1 hour at RT.

3.5.3 Immunohistochemical staining and analysis of microglial phagocytosis

Microglia in adult brain slices were identified by staining with Iba-1 (Wako Chemicals). Fixed slices were permeabilized in 2 % TX in PBS for 4 hours at RT on a shaker, then unspecific binding sites were blocked by incubation in 10 % NGS/ 2 % TX/ 2 % BSA for 2 hours at RT. Primary antibody Iba-1 was diluted at 1:300 in 5 % NGS/ 0.3 % TX in PBS and incubated with slices over night at 4 °C. The next day, slices were washed 3 times in 1x PBS and secondary antibody (goat-anti-rabbit Alexa® Flour 568, 1:300 in

PBS/ 5 % NGS/ 0.3 % TX) was incubated for 2 hours at RT. After washing the slices 3 times with 1x PBS, they were counterstained with Draq5 (1:1000 in PBS, eBioscience) for 10 minutes and then mounted with Microscopy Aquatex (Merck). For analysis of microglial phagocytosis, 15 µm thick z-stacks with a step size of 1 µm, beginning from the top of the slice where the microspheres are located, were taken at 40x magnification using a confocal laser scanning microscope (LSM 510 META, Zeiss). 4 - 5 z-stacks per slice were analyzed by determining the percentage of phagocytic microglia per field of view using the ImageJ cell counter plugin. Furthermore, phagocytic cells were grouped according to the number of microspheres they have taken up, to determine the phagocytosis grade of microglia, with 1 - 3 microspheres = grade 1; 4 - 6 = grade 2; 7 - 10 = grade 3; > 10 = grade 4.

3.6 Primary cell culture

3.6.1 Preparation of mixed glial culture

Mixed glial cultures were prepared from newborn mouse brains (postnatal day 2 – 5), as previously described[126]. In brief, cortical tissue was isolated, freed from meninges and adherent blood vessels, cross-chopped and incubated in 1x trypsin/EDTA for 5 min at 37 °C, before being triturated into a single cell suspension. Cells were then passed through a 70 µm nylon cell strainer, centrifuged (5 min, 1000x g) and resuspended in pre-warmed Dulbecco's modified Eagle's medium (DMEM; Invitrogen), supplemented with 10 % fetal bovine serum and 50 U/ ml penicillin/ streptomycin (Invitrogen). Cells were maintained in T75 flasks at 37 °C in a 5 % CO_2 humidified atmosphere. Culture media was replaced every three to four days until cells reached confluency.

3.6.2 Isolation of microglia and astrocytes from mixed glia culture

To isolate microglia from a mixed glial culture, flasks were tapped vigorously several times to remove the cells from the astroglia monolayer. Culture medium with suspended cells was centrifuged (1000x g, 5 min) and cells were counted using an improved Neubauer chamber. After removal of microglia from the mixed glia culture, remaining cells were trypsinized for 5 min at 37 °C and suspended in fresh pre-warmed culture

medium. In order to remove any residual microglia cells from the culture, a method described by Losciuto et.al., 2012 was carried out, which is based on the antigen–antibody-mediated magnetic cell sorting system using CD11b MicroBeads (Miltenyi Biotech). This technique allows to rapidly obtain purified astrocyte cultures after microglia depletion[127]. Therefore, cells from one T75 flask were centrifuged and resuspended in 180 μl separation buffer (MACS buffer; PBS, pH 7.2, 0.5 % BSA and 2 mM EDTA) and 20 μl CD11b MicroBeads (MicroBeads conjugated to monoclonal rat anti-mouse CD11b antibody). After 20 min incubation at 4 °C, during which CD11b positive cells were magnetically labeled with CD11b MicroBeads, cells were washed in MACS buffer, centrifuged (1000x g, 5 min) and resuspended in 1 ml MACS buffer. The cell suspension was applied on two LS columns (Miltenyi Biotech), fixed into the MidiMACS magnetic separation unit (Miltenyi Biotec). Columns were washed three times with MACS Buffer and unlabeled, CD11b negative cells which passed through the columns were collected, centrifuged (1000x g, 5 min) and counted. Microglia and purified astrocytes were plated at 5x 10^4 cells/ well in either 96-well plates for stimulation experiments or on cover slips placed in 24-well plates for staining.

3.6.3 Immunocytochemistry of primary glia cells

To evaluate the purity of primary microglia and astrocyte cultures, cells were stained for specific microglia and astrocyte markers. Therefore, cells were cultured for three days on cover slips and then washed 2x in PBS. Microglia were fixed for at least 1 hour and astrocytes for 10 minutes in 4 % PFA at RT. After washing the cells 3x in PBS, they were incubated in blocking buffer (1x PBS containing 0.3 % TX and 10 % NGS) for 1 hour at RT. Primary antibodies were diluted in 1x PBS/ 0.3 % TX/ 5 % NGS and incubated for 2 hours at RT. After rinsing the cells three times with 1x PBS, they were incubated with species specific fluorescently labelled secondary antibodies (Table 6). Secondary antibodies were diluted in 1x PBS/ 0.3 % TX/ 5 % NGS and cells were incubated for 1 h on a shaker at RT. After rinsing the cells three times with 1x PBS, they were mounted with DAPI containing aqueous mounting medium (Fluoroshield Mounting Medium with DAPI, abcam®). Microscopic analysis was carried out using a fluorescence microscope (Zeiss Axio Observer Z1) with the software Axio vision 4.

Table 6: Primary and secondary antibodys used for immunofluorescence of primary cells

Primary antibody	Host	Dilution	Company	Secondary antibody	Host	Dilution	Company
Iba-1	rabbit	1:500	Wako	**Alexa Fluor® 568 Anti-rabbit IgG**	goat	1:300	Dianova
GFAP	rabbit	1:1500	Dako	**Alexa Fluor® 568 Anti-rabbit IgG**	goat	1:300	Dianova
GLAST-1	rabbit	1:250	Abcam	**Alexa Fluor® 568 Anti-rabbit IgG**	goat	1:300	Dianova

3.6.4 Stimulation of primary glia cells

Microglia and astrocytes were kept in culture for two days after being plated in 96 wells. Culture medium was discarded and LPS (1 µg/ ml) and IFNγ (100 U/ ml)[102] diluted in serum-free culture medium was added to stimulate the cells. Equivalent amount of PBS in serum-free medium was used as stimulation negative control. After 6, 12 and 24 hours, medium was collected, snap frozen in liquid nitrogen and stored at -80 °C until biochemical analysis. Cells were dissolved in 500 µl TriFast and stored at -80 °C for subsequent RNA analysis.

3.6.5 Phagocytosis of primary microglia after stimulation

Microglia cultures and microglia/astrocyte co-cultures were used for stimulation with recombinant IL-12 (Peprotech) and subsequent phagocytosis assay. Two days after plating on cover slips in 24-well plates, cells were stimulated with IL-12 (10 ng/ml) or LPS diluted in serum-free culture medium for 24 hours. PBS in serum-free medium was used as stimulation control. Yellowgreen fluorescent microspheres were prepared as described in chapter 3.5.2 and added to the cells at a concentration of 8.4×10^6 microspheres per well. Cells were incubated with the microspheres for 30 minutes at 37 °C before being washed twice in 1x PBS for 5 minutes on a shaker and fixed in 4 % PFA for 1 hour at RT. Cells were then rinsed twice in 1x PBS, stained for Iba-1 and mounted, as described in chapter 3.6.3. Per stimulation condition, 9 – 11 images were taken using a fluorescence microscope (Zeiss Axio Observer Z1) and analyzed by determining the percentage of phagocytic microglia per image using the ImageJ cell counter plugin.

3.7 Flow cytometry

3.7.1 Flow cytometric analysis of blood immune cells

Blood from *APP23* mice was analyzed by FACS to determine blood immune cell composition after peripheral anti-p40 antibody treatment. Mice were sacrificed and 50 µl of blood was collected in 200 µl 1x PBS/ 20 mM EDTA. After red blood cell lysis in 150 mM NH_4Cl, 10 mM $KHCO_3$, 0,1 mM EDTA in ddH_2O for 5 minutes, the cells were centrifuged (1200x rpm, 7 min) and resuspended in 100 µl FACS Buffer (0.5 % BSA in 1x PBS). 0.5 µl Fc-Block (1:200, BioLegend) was added (10 min incubation) to block unspecific binding of the Fc-receptors on cells (CD16/ CD32) via the Fc domain of the antibodies. The respective surface antibodies (Table 7) were added at their specific dilution and incubated for 20 min at 4°C in the dark. Following washing in 500 µl FACS buffer the cells were resuspended in 200 µl FACS buffer. The fluorescence cell properties were measured with BD FACS Canto TM II (Becton Dickinson) and the data was analyzed with FlowJo 7.6 software (Tree Star Inc.) and MS-Excel.

Table 7: FACS antibodies used for identification of blood immune cell composition

Antibody-fluorochrome	Dilution	Company
CD5-PE	1:400	BioLegend
B220-V450	1:400	BD Bioscience
CD11b-FITC	1:400	BioLegend

3.7.2 Flow cytometric analysis of primary astrocyte cultures

To determine the abundance of microglia in the primary astrocyte culture, cells were stained with microglia-specific cell surface markers and analyzed by flow cytometry. Therefore, astrocytes before and after MACS procedure were blocked in Fc-Block and stained with antibodies (Table 8) as described in chapter 3.7.1.

Table 8: Antibodies used for FACS analysis of primary astrocytes

Antibody-fluorochrome	Dilution	Company
CD11b-PE	1:100	BioLegend
CD45-APC	1:100	BD Pharmingen

After washing of the cells, they were resuspended in 200 µl FACS buffer. 1 µl of PE-labelled propidium iodide (PI) was added to detect dead cells. The fluorescence cell properties were measured with BD FACS Canto TM II (Becton Dickinson) and the data was analyzed with FlowJo 7.6 software (Tree Star Inc.) and MS-Excel.

3.7.3 FACS sorting of isolated CD11b$^+$ cells

To ensure high purity of microglia cells, the CD11b$^+$ cell population isolated by MACS (see chapter 3.4) was subjected to FACS sorting to remove cell debris, dead cells and residual CD11b$^-$ cells from the cell suspension. After the MACS procedure, CD11b$^+$ cells were centrifuged and resuspended in 200 µl MACS buffer. Therefore cells were incubated with Fc-Block and with cell surface antibodies (3.7.1.

Table **9**) as described in chapter 3.7.1.

Table 9: Antibodies used for FACS sorting

Antibody-fluorochrome	Dilution	Company
CD11b-PE	1:100	BioLegend
CD45-APC	1:100	BD Pharmingen

After washing, cells were resuspended in 200 µl FACS buffer. 1 µl DAPI was added to detect dead cells. Cells were sorted for DAPI-negative (living cells) and CD11b$^+$ / CD45^{intermediate} positivity (Figure 9) at the Flow Cytometry Core Facility (FCCF) of the Deutsches Rheuma-Forschungszentrum (DRFZ) in Berlin.
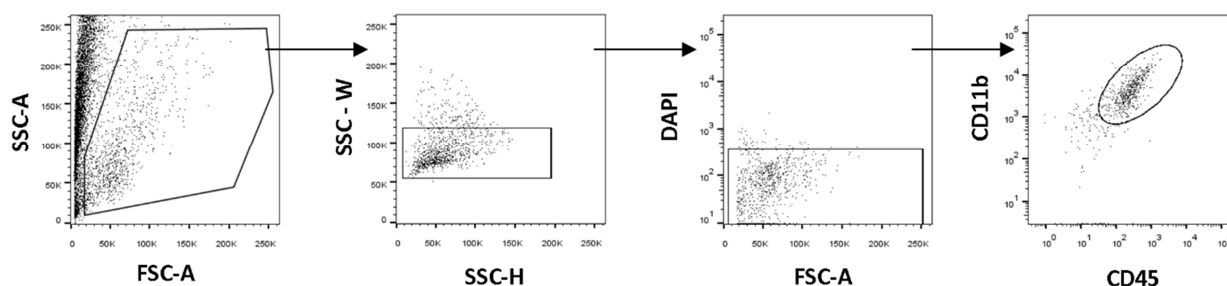

Figure 9: Gating strategy for FACS-sort of cortical microglia.
MACS-isolated microglia were subjected to FACS-sort for DAPI-negative, CD11b^{pos} and CD45^{int} cells.

After FACS sorting, CD11b$^+$ and CD11b$^-$ cell populations were dissolved in TriFast reagenz and stored at -80°C until RNA analysis.

3.8 Statistics

Statistical analyses were performed using the GraphPad Prism 5 Software. Differences between groups were evaluated by Student's t-test for pairwise comparison of experimental groups or by one-way ANOVA with Dunnett's multiple comparison or Tukey's multiple comparison post-test for comparison of more than two experimental groups, as indicated. Statistical significance is indicated as follows: * $p < 0.05$, ** $p < 0.01$ and *** $p < 0.001$.

4.   Results

Previous work in the laboratory of Prof. Heppner has demonstrated that genetic deficiency of p40, the common subunit of the hetero-dimeric cytokines IL-12 and IL-23, has a major effect on Aβ plaque pathology in the AD mouse model *APPPS1*. The lack of p40 resulted in a significant reduction in Aβ plaque burden in *APPPS1* mice at the age of 120 days and 250 days[121] (also see chapter 1.4). In light of these findings this thesis aimed at determining the mechanism which lead to the observed Aβ reduction upon p40 deficiency, to define cellular players and downstream signaling pathways in the brain, and to evaluate whether pharmacological p40 reduction ameliorates Aβ-related pathology as a potential therapeutic strategy.

4.1   Aβ and sAPPβ levels in pre-depositing *APPPS1* mice deficient in p40

The finding of reduced Aβ plaque burden upon genetic deficiency of p40 raises the question whether the absence of p40 affects steady-state levels of cerebral Aβ in young *APPPS1* mice, before Aβ plaques start to form. Possible differences detectable at an early time-point of Aβ pathology would indicate that Aβ production is changed and explain the differences in plaque load in later stages of the pathology. To address this, *APPPS1* mice which lack p40 were analyzed at the age of 7 weeks, a time point when this mouse line does not show any Aβ deposition in plaques yet[36]. Frozen brain hemispheres of p40-deficient *APPPS1* mice and *APPPS1* littermates with functional p40 as control were homogenized according to a 4-step extraction protocol[124], which allows to analyze soluble proteins from aggregated proteins separately. The obtained TBS-, TX- and SDS-extracted protein fractions were subjected to the Meso Scale Discovery (MSD) electrochemiluminescent Immunoassay using the MSD 6E10 assay, to determine Aβ levels in each fraction. The FA fraction, which contains Aβ from densely aggregated core plaques, was not analyzed in this experiment, since mice at this age do not exhibit dense plaques yet. Young p40-deficient *APPPS1* mice show in all protein fractions a tendency towards slightly higher Aβ levels compared to *APPPS1* control mice (Figure 10). This effect was not significant in any fraction, except for the TX fraction. Taken together these data, which show slightly higher Aβ levels in young, pre-

depositing *APPPS1* mice which lack p40, do not explain the observed reduced Aβ pathology in older mice and indicate no major difference in steady state Aβ production upon p40 deficiency.
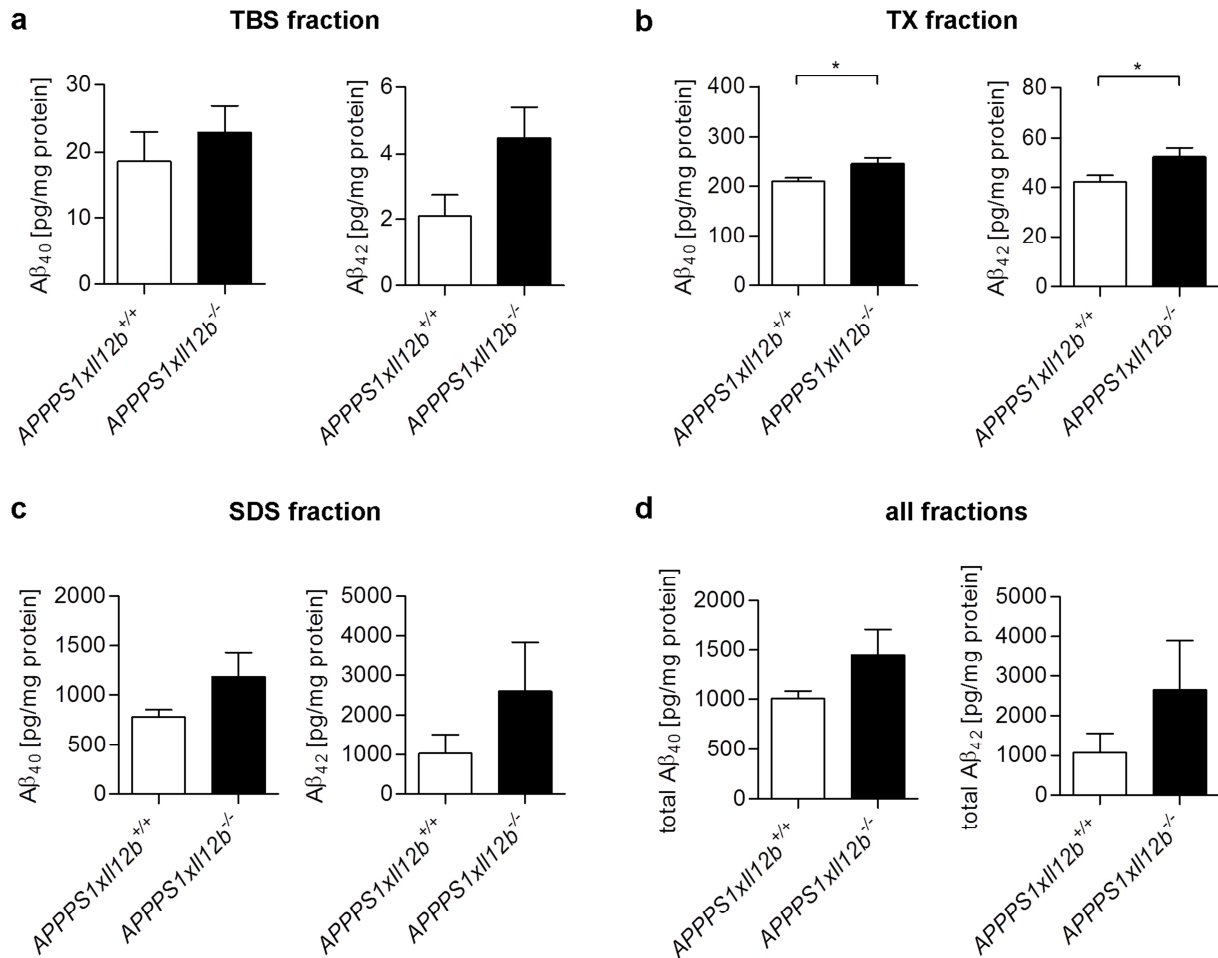

Figure 10: Cerebral Aβ40 and Aβ42 levels in young, pre-depositing *APPPS1* mice deficient in *Il12b*. Frozen brain tissue of 49 day old *Il12b*-deficient *APPPS1* mice and *APPPS1* mice with functional *Il12b* was homogenized consecutively in (a) TBS, (b) TX and (c) SDS buffer and supernatants of each fraction were subjected to MSD analysis using the 6E10 Aβ Triplex assay. (d) Aβ40 and Aβ42 contents of all three fractions were combined to determine total Aβ levels (n = 9 per group). For statistical analysis student's t-test was used.

In addition to steady state Aβ levels measured during an early time-point of Aβ pathology, analyzing APP processing and particularly β-secretase cleavage as the initial step of Aβ generation can indicate whether Aβ production is altered. Changes in amyloidogenic APP processing facilitated by β-secretase in young, pre-depositing p40-deficient *APPPS1* mice compared to *APPPS1* mice with functional p40 signaling could lead to the observed decrease in amyloid plaque burden at a later age. Cleavage of APP by β-secretase results in the generation of a soluble APPβ fragment (sAPPβ),

which can be measured as an indicator of β-secretase activity. To determine if APP cleavage by β-secretase is changed, the sAPPβ fragment was measured in the TBS-extracted protein fraction using the MSD sw sAPPβ assay. Soluble APPβ levels were not significantly altered in young *APPPS1* mice which lack the p40 subunit, compared to *APPPS1* control mice (Figure 11). This indicates that APP processing by β-secretase is not changed upon p40 deficiency in young, pre-depositing *APPPS1* mice**.**
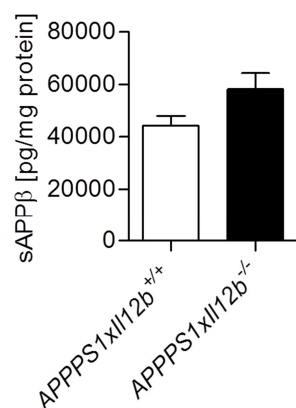

Figure 11: sAPPβ levels in brain homogenates of young, pre-depositing *APPPS1* mice deficient in *Il12b*.
TBS-extracted protein fraction of 49 day old *Il12b*-deficient *APPPS1* mice and *APPPS1* mice with functional *Il12b* was subjected to MSD analysis using the sw sAPPβ assay (n = 9 per group). For statistical analysis student's t-test was used.

4.2 Aβ levels in the plasma of *APPPS1* mice upon p40 deficiency

Aβ peptide can be transported from the CNS to the peripheral blood via the blood-brain barrier. A balanced Aβ efflux is mainly facilitated by the low-density lipoprotein receptor-related protein (LRP), P-glycoprotein (P-gp or ABCB1) and other ATP-binding cassette (ABC) transporters such as ABCA, ABCG2 and ABCC1[128]. In the AD brain as well as in AD mouse models, it was proposed that Aβ clearance from the brain to the periphery is impaired, leading to Aβ retention in the brain[129–132]. To analyze whether peripheral Aβ levels in the blood are altered in the absence of p40, which could hint towards changes in Aβ efflux mechanisms from the brain to the circulation via the blood-brain barrier, $A\beta_{40}$ and $A\beta_{42}$ levels in the plasma of young, pre-depositing *APPPS1* mice and older mice with an established disease phenotype were measured by electrochemiluminescent Immunoassay using the MSD 4G8 assay. $A\beta_{40}$ and $A\beta_{42}$

content in the blood of young (Figure 12 a) and old *APPPS1* mice (Figure 12 b) did not differ between mice lacking p40 protein and mice with functional p40, which gives no indication that Aβ efflux from the brain to the blood is altered upon p40 deficiency or that the lack of p40 disturbs peripheral Aβ homeostasis.
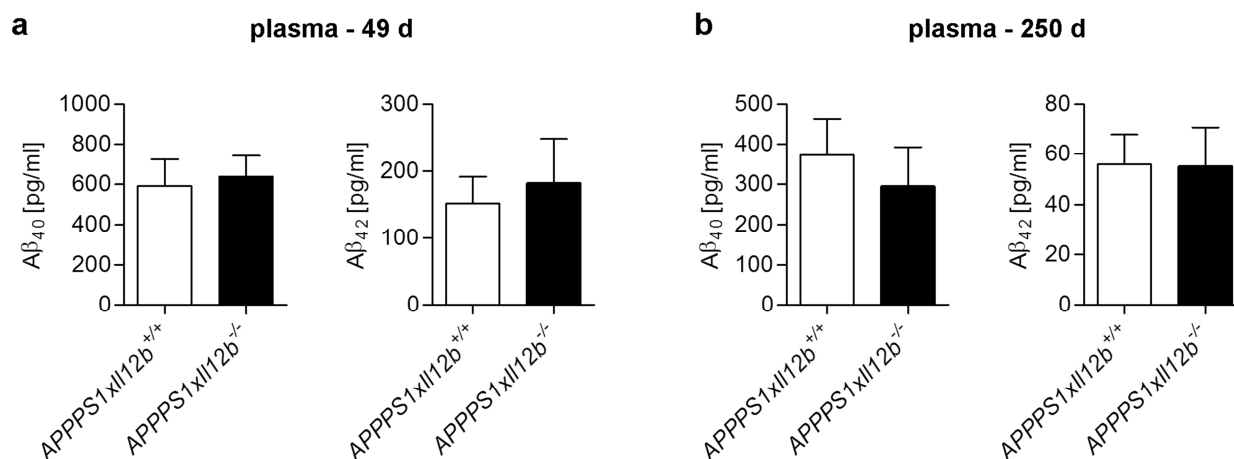

Figure 12: Aβ$_{40}$ and Aβ$_{42}$ levels in the plasma of young, pre-depositing and aged *APPPS1* mice deficient in *Il12b*.
Aβ levels were determined in the plasma of *Il12b*-deficient *APPPS1* mice and *APPPS1* with functional *Il12b* at (a) 49 days of age and (b) 250 days of age using the Meso Scale 4G8 Aβ Triplex assay (49 d n = 9, 250 d n = 9 - 11). For statistical analysis student's t-test was used.

4.3   Influence of IL-12 / IL-23 pathways on microglial phagocytosis

Microglia are the brain's intrinsic macrophages and thus capable of phagocytosis. Several studies have demonstrated that microglia are able to phagocytose and degrade Aβ[133–135], however clearance of Aβ by microglial phagocytosis seems to be either inefficient or inadequate in the context of Alzheimer's disease[119]. Phagocytosis capacity of microglia has been shown to be impaired in mice with AD-like pathology[136]. Furthermore, stimulation of microglia with the pro-inflammatory cytokine TNFα decreased microglial phagocytosis activity[120], indicating that inflammatory mediators can affect the ability of microglia to phagocytose. Hence, we sought to determine if the presence or absence of IL-12 / IL-23 alters phagocytic capacity of microglia.

4.3.1 Microglial phagocytosis in adult brain slices upon p40 deficiency

To investigate if p40 deficiency affects microglial phagocytosis, a phagocytosis assay *in situ* using adult brain slices was conducted[136]. Therefore, acute brain slices from wt *(Il12b^{+/+}), Il12b^{-/-}, APPPS1xIl12b^{+/+}* and *APPPS1xIl12b^{-/-}* mice were prepared and incubated with fluorescent microbeads that can be taken up by microglia. Afterwards, slices were fixed and stained with the microglia-specific marker Iba-1. To analyze phagocytosis of microbeads by microglia, confocal z-stacks were taken and the percentage of phagocytic microglia was determined. Orthogonal views of 15 µm confocal z-stacks show the uptake of microbeads by Iba-1-positive microglia in acute brain slices of the different genotypes (Figure 13 a). The number of microglia is significantly higher in slices of *APPPS1* mice compared to non-transgenic animals, while the genetic deficiency of p40 did not affect the frequency of Iba-1- positive cells (Figure 13 b). No difference in phagocytic capacity of microglia in brain slices of non-transgenic wt and *Il12b^{-/-}* can be detected, however the percentage of phagocytic microglia in brain slices of *APPPS1xIl12b^{+/+}* is significantly decreased compared to wt (Figure 13 c), which is consistent with previously published results[136]. Notably, phagocytosis of microbeads is slightly improved in brain slices of *APPPS1* mice which lack p40. This effect was most pronounced in cells that engulfed a low number of beads (1 – 3 beads per cell), as assessed in an analysis where the phagocytic cells were grouped according to the number of beads they phagocytosed (Figure 13 d).
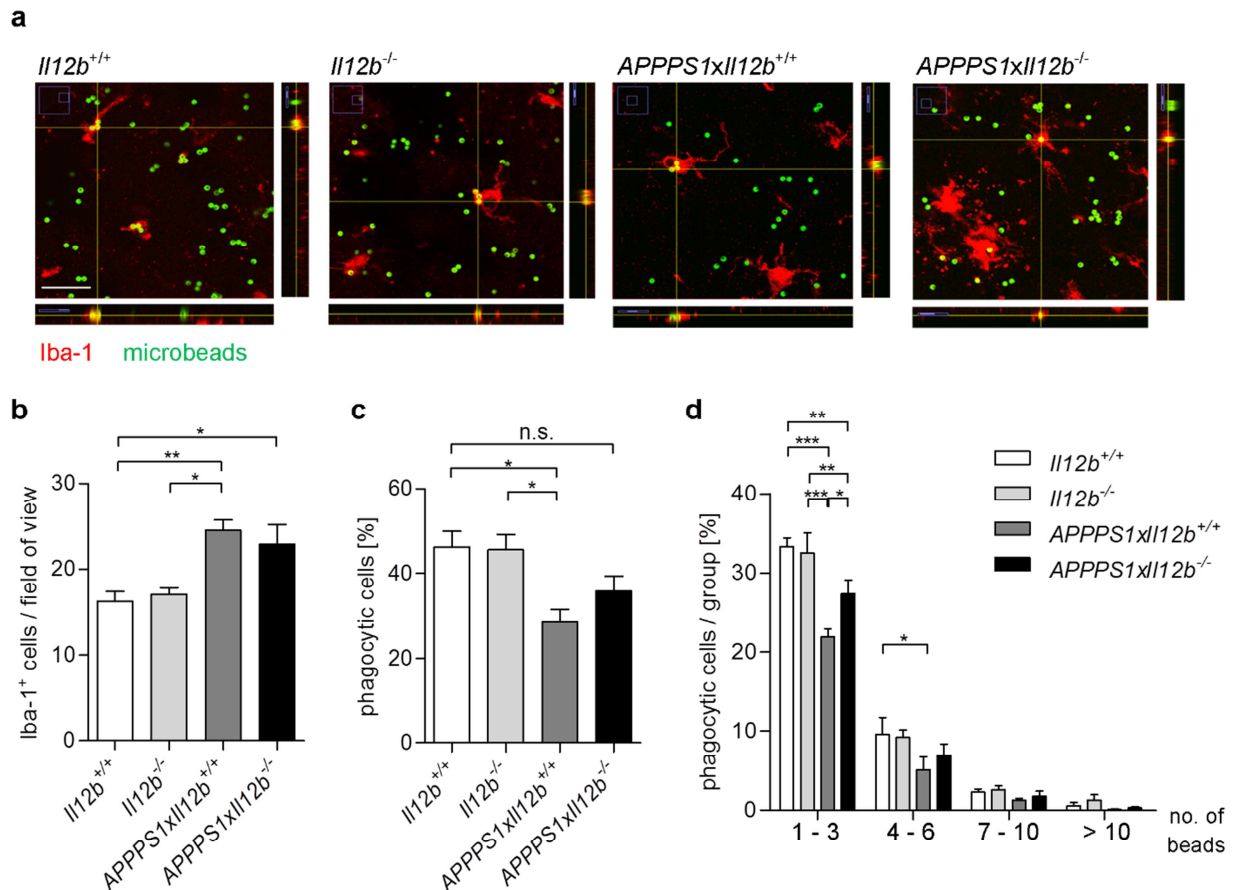
Figure 13: Phagocytic activity of microglia in adult acute brain slices of mice deficient in *Il12b*. Organotypic brain slices prepared from 90 day old wt (*Il12b^{+/+}*), *Il12b^{-/-}*, *APPPS1xIl12b^{+/+}* and *APPPS1xIl12b^{-/-}* mice were incubated with fluorescent microbeads to analyze phagocytic microglia. (a) Representative orthogonal views from 15 μm confocal z-stacks showing uptake of fluorescent microbeads (in green) by microglia (labelled with Iba-1, red) in brain slices of *Il12b^{+/+}*, *Il12b^{-/-}*, *APPPS1xIl12b^{+/+}* and *APPPS1xIl12b^{-/-}* mice. (b) Number of Iba-1 positive cells per field of view for all four different genotypes. (c) Percentage of phagocytic microglia of all genotypes. (d) Phagocytic microglia of each genotype were grouped according to the number of engulfed microbeads. scale bar 20 μm, n = 4 mice per group, for statistical analysis one-way ANOVA, followed by Tukey's Multiple Comparison Test was used.

Taken together, in wt mice the absence of p40 did not affect baseline phagocytic activity of microglia. In *APPPS1* mice, which showed lower phagocytic capacity at baseline, the lack of p40 resulted in increased phagocytic activity, thus rescuing the *APPPS1*-dependent reduction in microglial phagocytosis. Stereological analysis of Aβ plaque load using the Stereoinvestigator System in the 90 day old mice showed that the p40-deficient *APPPS1* mice have a significantly lower cortical area that is covered with Aβ compared to *APPPS1* mice with functional p40 signaling (Figure 14), which is in line with previous results demonstrating reduced Aβ plaque burden in the absence of p40[121]. Since it was shown that Aβ deposition in plaques negatively correlates with

phagocytic activity of microglia[136], the finding that phagocytosis is improved could be due to the difference in plaque burden between *APPPS1xII12b^{-/-}* and control *APPPS1* mice at the time of analysis, and not necessarily due to a direct effect of p40 on phagocytosis capacity of microglia.
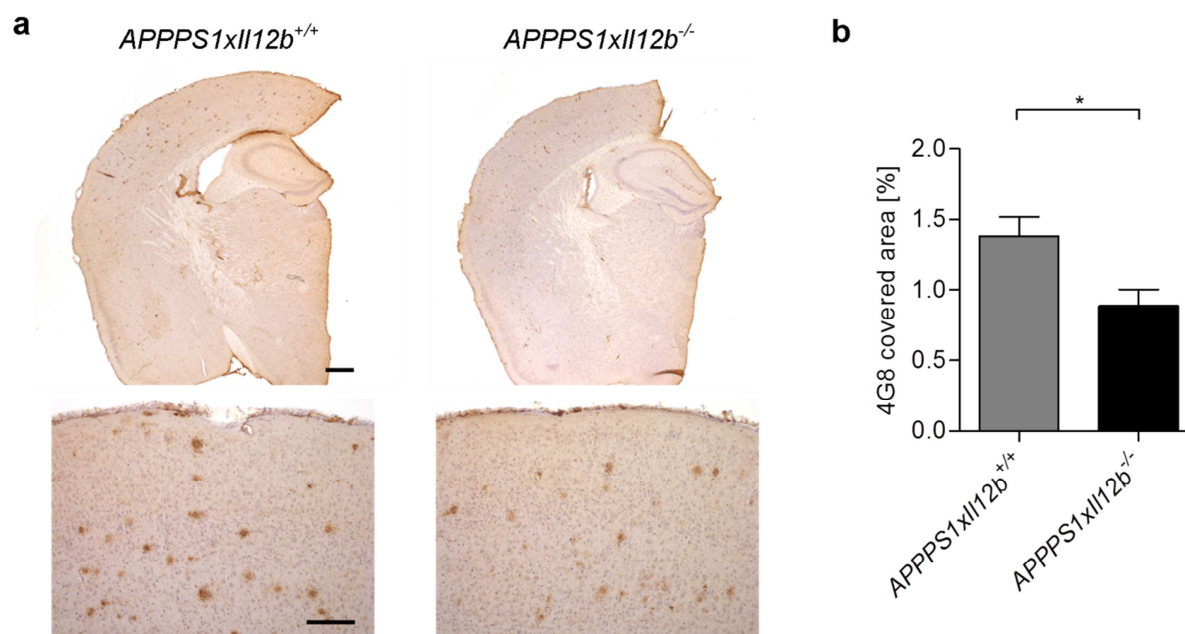

Figure 14: Histological analysis of Aβ plaque burden in *APPPS1* mice deficient in *II12b*.
Aβ burden in 90 day old mice was assessed by immunohistochemical staining using the amyloid-β reactive antibody 4G8. (a) Representative images of 4G8 staining in *APPPS1* mice deficient in *II12b* compared to *APPPS1* mice with functional *II12b* at low magnification (upper row, scale bar 500 µm) and higher magnification (lower row, scale bar 200 µm). (b) Stereological quantification of the area covered by 4G8 was assessed using the Stereo Investigator system. n = 4. For statistical analysis the student's t-test was used.

4.3.2 Phagocytosis of primary microglia upon IL-12 stimulation

Since microglial phagocytosis activity is affected by the absence of p40 signaling in acute brain slices of *APPPS1* mice (chapter 4.3.1), we next sought to determine whether p40 directly affects microglial phagocytosis. To find out whether p40 has a direct effect on phagocytosis activity of microglia, primary microglia cells isolated from neonatal mixed glia culture were stimulated with IL-12 for 24 hours and the capacity of microglia to take up fluorescent microbeads after the stimulation was quantified. Since previous data point to the fact that non-microglial brain cells, possibly astrocytes, are involved in the IL-12 / IL-23 signaling pathway[121] (see chapter 4.6), and thus the

presence of astrocytes might be necessary to enable functional effects of IL-12 stimulation, we also included primary microglia/astrocyte co-cultures in the analysis. To address whether the primary cultures per se are able to react to stimulation, they were also treated with LPS, which has been shown to increase microglia phagocytosis *in vitro*[137]. Incubation of primary microglia cultures with fluorescent microbeads for 30 minutes resulted in approximately 70 % phagocytic microglia in control-treated cultures (Figure 15 a, b). While the percentage of phagocytic cells was significantly increased after stimulation with LPS, IL-12 stimulation of primary microglia did not alter phagocytic activity compared to control treatment (Figure 15 b). Microglia/astrocyte co-cultures showed a significantly higher phagocytic capacity of microglia upon control- and IL-12-treatment compared to pure microglia cultures, while no such changes could be observed after LPS treatment (Figure 15 d). The fact that phagocytosis activity of LPS-stimulated microglia did not differ between single cell cultures and microglia/astrocyte co-cultures is most likely due to the high phagocytosis activity per se in the microglia single cell cultures treated with LPS, which was already close to the upper bound of 100 % of phagocytic cells that cannot be further markedly increased. Even though the presence of astrocytes affected the general activity of microglia to phagocytose, the different treatment regimens did not affect microglia phagocytosis in the co-cultures (Figure 15 c). Notably, the percentage of phagocytic microglia was not altered after treatment with IL-12 in neither microglia nor microglia/astrocyte co-cultures, which indicates that IL-12 does not directly affect phagocytic activity of primary neonatal microglia *in vitro.*
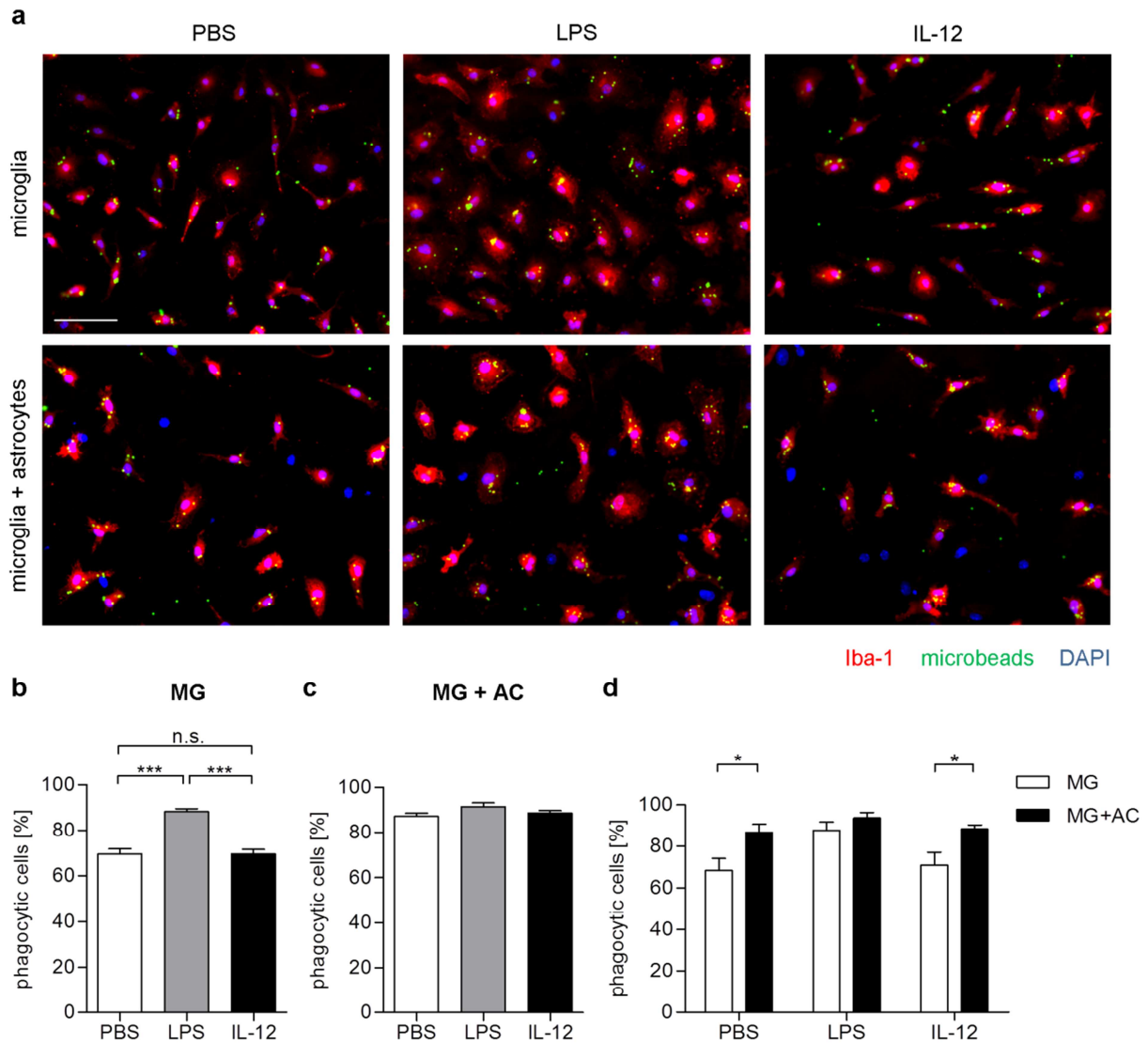
Figure 15: Phagocytic activity of primary microglia after stimulation *in vitro*.
Primary microglia cultures (MG) and microglia and astrocyte (AC) co-cultures (MG+AC) were stimulated with LPS (1 µg/ml) or IL-12 (10 ng/ml) for 24 hours, before fluorescent microbeads were added to analyze microglial phagocytosis. (a) Representative images of microglia cultures (upper panel) and microglia/astrocyte co-cultures (lower panel) stimulated with LPS, IL-12 or control-treated with PBS in medium, showing uptake of fluorescent microbeads (in green) by microglia (immunofluorescently labelled with Iba-1, red). Quantification of phagocytic cells in (b) microglia cultures and (c) microglia/astrocyte co-cultures after stimulation. (d) Comparison of phagocytic activity between microglia and microglia/astrocyte co-cultures after stimulation. scale bar 100 µm, n = 3 independent experiments, for statistical analysis one-way ANOVA, followed by Tukey's Multiple Comparison Test was used.

4.4 Inflammatory profile of *APPPS1* mice upon p40 deficiency

It was previously demonstrated that manipulation of specific immune pathways influences the gene expression profile and the activation state of microglia. Genetic

deficiency of the NLRP3 inflammasome resulted in a decrease of pro-inflammatory markers and increased expression of anti-inflammatory genes, which are associated with an altered microglial phenotype and beneficial Aβ clearance function[80]. Another recent example is that the deficiency of IL-10 leads to the selective modulation of innate immune genes that drive innate immune response in favor of Aβ phagocytosis by microglia[83]. Similarly, the absence of the pro-inflammatory immune pathways of IL-12 and IL-23 in the AD-prone brain could result in an altered expression profile of pro- and anti-inflammatory markers and in changes of the activation phenotype of brain-intrinsic microglia cells. To address whether this is the case, CD11b-positive microglia cells from brains of *APPPS1* mice deficient in p40 and *APPPS1* control were separated from CD11b-negative brain cells, and both cell populations were analyzed for gene expression changes of different immune mediators. Additionally, expression of inflammatory mediators was analyzed in whole brain lysates of older animals, in *APPPS1xIl12b$^{+/+}$* and *APPPS1xIl12b$^{-/-}$* mice at 250 days of age.

4.4.1 Cell-specific analysis of gene expression levels of inflammatory mediators in 90 day old *APPPS1xIl12b$^{-/-}$* mice

To analyze the effect of p40 deficiency on gene expression in different brain cell populations, isolated CD11b-positive (CD11b^{+}) microglia and CD11b-negative (CD11b^{-}) brain cells from 90 day old mice were subjected to qPCR analysis of different pro-inflammatory (*il-1β, tnfα, il-6, nfκb, nos2*) and anti-inflammatory *(il-10, tgf-β, cd206)* mediators, as well as *apoe*, which has long been known as a major genetic risk factor for AD and is believed to affect Aβ aggregation and clearance in the brain[138],[139]. In addition, expression of microglial receptors associated with phagocytosis and inflammation (*cd36, trem-2, msr-1*), which were recently implicated in Aβ pathogenesis[70,140,141], was analyzed in CD11b-positive brain cells. Gene expression analysis revealed no significant differences in any of the genes analyzed between *APPPS1* mice with functional *Il12b* and *APPPS1* mice deficient in *Il12b* (Figure 16). Notably, expression of prominent target genes of IL-12 and IL-23 signaling in the peripheral compartment, namely *ifnγ*, *il-17a* and *il-17f*, were hardly detectable neither in the CD11b-positive nor in the CD11b-negative brain cell population and hence, were not depicted here. This analysis demonstrates that gene expression of the examined pro-

and anti-inflammatory markers in CD11b-positive and CD11b-negative brain cell populations isolated from 90 day old *APPPS1* mice is not affected by the lack of p40, at least at the analyzed time point.
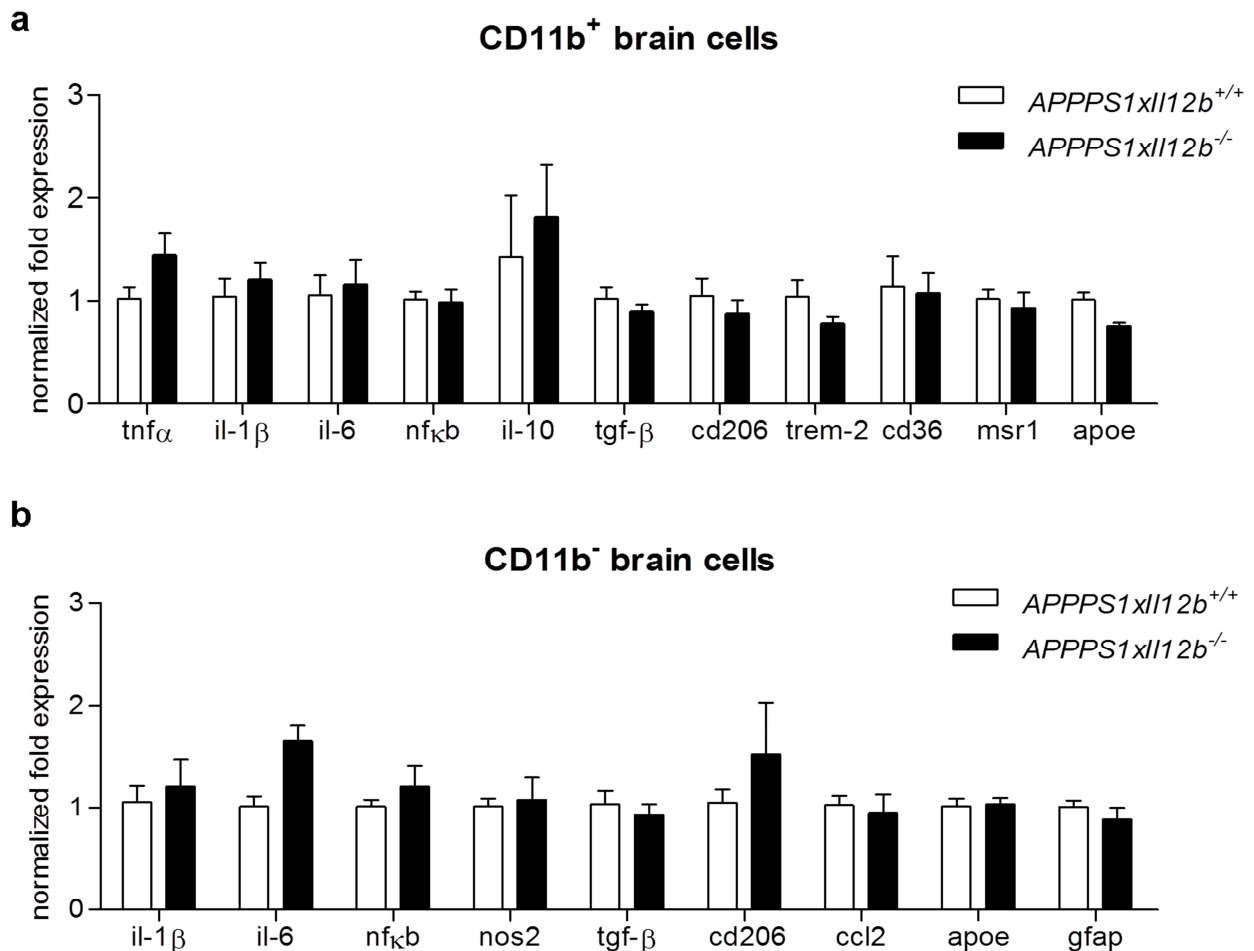

Figure 16: Analysis of gene expression levels of inflammatory mediators in CD11b$^+$ and CD11b$^-$ brain cells of *APPPS1* mice deficient in *Il12b*.
Fold expression of different pro- and anti-inflammatory genes in (a) CD11b$^+$ and (b) CD11b$^-$ brain cells of 90 day old *APPPS1xIl12b$^{-/-}$* mice compared to control *APPPS1xIl12b$^{+/+}$* mice. Fold regulations were calculated from Ct values measured with qRT-PCR using the delta-delta Ct method, in relation to GAPDH levels. n = 4 mice per group, for statistical analysis two-way ANOVA with Bonferroni post-test was used.

4.4.2 Cytokine levels in brains of 250 day old *APPPS1xIl12b$^{-/-}$* mice

We next aimed to determine whether protein expression of pro- and anti-inflammatory molecules is affected by the lack of p40 at a later stage of Aβ pathology. Therefore whole brain lysates were analyzed using the MSD V-PLEX Plus Proinflammatory Panel 1 from *APPPS1* with functional p40 signaling compared to *APPPS1* deficient in p40 at

250 days of age, which marks a time-point of robust, progressed Aβ pathology. While IFNγ was not detectable in whole brain lysates using this assay, protein levels of IL-1β, TNFα, IL-6, IL-10, CXCL1, IL-2, IL-4 and IL-5 were not found to be different between *APPPS1xII12b⁺ᐟ⁺* and *APPPPS1xII12b⁻ᐟ⁻* mice (Figure 17). This demonstrates that the analyzed cytokines/chemokines in whole brain lysates were not affected by the absence of p40 in AD-prone mice during a progressed disease stage.
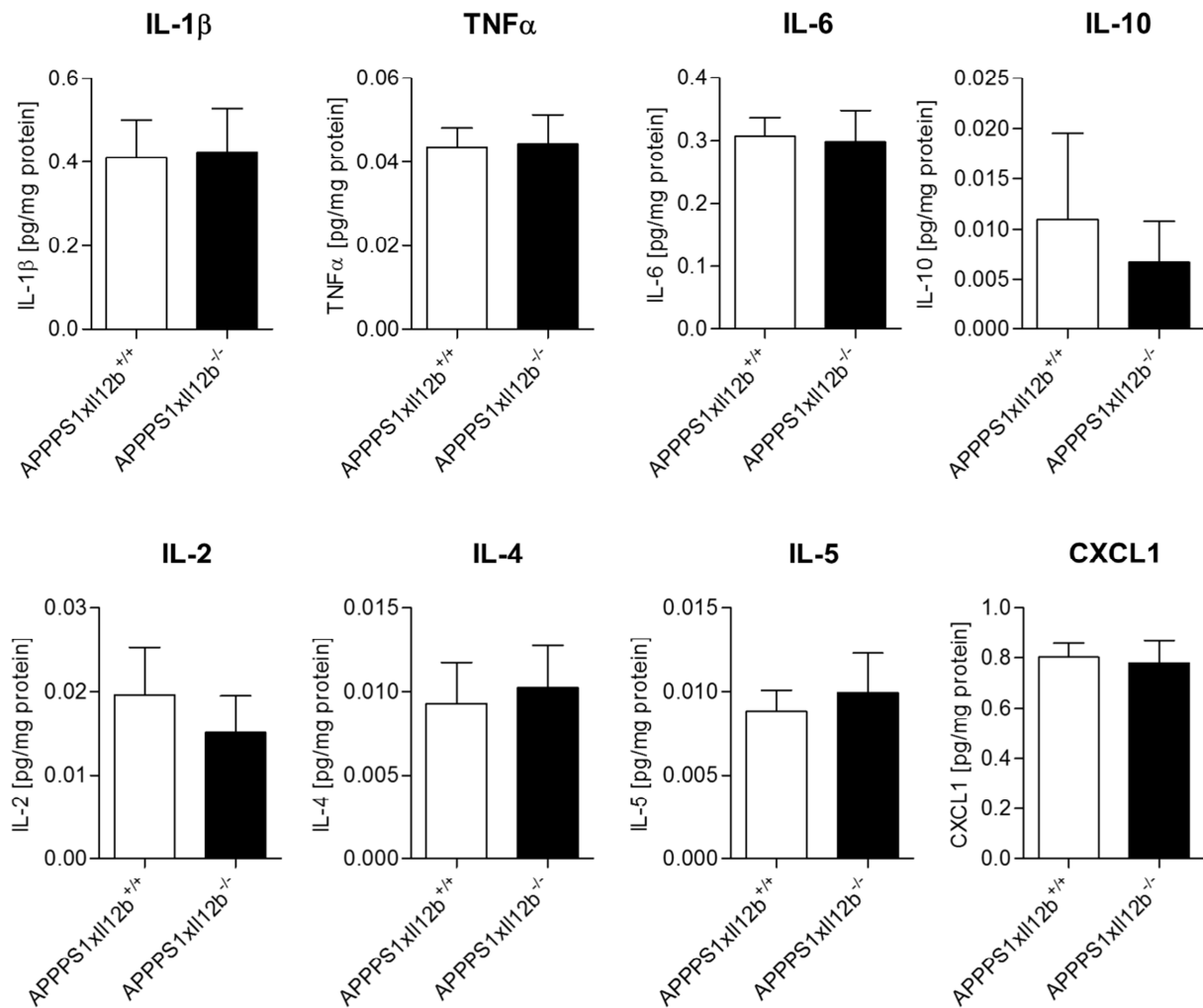

Figure 17: Cytokine levels in whole brain lysates of *APPPS1* mice deficient in *II12b*.
Levels of different pro- and anti-inflammatory markers in brain lysates of 250 day old *APPPS1xII12b⁻ᐟ⁻* mice compared to control *APPPS1xII12b⁺ᐟ⁺* mice, assessed using the Meso Scale V-PLEX Plus Proinflammatory Panel 1 (mouse) Kit. n = 5 mice per group, for statistical analysis the student's t-test was used.

4.5   Genetic deficiency of the IL-12 and IL-23 receptor in *APPPS1* mice

Genetic deficiency of either of the IL-12 or IL-23-related subunits in the AD mouse model *APPPS1* has been shown to have a drastic effect on Aβ plaque pathology[121]. IL-12 signals through its receptor composed of IL12Rβ1 and IL12Rβ2[142]. IL-23 also binds to IL12Rβ1 and another subunit called IL-23R[107]. Since both cytokines share a common receptor subunit which is essential for binding to the receptor, genetic deletion of IL12Rβ1 results in defective downstream signaling of both IL-12 and IL-23[143]. To analyze whether the deletion of the common IL-12 and IL-23 receptor subunit influences plaque burden, which would indicate that downstream receptor-mediated signaling facilitated by p40-binding target cells is responsible for the Aβ-modulating effect, *APPPS1* mice were crossed to mice that lack IL12Rβ1.

4.5.1   Aβ plaque burden in *APPPS1* mice deficient in the IL-12 and IL-23 receptor

To investigate whether genetic ablation of the common receptor subunit of IL-12 and IL-23, *Il12rb1*, influences Aβ plaque burden similar to mice lacking p40, cortical brain sections of mice were analyzed at 120 days of age, a time point when *APPPS1* mice show robust Aβ plaque burden[36]. Cortical plaque load was assessed by immunohistochemical staining with the amyloid-β reactive antibody 4G8 and subsequent stereological quantification of cortical area which is covered by Aβ, using the Stereoinvestigator system. Deletion of IL12Rβ1 receptor subunit in *APPPS1* mice resulted in a significantly reduced Aβ plaque burden, compared to control mice with functional receptor signaling (Figure 18 a, b). In addition, the number of microglia in the cortex of *APPPS1* mice, as determined by staining with the Iba-1 antibody and stereological quantification, was also significantly reduced in the absence of IL12Rβ1 (Figure 18 c, d).

Taken together, these results demonstrate that, consistent with the finding of reduced Aβ plaque deposition upon IL-12 and IL-23 deficiency[121] (chapter 1.4), the constitutive absence of the receptor subunit IL12Rβ1, which is required for the conduction of IL-12 and IL-23-mediated signals, likewise leads to a drastic reduction in Aβ plaque pathology and reduced microglia response. This finding indicates that IL-12 and IL-23 exert their effect on Aβ plaque pathology through binding to their respective receptors.
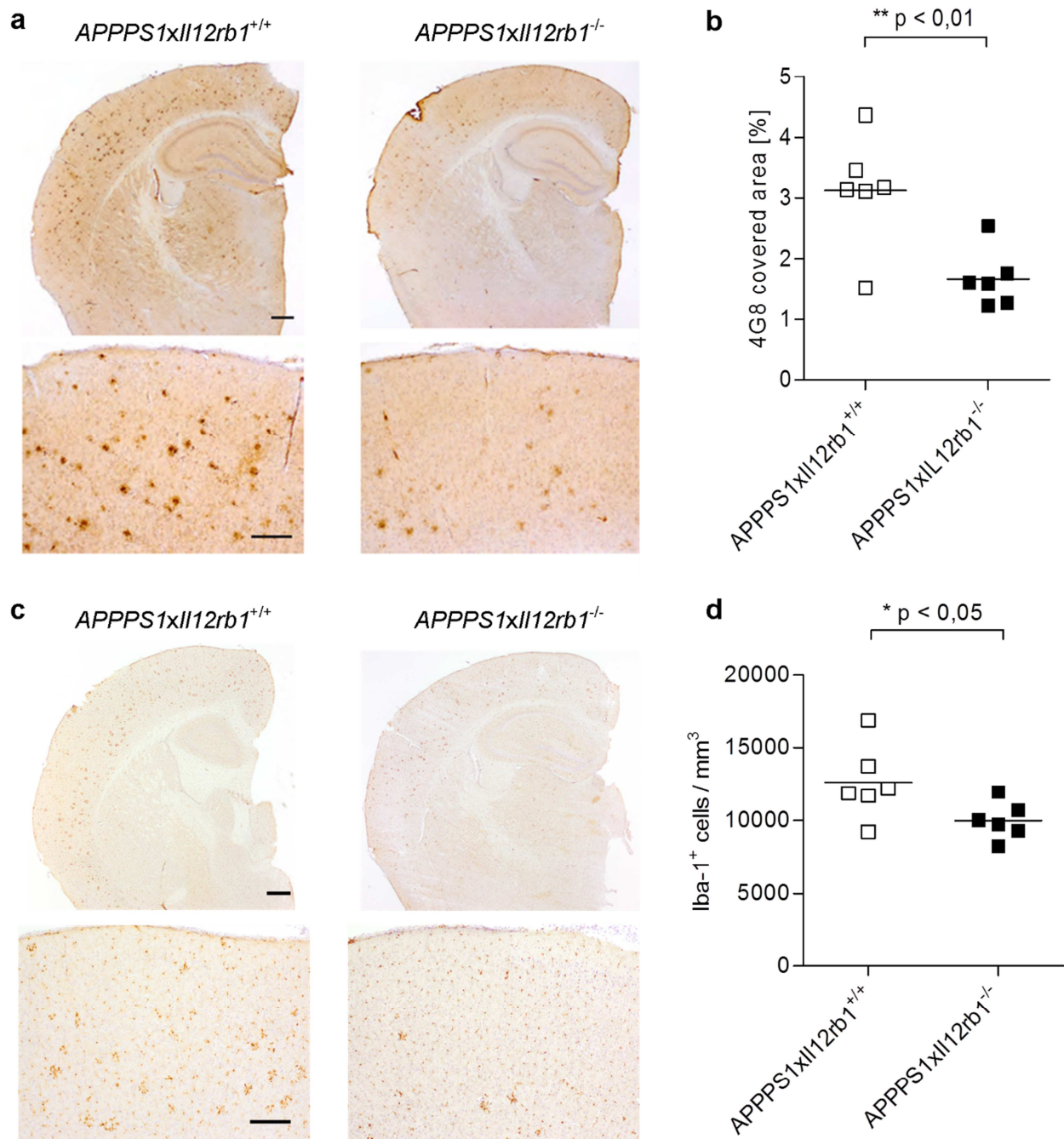
Figure 18: Histological analysis of cerebral Aβ plaque burden and microglia number in *APPPS1* mice deficient in *Il12rb1*.

Aβ burden was assessed by immunohistochemical staining using the 4G8 antibody (a, b), microglia number was determined by immunohistochemical staining using the Iba-1 antibody (c, d). (a) Representative images of 4G8 staining in *APPPS1* mice which lack IL12Rβ1 compared to *APPPS1* mice with functional IL12Rβ1 at low magnification (upper row, scale bar 500 μm) and higher magnification (lower row, scale bar 200 μm). (b) Stereological quantification of the area covered by 4G8 as assessed using the Stereo Investigator system. (c) Representative images of Iba-1 staining in *APPPS1* mice deficient in IL12Rβ1 and with functional IL12Rβ1 at low magnification (upper row, scale bar 500 μm) and higher magnification (lower row, scale bar 200 μm), n =6. For statistical analysis student's t-test was used.

4.5.2 Cytokine levels in brains of *APPPS1* mice deficient in the IL-12 and IL-23 receptor

Since genetic deficiency of *IL12rb1* in *APPPS1* mice lead to a reduction in Aβ plaque burden and microglia activation similar to mice deficient in p40, we further aimed to determine whether protein levels of different pro- and anti-inflammatory molecules in the brain were changed in the absence of IL12Rβ1. Upon p40 deficiency, however, we did not observe differences in cytokine levels (chapter 4.4.2). To address whether cytokine levels were increased in *APPPS1* mice in general, wt control animals were included in the analysis. Whole brain lysates from wt, *APPPS1* with functional IL12Rβ1 and *APPPS1* deficient in IL12Rβ1 were analyzed using the MSD V-PLEX Plus Proinflammatory Panel 1. The analysis was carried out at 120 days of age, which is the time-point where we observed a reduction in Aβ plaque burden (chapter 4.5.1). While cytokine levels appeared to be generally increased in *APPPS1* brains compared to wt, demonstrating an elevated inflammatory milieu in AD-prone brains, protein levels of IL-1β, TNFα, IL-6, IL-10, CXCL1, IL-2, IL-4 and IL-5 were not found to be significantly different between *APPPS1xIl12rb1*^{+/+} and *APPPS1xIl12rb1*^{-/-} mice (Figure 19). Similar to the previous analysis using whole brain homogenates of 250 day old *APPPS1* mice with functional or deficient p40 signaling (chapter 4.4.2), IFNγ as one of the major downstream targets of IL-12 was not detectable in whole brain lysates of 120 day old *APPPS1xIl12rb1*^{+/+} and *APPPS1xIl12rb1*^{-/-} mice. Taken together, this demonstrates that levels of the analyzed cytokines/chemokines in whole brain lysates were not affected by the absence of IL12Rβ1 in AD-prone mice.
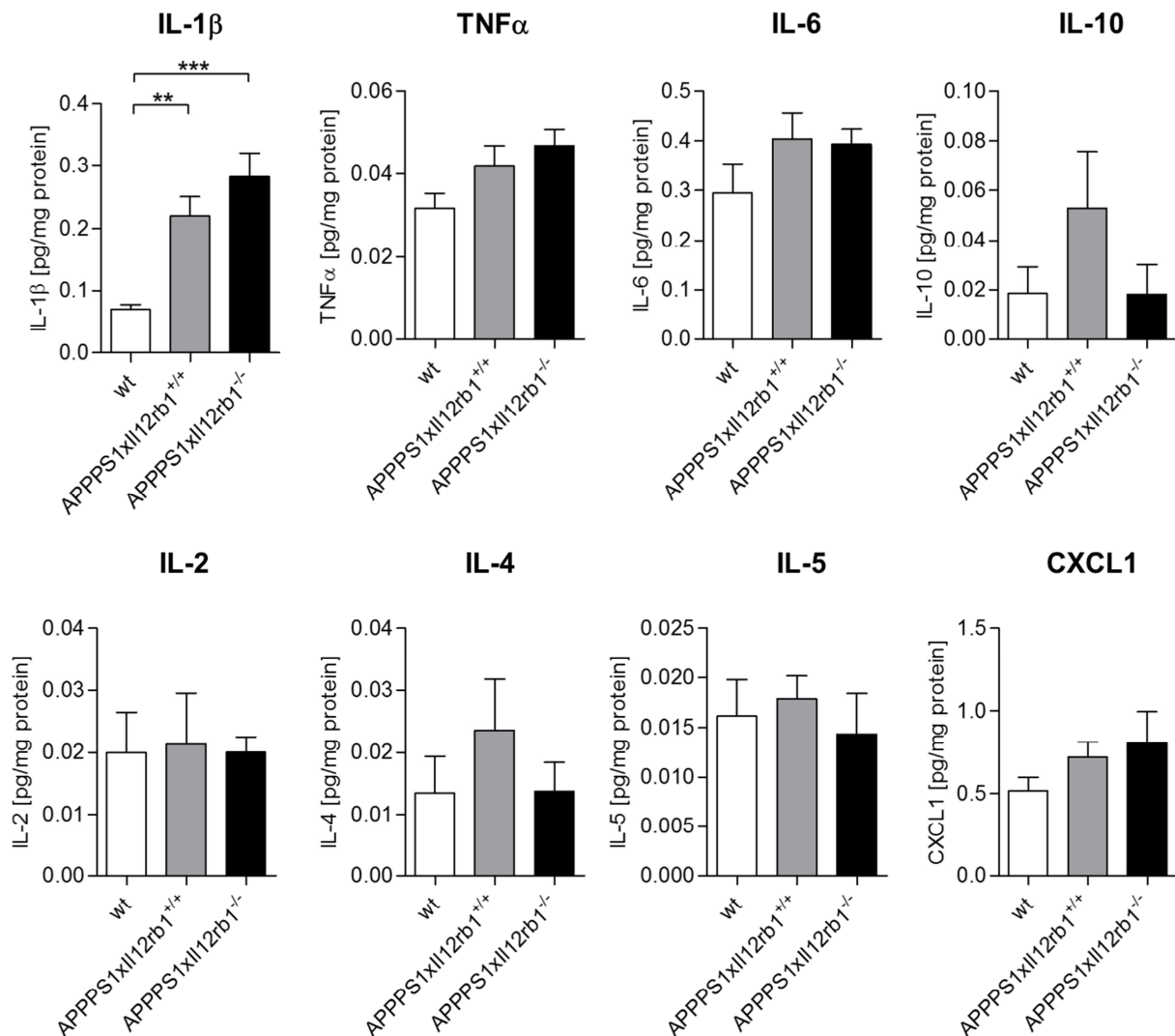
Figure 19: Cytokine levels in whole brain lysates of *APPPS1* mice deficient in *Il12rb1*.
Levels of different pro-and anti-inflammatory markers in brain lysates of 120 day old *APPPS1xIl12rb1*^{+/+}
and *APPPS1xIl12rb1*^{-/-} mice compared to wt control mice, assessed using the Meso Scale V-PLEX Plus
Proinflammatory Panel 1 (mouse) Kit. n = 4 - 5 mice per group, for statistical analysis one-way ANOVA
with Bonferroni post test was used.

4.6   Histological analysis of STAT4 in the brain

The finding that IL-12 / IL-23 receptor-mediated signaling facilitated by p40-binding cells
is responsible for the impact on Aβ deposition, emphasizes the necessity to identify the
brain-intrinsic target cells of p40 signaling. STAT4 has been shown to be mediating
intracellular downstream effects of both IL-12 and IL-23[106,107], and thus, identification of
the cell-specific expression pattern of STAT4 allows a conclusion on potential target
cells of p40 signaling. Since the abundance of STAT4 in the brain until now has not

been addressed to our knowledge, we sought to detect STAT4 by immunohistochemistry in brains of wt and *APPPS1* mice.

4.6.1 Localization of STAT4 in wt and *APPPS1* brains

To identify the cellular localization of STAT4 in the brain, immunohistochemical analysis in wt and *APPPS1* brain slices was conducted. In wt brains, STAT4 immunopositivity can be detected exclusively in the region of the lateral ventricle, but not in the cortex, while in brains of *APPPS1* mice STAT4 is also present in cortical cells (Figure 20). This indicates that cortical brain cells express STAT4 in the presence, but not in the absence of Aβ pathology.
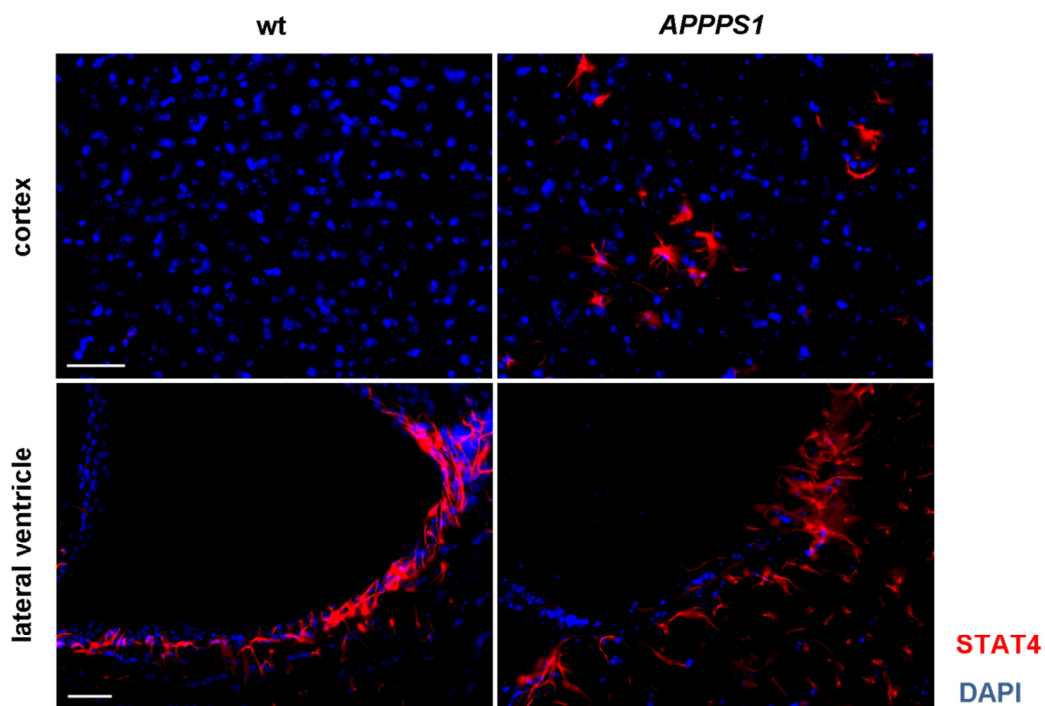

Figure 20: Immunofluorescent staining of STAT4 in wt and *APPPS1* brains.
STAT4 immunopositivity in the cortex (upper panel) and lateral ventricle (lower panel) of wt (left panel) and *APPPS1* mice (right panel). Scale bar 50 μm.

4.6.2 Co-localization of STAT4 with cell-specific markers in wt and *APPPS1* brains

To determine which cells express STAT4 in the brain, a co-localization study with microglial marker CD68 and astrocyte marker GFAP was conducted in brains of wt and

APPPS1 mice. In wt brains STAT4 immunopositivity was only detected in the region of the lateral ventricle, where it co-localized with GFAP, but not with CD68 (Figure 21 a). In the brain of *APPPS1* mice, STAT4 was also detectable in the cortex and showed co-localization with GFAP and not with CD68 (Figure 21 b).
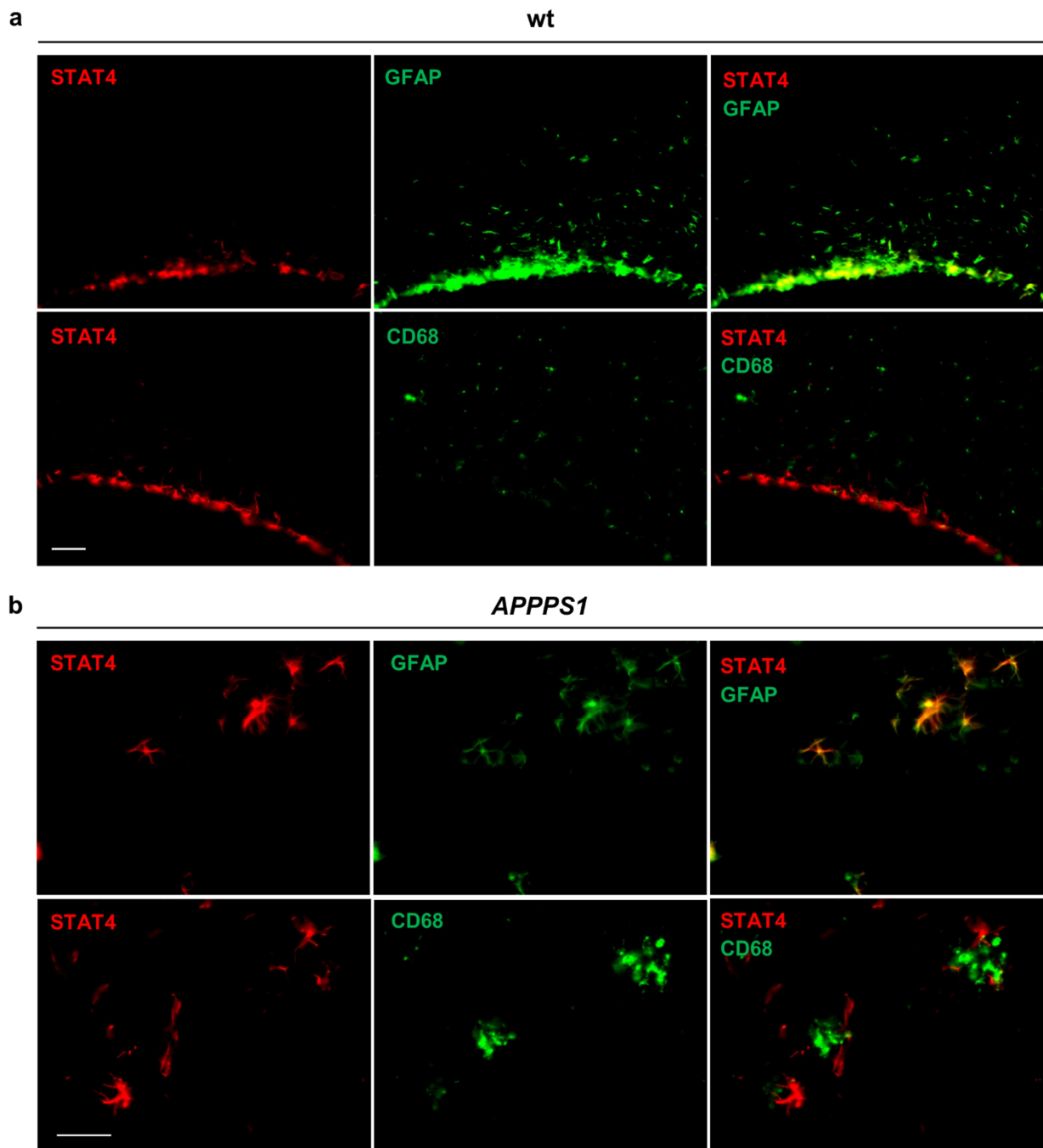

Figure 21: Co-localization of STAT4 with cell-specific markers in the brain of wt and *APPPS1* mice. Immunofluorescent double staining of STAT4 with astrocyte-specific GFAP and microglia-specific CD68 in brain slices of (a) wt and (b) *APPPS1* mice. Scale bar 50 μm.

This demonstrates that STAT4 is expressed in GFAP-positive cells around the lateral ventricle in wt brains and, additionally, in GFAP-positive astrocytes in the cortex of *APPPS1* mice, which indicates that astrocytes in mice with AD-like pathology might be the direct target cells of p40 signaling and could facilitate downstream effector function of IL-12 and IL-23. Since STAT4 immunopositivity appeared in a regional pattern in the cortex of *APPPS1* mice, we further investigated the distribution of STAT4-positive cells in relation to Aβ plaques. Therefore, a double staining of STAT4 and Aβ-specific antibody 4G8 was conducted in brain sections of *APPPS1* mice. Immunofluorescent images revealed the location of STAT4-positive cells in close proximity to Aβ plaques (Figure 22), indicating that GFAP-positive astrocytes specifically around Aβ plaques express STAT4 in the cortex of *APPPS1* mice.
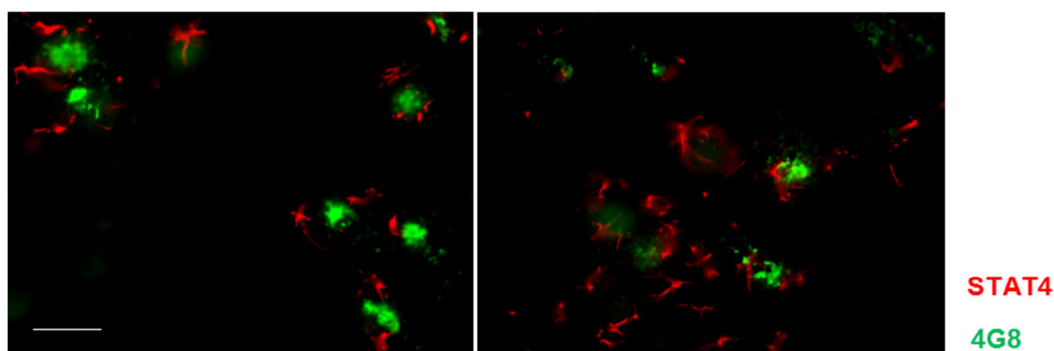

Figure 22: Immunofluorescent staining of STAT4 and Aβ plaques in the cortex of *APPPS1* mice. Immunofluorescent double staining of STAT4 and Aβ-specific 4G8 antibody in the cortex of *APPPS1* mice. Scale bar 50 µm.

Taken together, immunofluorescent analysis showed that STAT4 as the common downstream mediator of both IL-12 and IL-23 is up-regulated by astrocytes in close proximity to Aβ plaques in the cortex of *APPPS1* mice. The fact that STAT4 as a prominent member of the IL-12 and IL-23 induced signaling pathway is specifically expressed upon Aβ pathology emphasizes the relevance of this pathway in AD-prone mice and suggests that astrocytes might be possible downstream effector cells of IL-12 and IL-23 signaling.

4.7   Expression of IL-12-related subunits upon stimulation *in vitro*

Previous studies in the laboratory of Prof. Heppner have demonstrated that microglia up-regulate the p40 subunit in the brain and GFAP-positive non-microglia cells, possibly astrocytes, up-regulate the *Il12rb1* receptor subunit in the context of AD[121]. Moreover, as shown in the previous chapter, STAT4 as a central downstream mediator is expressed by GFAP-positive astrocytes in the AD-prone brain, indicating that astrocytes appear to be the principal effector cells downstream of p40. To further confirm this, we sought to analyze the ability of primary microglia and astrocytes to express IL-12 and IL-12 receptor subunits upon stimulation *in vitro*.

4.7.1   Preparation of primary microglia and astrocyte cultures

Primary mixed glial cultures were prepared from neonatal mouse brains. When the cultures were confluent, microglia were isolated by shaking them off from the astrocyte monolayer. Several reports emphasized the effect of residual microglia in astrocyte cultures, which even when present only at minor amounts in the culture can be responsible for effects that are falsely attributed to astrocytes[144,127]. In order to avoid this effect, astrocyte cultures were subjected to magnetic cell sorting using CD11b MicroBeads, to deplete residual microglia from the astrocyte population. Flow cytometric analysis before and after purification using the MACS technique showed effective removal of CD11b$^+$/CD45$^+$ microglia from the astrocyte cultures (Figure 23 c, d). Immunohistochemical stainings with markers specific for microglia (Iba-1) and astrocytes (GFAP, Excitatory Amino Acid Transporter 1 (EAAT1)) demonstrated the purity and viability of the cultures after the MACS procedure (Figure 23 a, b). While not all astrocytes were immunopositive for GFAP, they were all labeled by EAAT1.
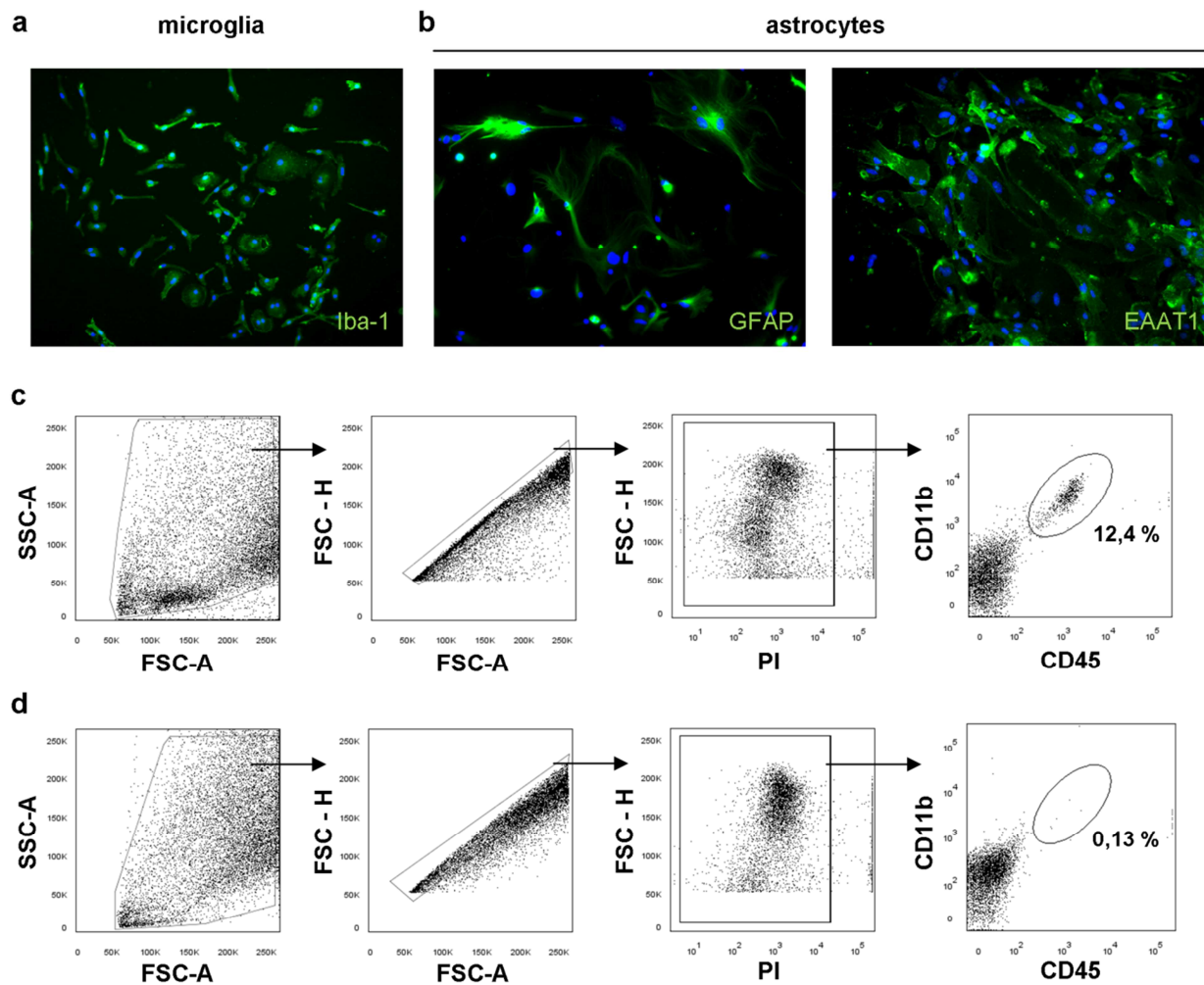
Figure 23: Primary cell culture of neonatal microglia and astrocytes.
Representative pictures of (a) primary microglia, showing Iba-1 immunoreactivity, and (b) primary astrocytes, immunopositive for GFAP and EAAT1, isolated from mixed glia culture. (c, d) Abundance of microglia in astrocyte cultures before and after purification using magnetic cell sorting. FACS analysis of astrocyte culture (c) before MACS sorting showing 12,4% of CD11b$^+$/CD45$^+$ microglia and (d) after MACS sorting, showing 0,13% of CD11b$^+$/CD45$^+$ cells.

4.7.2 Cytokine secretion by primary microglia and astrocytes upon stimulation

Next, pro-inflammatory cytokine secretion by primary microglia and astrocyte cultures was measured upon stimulation. Microglia and astrocyte cultures from either *Il12b$^{-/-}$* neonatal brains or control littermates (*Il12b$^{+/+}$*) were stimulated with LPS or LPS and IFNγ for 24 hours, equal amounts of the vehicle PBS in medium served as control. The protein levels of the pro-inflammatory cytokine TNFα as well as p40 were measured in the supernatant by ELISA. Unstimulated primary microglia secrete rarely any TNFα or IL-12p40. Stimulation with LPS or the combination of LPS and IFNγ similarly induced

TNFα production by wt and *Il12b*^{-/-} microglia. In contrast, astrocyte cultures did not show an induction of TNFα upon stimulation (Figure 24 a). This is in line with previous reports which demonstrated that clearing astrocyte cultures from residual microglia using the MACS technique effectively prevented secretion of TNFα by astrocyte cultures after LPS and IFNγ stimulation[127]. This shows that primary astrocytes alone do not secrete TNFα upon LPS stimulation, but that this effect is attributed to residual microglia in astrocyte cultures.
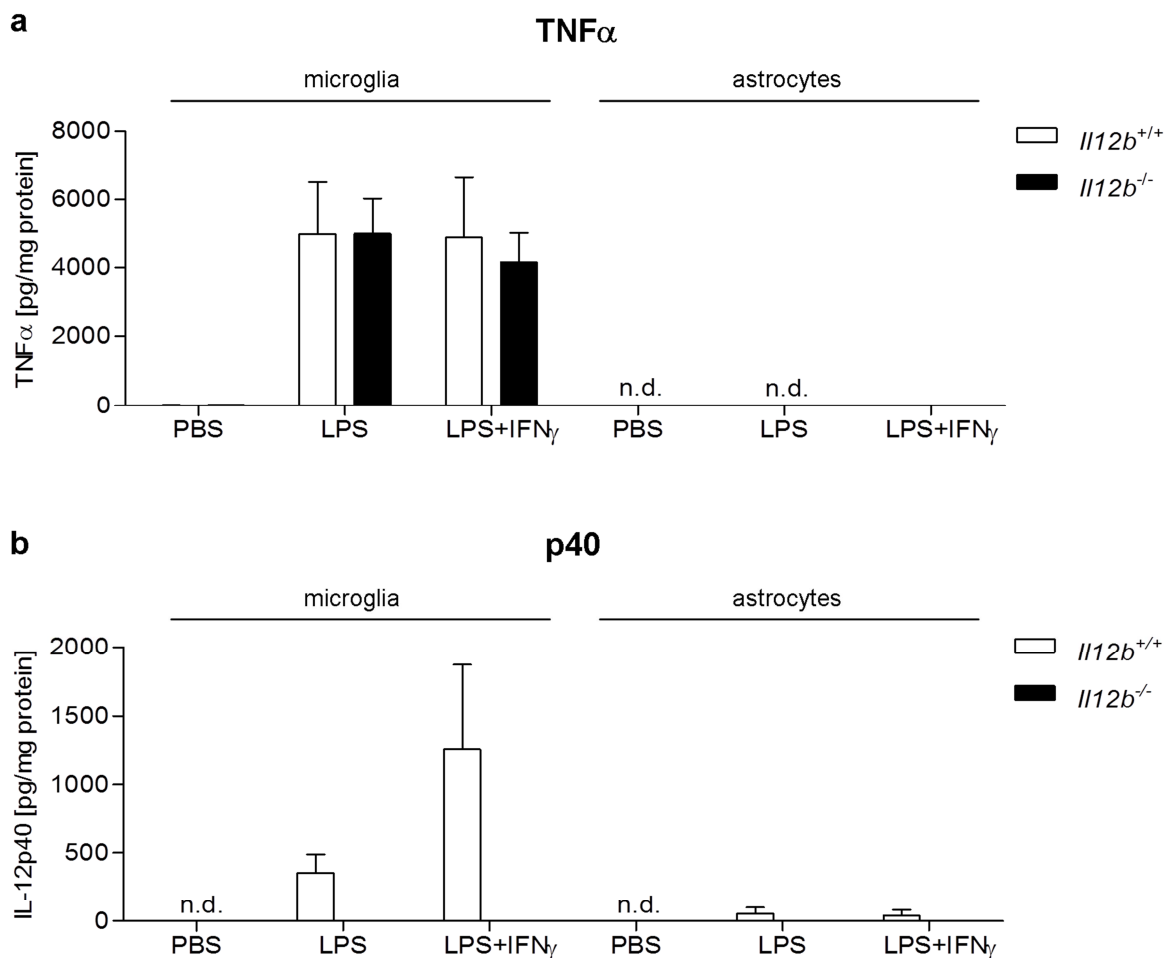

Figure 24: Induction of pro-inflammatory cytokines in primary microglia and astrocytes after stimulation.
Microglia and astrocytes from wt (*Il12b*^{+/+}) and *Il12b*^{-/-} neonatal brains were stimulated with LPS (1 µg/ml) or LPS and IFNγ (100 U/ml) for 24 hours. PBS in medium served as control. Cell culture supernatants were collected and analyzed for protein levels of (a) TNFα and (b) IL-12p40. Amounts of detected protein were normalized to total protein content. n = 4 (microglia), n = 3 (astrocytes)

IL-12p40 secretion could be observed by wt microglia after stimulation, while *Il12b*^{-/-} microglia, used as a negative control, did not show detectable levels of p40 in the medium. Production of IL-12p40 was increased about 3-fold after stimulation with LPS

and IFNγ, compared to LPS alone. This observation is consistent with previous reports that show that LPS alone has a mild effect on p40 secretion, while the combination of LPS and IFNγ highly induces p40 production in microglia and peripheral macrophages[102,101]. In addition, in wt astrocyte cultures p40 secretion was only detectable at very low levels after stimulation (Figure 24 b). These results show that the combination of LPS and IFNγ is a potent inducer of IL-12p40 secretion in primary microglia, but not in primary astrocytes.

4.7.3 Time-course dependent gene expression of IL-12-related subunits upon stimulation

Microglia were shown to up-regulate *Il12b* in AD-prone mice *in vivo*[121], (chapter 1.4) and were able to express *Il12b* and secrete p40 protein after stimulation *in vitro* (chapter 4.7.2). We assume that astrocytes are the direct target and downstream effector cells of microglia-released p40, since *gfap*-positive brain cells up-regulate *Il12rb1* in *APPPS1* mice[121] and express STAT4 as a known common downstream mediator of IL-12 and IL-23 (chapter 4.6.2). To further confirm this, we investigated the ability of microglia and astrocytes to express the different subunits of IL-12 and IL-12 receptor after pro-inflammatory stimulation *in vitro*. Therefore, primary microglia and astrocytes were stimulated with LPS and IFNγ for 6, 12 and 24 hours and gene expression analysis was conducted by quantitative PCR. Gene expression of *Il12b*, coding for p40, the common subunit of IL-12 and IL-23, was highly up-regulated upon stimulation with LPS and IFNγ in microglia after 6 hours, which decreased after 24 hours of stimulation (Figure 25 a). In contrast, astrocytes show a much lower induction of *Il12b* after stimulation compared to microglia. In accordance with the gene expression data, p40 protein levels increased over time in the supernatant of stimulated microglia, and were rarely detectable in supernatant of astrocyte cultures (Figure 25 e). *Il12a*, the IL-12-specific subunit, is up-regulated exclusively by microglia after stimulation, but not by astrocytes. The common receptor subunit of IL-12 and IL-23, *Il12rb1*, is up-regulated by both microglia and astrocytes after stimulation. However, astrocytes up-regulate *Il12rb1* to a higher degree than microglia. *Il12rb2*, the IL-12-specific receptor subunit is exclusively up-regulated by astrocytes after LPS and IFNγ stimulation, but not by microglia (Figure 25 a – d). These data demonstrate that microglia react towards pro-inflammatory stimuli by mainly expressing the IL-12 subunits, while astrocytes mainly up-regulate the IL-12 receptor

subunits *in vitro*, which supports the hypothesis that microglia are the source of IL-12 and astrocytes the potential p40-binding target cells.
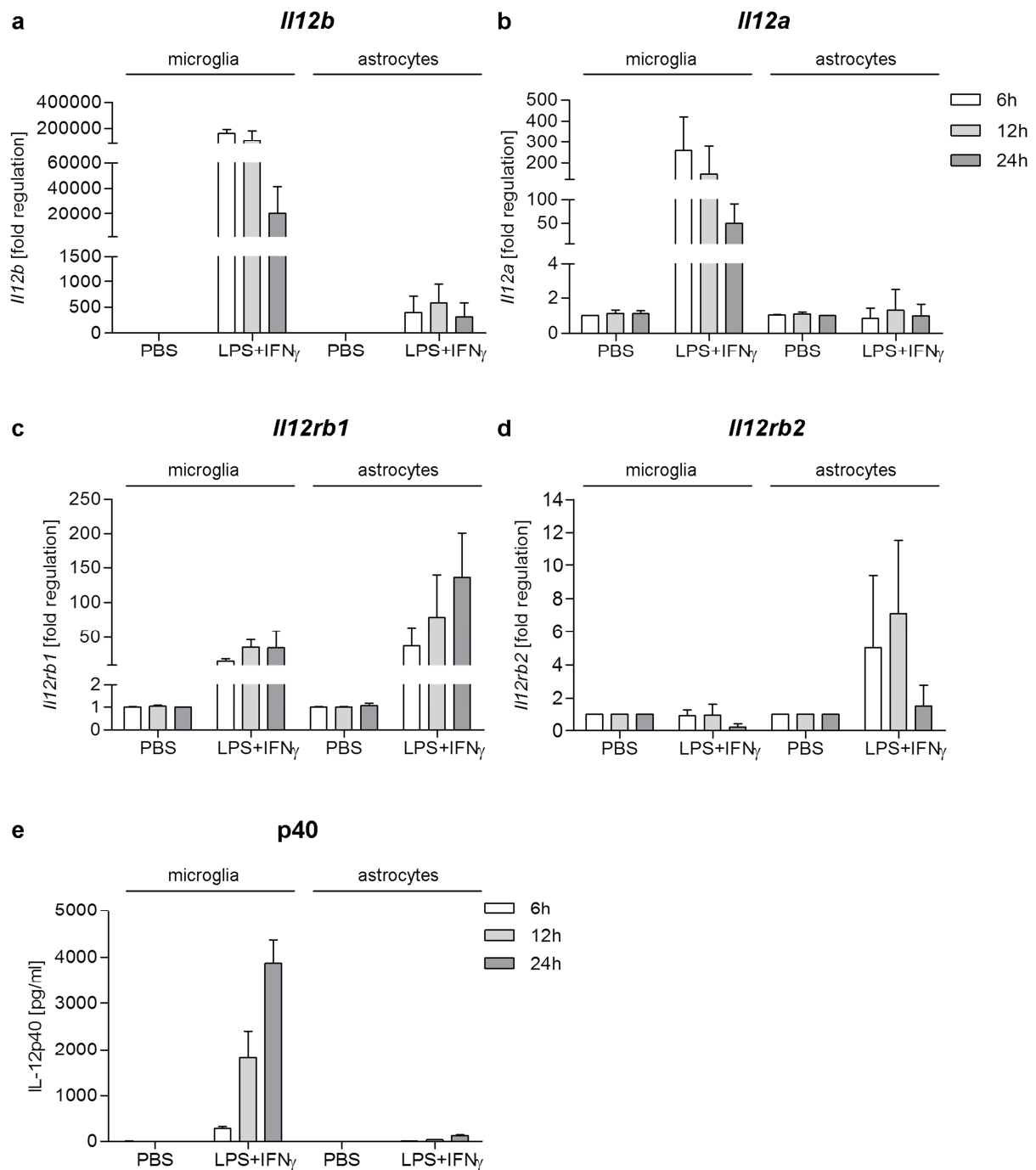

Figure 25: Induction of IL-12 and IL-12 receptor subunits in primary microglia and astrocytes after stimulation.
Microglia and astrocytes from wt neonatal brains were stimulated with LPS (1 µg/ml) and IFNγ (100 U/ml) for 6, 12 and 24 hours. PBS in medium served as control. Gene expression changes of (a) *Il12b*, (b) *Il12a*, (c) *Il12rb1* and (d) *Il12rb2* were analyzed by qPCR. (d) Cell culture supernatants were analyzed for IL-12p40 production. n = 3 independent experiments.

4.8 Intracerebroventricular application of anti-p40 antibody to aged *APPPS1* mice

Previous data in the laboratory of Prof. Heppner showed that pharmacological blockade of the IL-12 / IL-23 pathway by application of a p40 neutralizing antibody (anti-p40) significantly decreased Aβ plaque load in *APPPS1* mice, when treatment was started before onset of plaque deposition[121]. To find out whether anti-p40 antibody treatment also has a behavioral effect on an already established disease phenotype, aged *APPPS1* mice were treated with the p40 neutralizing antibody and cognitive performance was assessed in different behavioral tests. *APPPS1* mice only develop a mild behavioral phenotype, which is detectable at 8 months of age[36] and is restricted to a few behavioral tests. In consideration of this and previous results which show that brain intrinsic and not peripheral p40 levels modulate amyloidosis[121], anti-p40 antibodies or isotype control antibodies were directly and constitutively applied into the lateral ventricle of the brain using a mini-osmotic pump, starting at 190 days of age. Behavioral performance was assessed in different cognitive tests. To investigate whether anti-p40 treatment of aged *APPPS1* mice affects Aβ plaque pathology, brains were subjected to histological and biochemical analysis of Aβ burden.

4.8.1 Behavioral analysis of anti-p40 treated aged animals

To determine whether anti-p40 treatment has an effect on the behavioral phenotype of aged mice, the behavioral performance of wt and *APPPS1* mice, treated for 6 weeks with either anti-p40 or isotype control antibody, was assessed by the Open field test, the Novel object recognition test and the Barnes maze test. To determine whether mice show any abnormalities in general locomotor function due to the treatment or the carrying of mini-osmotic pumps, locomotor activity and the distance mice travelled were measured in the Open field arena. No major differences in the percentage of locomotor activity (Figure 26 a) or the distance travelled (Figure 26 b) were observed between the groups, indicating that the animals showed normal locomotor function after the icv treatment.
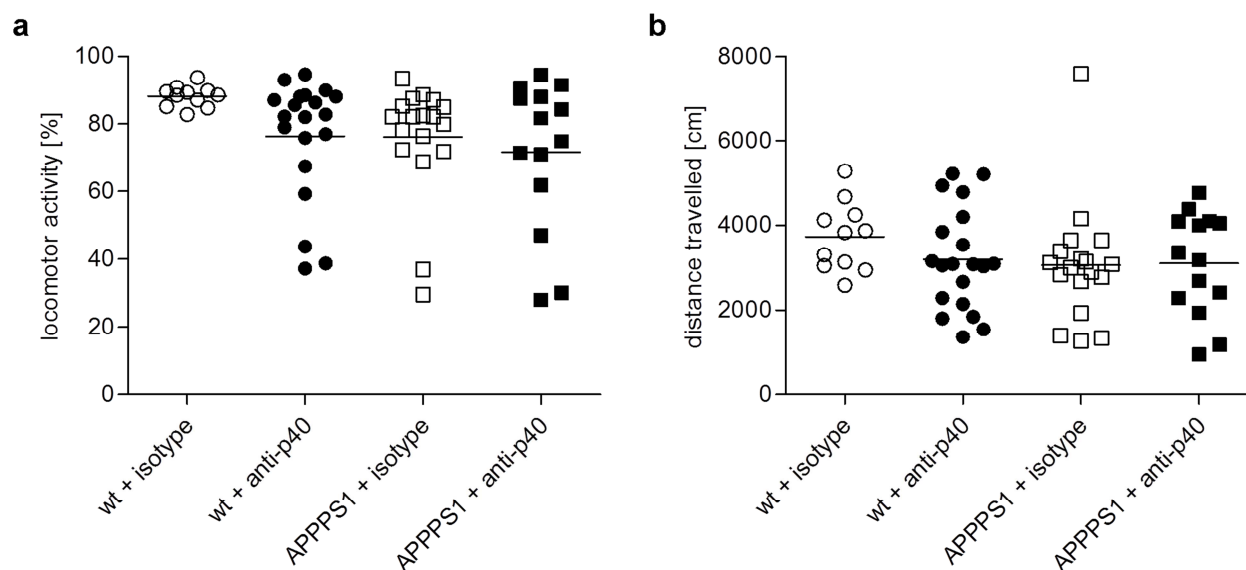
Figure 26: Open field test of aged mice after icv antibody treatment.
Aged wt and *APPPS1* mice underwent behavioral test 6 weeks after start of icv antibody delivery. To assess general locomotor function after icv treatment, (a) locomotor activity and (b) distance travelled in the Open field was analyzed. n = 11 – 20. For statistical analysis one-way ANOVA with Dunnett's post hoc test was used. Adapted from Vom Berg et.al. *Nature Medicine*, 2012[121].

It was reported that *APPPS1* mice show impairments in spatial learning at the age of 8 months[36]. To determine whether anti-p40 antibody treatment influences cognitive function in aged mice, behavioral tests to analyze spatial learning and object recognition were conducted. To assess spatial learning and memory in the antibody-treated *APPPS1* and wt mice, the latency to reach the target in a Barnes maze paradigm was analyzed. In the short-term retention memory trial *APPPS1* mice treated with isotype control antibody showed a significant deficit in spatial memory, compared to wt control mice (Figure 27 a, b). This deficit in spatial learning was substantially improved in *APPPS1* mice which received anti-p40 antibody. In the Novel object recognition task, isotype control-treated *APPPS1* mice show an obvious impairment compared to wt mice, as measured by reduced exploration and visits of the new object (Figure 27 c, d), which was reversed to wt levels after treatment with anti-p40. These results demonstrate that cognitive deficits which exist in 8 month old *APPPS1* mice are ameliorated by icv delivery of anti-p40 antibodies.
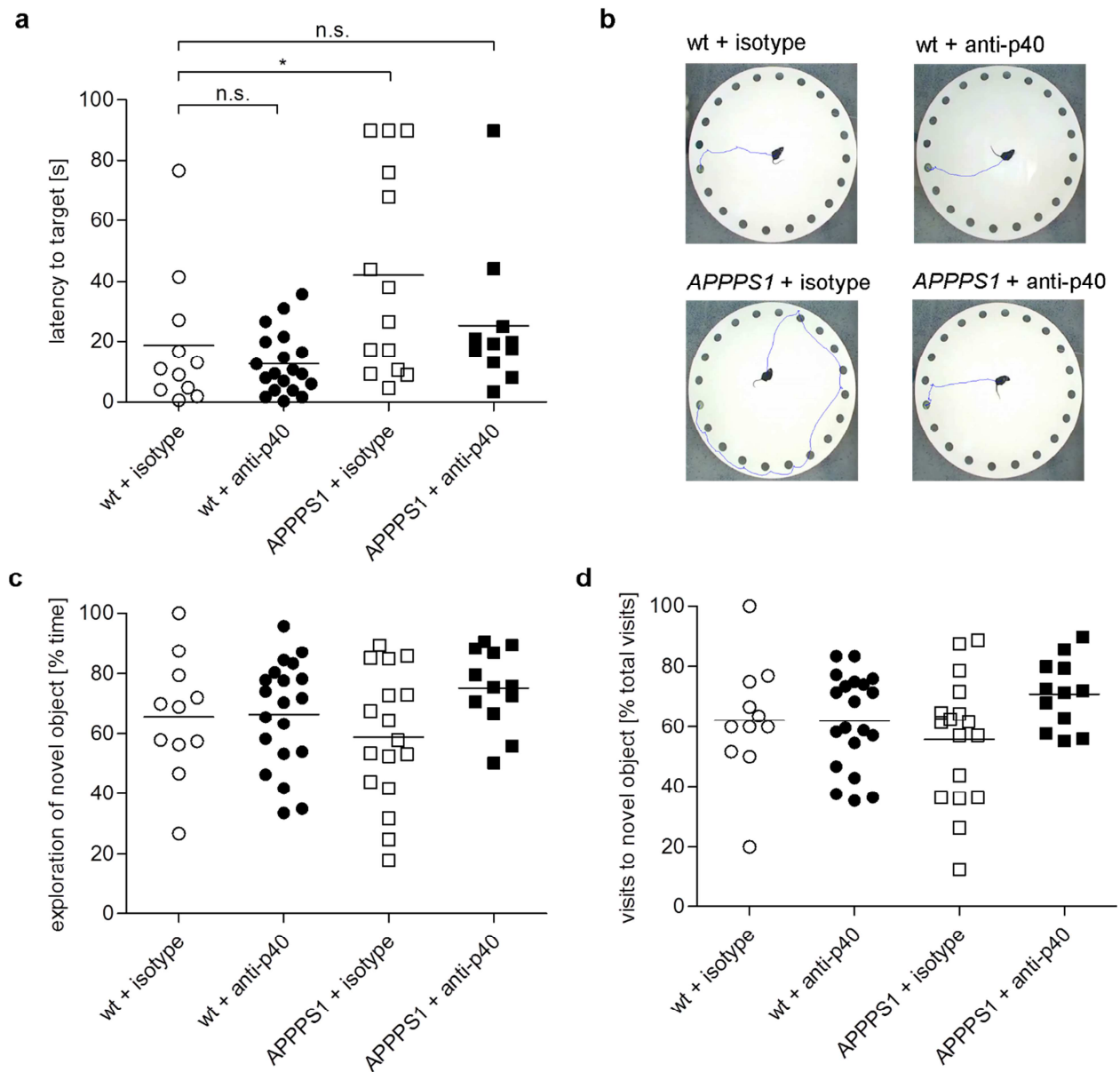
Figure 27: Barnes maze and Novel object recognition test of aged mice after icv antibody treatment.
Aged wt and *APPPS1* mice underwent behavioral tests 6 weeks after start of icv antibody delivery. (a) Quantification of latency to reach target in the short term retention trial and (b) representative pathway tracking pictures in the Barnes maze test. (c) Percentage of time spent exploring the novel object and (d) percentage of visits to new object in the Novel object recognition test. n = 11 – 20. For statistical analysis one-way ANOVA with Dunnett's post hoc test was used. Adapted from Vom Berg et.al. *Nature Medicine*, 2012[121].

4.8.2 Histological analysis of Aβ plaque burden after anti-p40 antibody treatment

To determine whether long-term icv application of anti-p40 to aged *APPPS1* mice modulated Aβ plaque deposition, brains of experimental mice were sampled for histological analysis of Aβ plaque burden. Therefore, cerebral sections of anti-p40 and isotype control antibody-treated *APPPS1* mice were stained with the conventional amyloid dye Congo red and immunohistochemically using the Aβ-specific antibody 4G8. While Congo red labels the compact core of Aβ plaques, the so-called "congophilic" plaques consisting of dense aggregated Aβ fibrils, the immunohistochemical stainings using the antibody 4G8 also label diffuse Aβ deposits besides amyloid containing Aβ plaque cores. Aβ plaque burden was evaluated by stereological quantification of Congo red- or 4G8 covered area using the Stereoinvestigator system. Histological and quantitative analysis of Congo red-covered area in *APPPS1* mice revealed no significant difference in amyloid plaque burden after treatment with anti-p40 or isotype control antibody (Figure 28 a, b). Likewise, Aβ plaque burden as assessed by immunohistochemical staining with 4G8 antibody showed no effect of the treatment on Aβ plaque load (Figure 28 c, d). This demonstrates that long-term delivery of anti-p40 antibodies into the brain of aged *APPPS1* mice, which already had an established disease phenotype at the start of the treatment, does not affect Aβ plaque deposition.
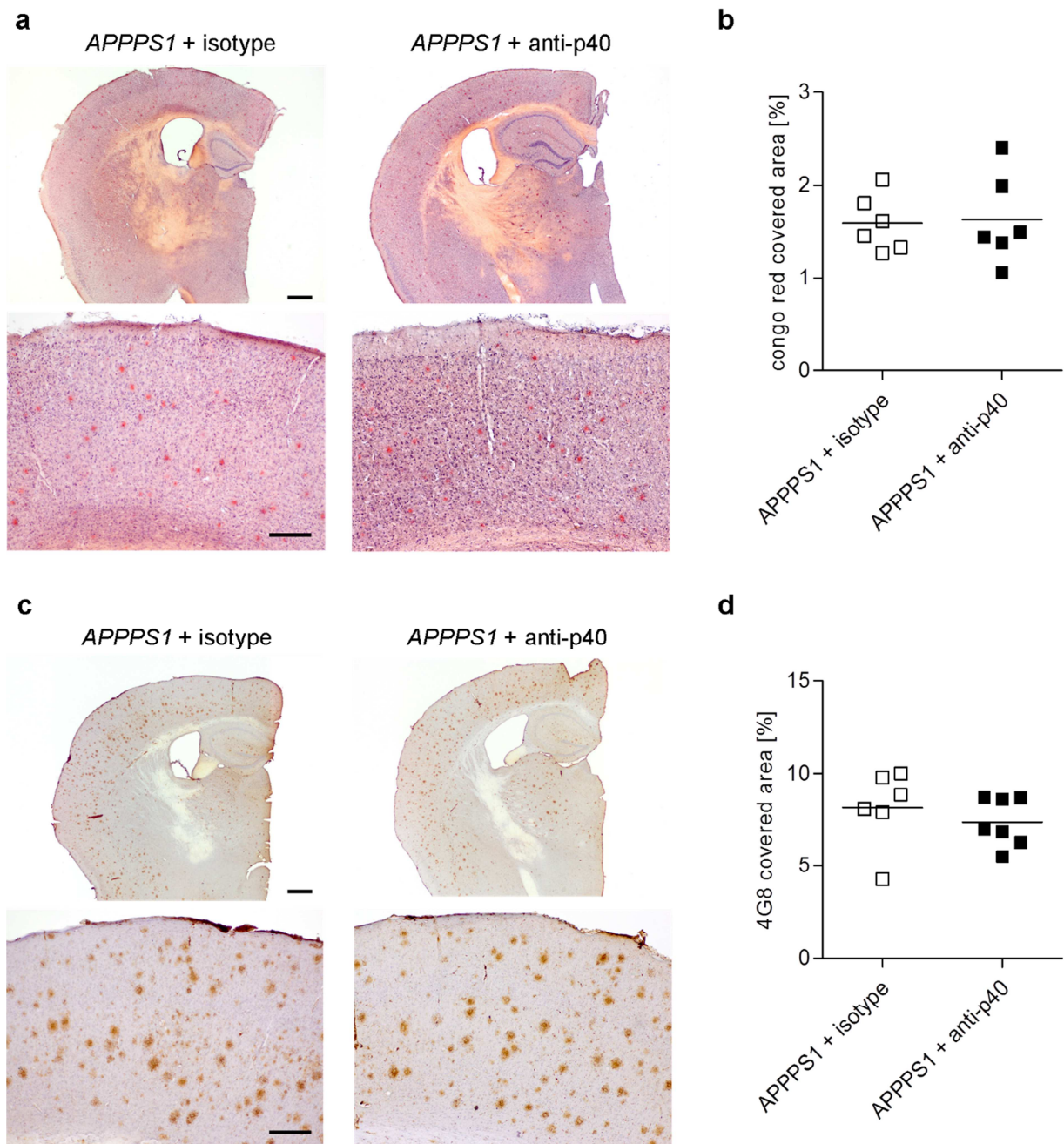
Figure 28: Histological analysis of cerebral Aβ plaque burden in aged *APPPS1* mice after icv antibody treatment.

Aβ burden was assessed by Congo red (a, b) and immunohistochemical staining using the 4G8 antibody (c, d). (a) Representative images of Congo red staining in *APPPS1* mice which received isotype control or anti-p40 antibody at low magnification (upper row, scale bar 500 μm) and higher magnification (lower row, scale bar 200 μm). (b) Stereomorphometric quantification of the area covered by Congo red as assessed using the Stereo Investigator system. (c) Representative images of 4G8 staining in *APPPS1* mice treated with isotype control or anti-p40 antibody at low magnification (upper row, scale bar 500 μm) and higher magnification (lower row, scale bar 200 μm). n = 6 - 7. For statistical analysis student's t-test was used. Adapted from Vom Berg et.al. *Nature Medicine*, 2012[121].

4.8.3 Biochemical analysis of Aβ plaque burden after anti-p40 antibody treatment

Histological analysis of Aβ plaque deposition revealed no differences between anti-p40 and isotype control-treated *APPPS1* mice. In order to analyze whether levels of soluble Aβ in the cortex of *APPPS1* mice were changed upon antibody treatment, frozen brain hemispheres were homogenized in a step-wise fashion in TBS-, TX-, SDS- and FA buffer, which allowed to measure amounts of soluble Aβ and aggregated, insoluble Aβ species separately[124]. Protein extracts from each fraction were subjected to electrochemiluminescence assay using the MSD 6E10 assay. $A\beta_{40}$ and $A\beta_{42}$ levels in the TX-, SDS- and FA-soluble fraction did not differ between *APPPS1* mice treated with anti-p40 and isotype control (Figure 29 b - d), which is consistent with the finding that insoluble or aggregated Aβ burden as determined by the histological analysis is unaltered (see chapter 4.8.2). However, soluble Aβ species in the brain parenchyma extracted in the TBS fraction are significantly reduced in the anti-p40 treatment group compared to the isotype control-treated animals (Figure 29 a). This reduction in soluble Aβ species in the cortex of anti-p40-treated mice may explain the observed effect on cognitive function (chapter 4.8.1), since soluble Aβ species have been proposed to be toxic to neurons and impair synaptic plasticity[23,24,145].

Taken together, blocking p40 by icv antibody delivery in the brain of aged *APPPS1* mice with an established Aβ pathology did not alter Aβ plaque deposition, but reduced soluble Aβ species and ameliorated performance in learning and memory tasks.
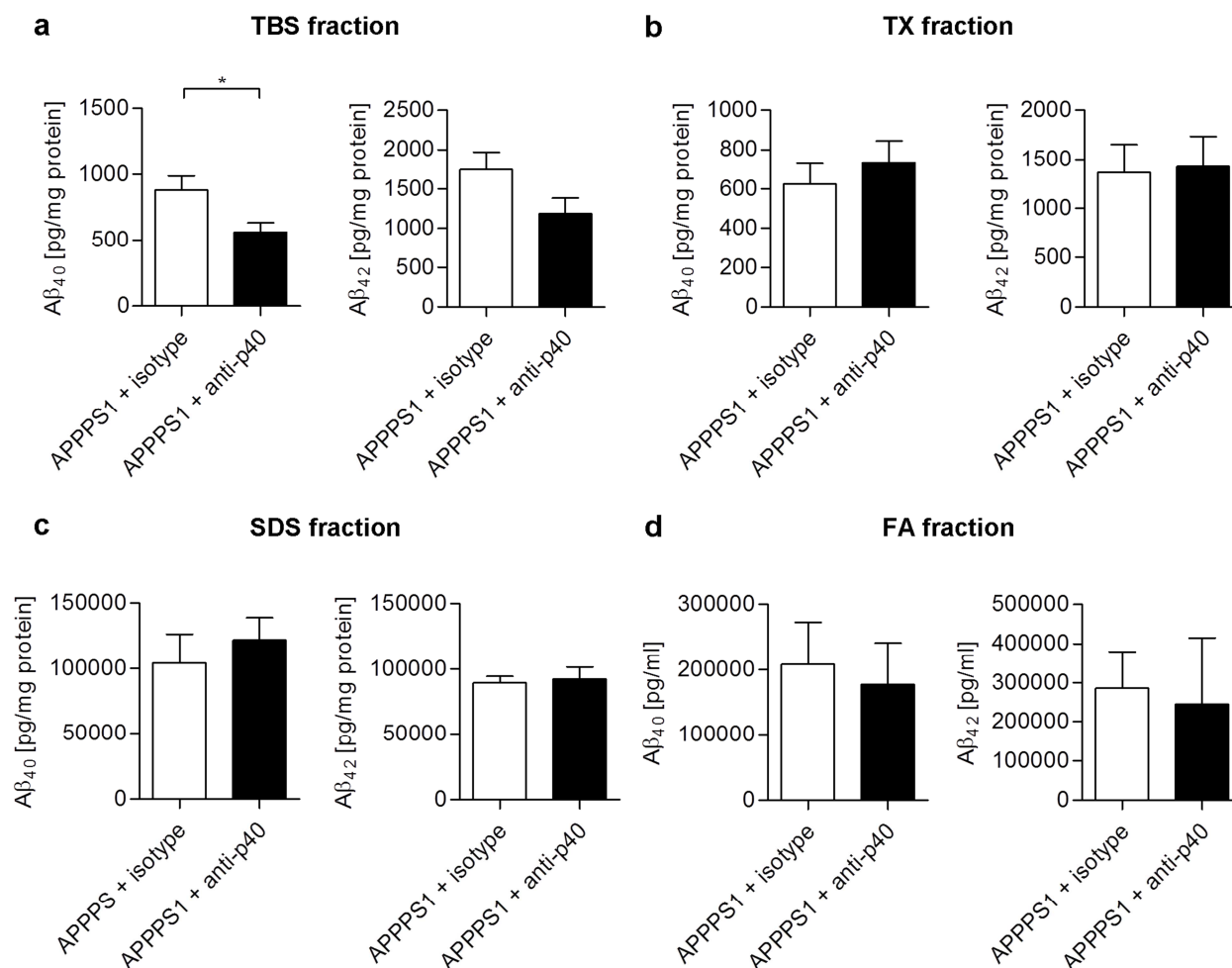
Figure 29: Cerebral Aβ$_{40}$ and Aβ$_{42}$ levels in brain homogenates of aged *APPPS1* mice after icv antibody treatment.
Frozen brain tissue of anti-p40 and isotype control antibody treated *APPPS1* mice was homogenized consecutively in TBS, TX, SDS and FA buffer and supernatants of each fraction was subjected to Meso Scale analysis using the 6E10 Aβ Triplex Assay. Aβ$_{40}$ and Aβ$_{42}$ protein levels were normalized to the amount of total protein in each fraction. n = 11. For statistical analysis student's t-test was used. Adapted from Vom Berg et.al. *Nature Medicine*, 2012[121].

4.9 Intraperitoneal application of anti-p40 antibody to aged *APP23* mice

Treatment with a p40 neutralizing antibody proved to be effective in reducing Aβ pathology when applied intraperitoneally (i.p.) in young *APPPS1* mice over the course of 3 months[121] and intracerebroventricularly to aged *APPPS1* mice for 2 months (chapter 4.8). In addition, icv anti-p40 treatment resulted in an improvement of cognitive deficits present in *APPPS1* mice. In order to evaluate whether the effect of the treatment is mouse line specific or can be reproduced in a different AD mouse strain,

aged *APP23* mice were treated with anti-p40 antibodies and analyzed for behavioral performance and Aβ pathology. *APP23* is an amyloidosis mouse model which is characterized by slower kinetics of Aβ plaque deposition than *APPPS1* mice, with first Aβ plaques appearing at approximately 6 months of age and a robust plaque burden at 12 months of age[37]. Cognitive deficits can be detected at 12 months of age[146] and are constitutively increasing with age[147]. Based on this knowledge and the finding that anti-p40 was effective when applied intraperitoneally[121], treatment of *APP23* mice was started at 12 months of age, with biweekly i.p. injections for 3 months. After 3 months, treatment was terminated and mice were subjected to behavioral analysis by the Open field test, Novel object recognition test and the Morris water maze test. To find out whether anti-p40 treatment of aged *APP23* mice affects Aβ plaque pathology, brains were subjected to histological and biochemical analysis of Aβ burden.

4.9.1 Detection and efficiency of anti-p40 in plasma and brain after i.p. treatment

First, to determine whether anti-p40 antibodies can be detected in the blood and in the brain after i.p treatment, the TBS-extracted protein fraction of the brain and plasma samples of anti-p40-treated *APP23* mice were subjected to Western Blot analysis using a goat-anti-rat secondary antibody to specifically detect the anti-rat raised p40 antibody. Figure 30 a shows representative samples of brain extracts and plasma of anti-p40-treated *APP23* mice, in comparison to 10 ng of p40-antibody used as a reference (light chain = 23 - 25 kDa, heavy chain = 53 kDa). While brain extracts of control animals injected with PBS did not show any signal, high amounts of anti-p40 can be detected in the plasma. In the brain, anti-p40 can be detected, although at a much lower amount than in the plasma (Figure 30 a). Since experimental animals were transcardially perfused before sampling of the brain, contamination of the brain by anti-p40 present in the plasma can be excluded. This demonstrates that low amounts of p40-antibodies were able to cross the blood brain barrier and reached the brain upon i.p. delivery. To further analyze the ability of anti-p40 to neutralize p40 protein after i.p. treatment *in vivo*, p40 levels in the plasma and TBS-extracted brain homogenates of anti-p40 and isotype control treated animals were measured by ELISA. In the plasma, anti-p40 treatment resulted in a reduction of p40 levels of 79,2% in the anti-p40 treatment group, while in the brain a substantial decrease of 59,6% was detected (Figure 30 b, c). This shows that i.p. anti-p40 treatment was efficient in reducing p40 levels *in vivo* and that even

though only small amounts of antibody reached the brain, brain intrinsic p40 levels were substantially decreased upon i.p. application.
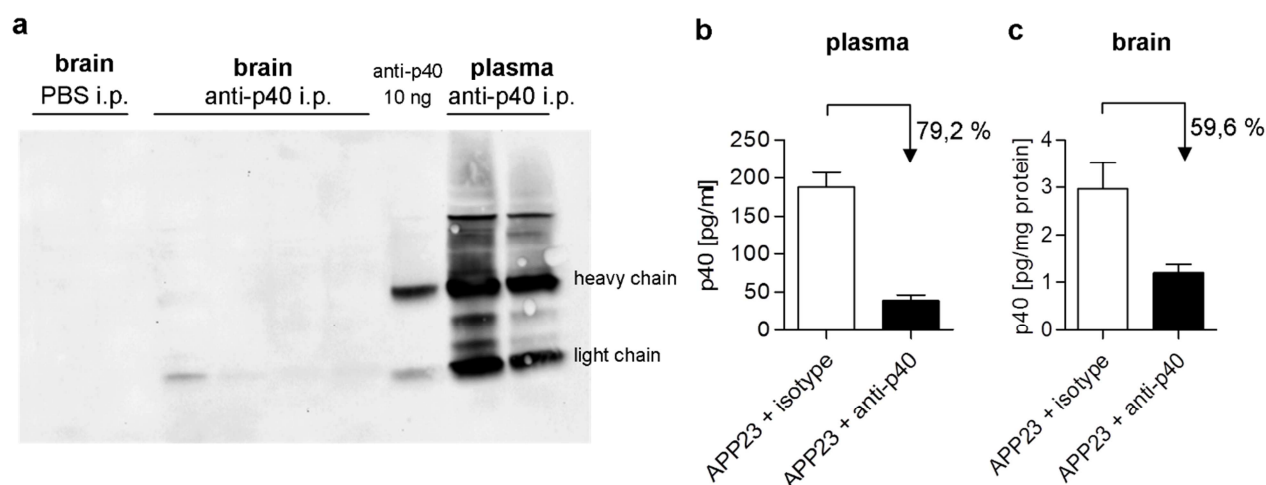

Figure 30: Detection and efficiency of anti-p40 antibody in plasma and brain after i.p. treatment. (a) Western Blot analysis of representative samples of brain homogenates and plasma from anti-p40 antibody treated *APP23* mice, showing light and heavy chain of rat-anti-mouse anti-p40 antibody, detected by anti-rat specific secondary antibody. IL-12 / IL-23p40 levels in (b) plasma and (c) brain in isotype and anti-p40 treated *APP23* mice. n = 15 - 16

4.9.2 Flow cytometric analysis of blood immune cells after i.p. anti-p40 treatment

Next, we wanted to evaluate whether long-term i.p treatment with anti-p40 influenced the composition of blood immune cells. IL-12 and IL-23 have been shown to play a central role in T cell development and differentiation[104,96]. Apart from its effect on T cells, IL-12 also acts on B cells, NK cells and antigen-presenting cells[88,91,92,104]. The systemic immune system has been reported to influence the progression of Aβ pathology[148,149]. Given the influence of IL-12 and IL-23 on adaptive and innate immune cells in the hematopoietic compartment, blocking of IL-12 and IL-23 function by injecting anti-p40 i.p. over 3 months could modulate blood immune cell composition. To monitor the effect of anti-p40 treatment on peripheral immune cells, the frequency of T cells, B cells and monocytes in the blood was analyzed by flow cytometry at the end of the experiment. Living single cells were gated for CD5^{+} T cells and B220^{+} B cells (Figure 31 a) and CD11b^{+} monocytes (Figure 31 b). The percentage of T cells, B cells and monocytic cells did not differ between anti-p40 and isotype control treated animals (Figure 31 c – e), which indicates that the composition of the main immune cells in the

blood was not affected by i.p. administration of p40-blocking antibodies to aged *APP23* mice.
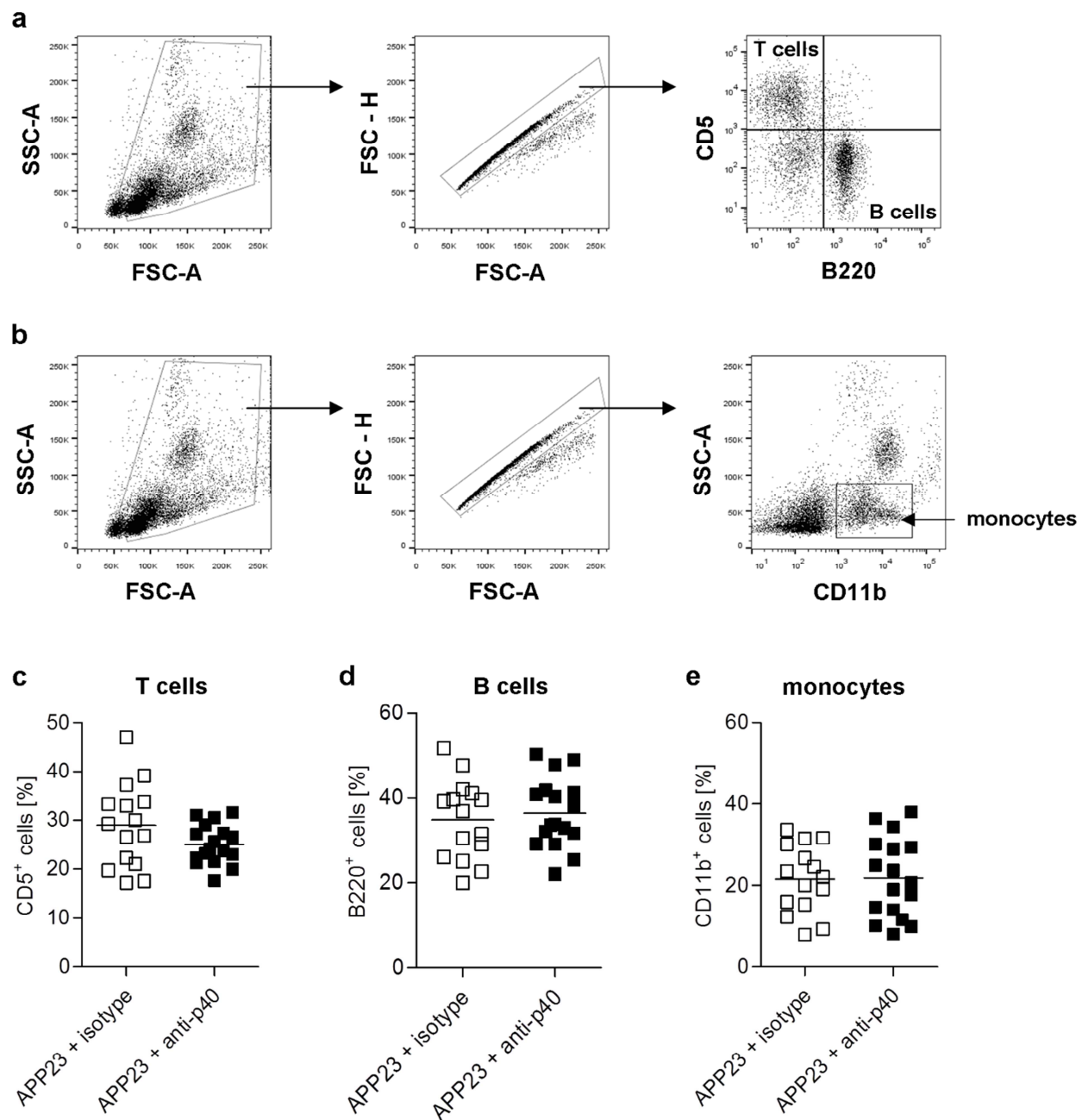

Figure 31: FACS analysis of blood immune cell composition after i.p. antibody treatment.
(a, b) Representative dot plots and gating strategy to analyze blood immune cells are displayed from an anti-p40 antibody treated animal. A gate in the SSC/FSC plot was set to exclude cell debris. From all living cells only single cells were gated for (a) CD5-positive T cells and B220-positive B cells, and (b) CD11b-positive monocytes. Quantification of (c) T cell, (d) B cell and (e) monocyte frequencies in isotype and anti-p40 antibody treated *APP23* mice. n = 15 – 17. For statistical analysis student's t-test was used.

4.9.3 Behavioral analysis of i.p. anti-p40 treated *APP23* mice

Intracerebroventricular application of anti-p40 antibody ameliorated cognitive function in aged *APPPS1* mice as assessed in the Barnes maze test as well as the Novel object recognition test (chapter 4.8). To find out whether long term i.p. application of anti-p40 to aged *APP23* mice has a similar effect on behavior, mice were subjected to the Open field, the Novel object recognition test and the Morris water maze test. The Morris water maze paradigm is commonly used to assess spatial learning and memory in AD mouse models, similar to the Barnes maze[150,147]. In an Open field arena, antibody-treated *APP23* mice were first tested for general locomotor activity to exclude any abnormalities in motor function due to the long term i.p. treatment. Analysis of the distance the mice travelled in the arena during the trial revealed no differences in locomotor activity between anti-p40 and isotype-treated groups (Figure 32 a). Subsequently, mice were tested for Novel object recognition. The quantification of the percentage of visits (Figure 32 b) and the time the mice spent near the new object (Figure 32 c) did not show a difference between the groups. Since the mice spent on average around 50 % of time and visits investigating the new object, no preference regarding the novel object could be detected in the isotype and anti-p40 treated animals.
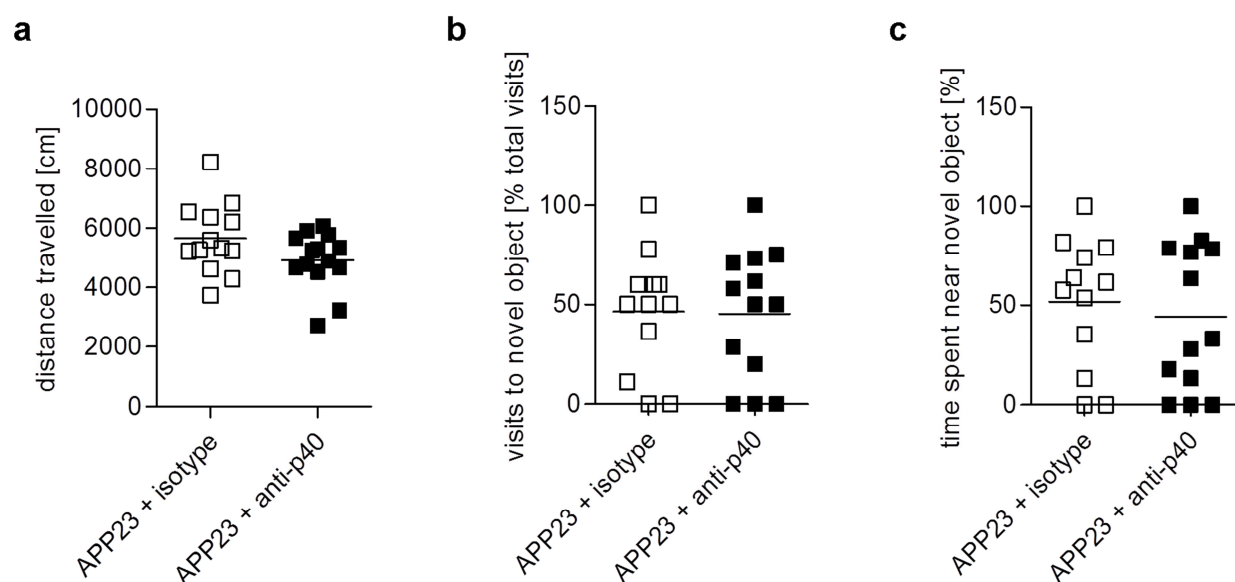

Figure 32: Open field and Novel object recognition test after i.p. antibody delivery in aged *APP23* mice.
(a) General locomotor activity is determined by analyzing the distance mice travelled in an open field arena. (b) Percentage of visits to novel object and (c) percentage of time spent near new object of *APP23* mice treated with either anti-p40 or isotype control antibody. n = 13 – 14. For statistical analysis the student's t-test was used.

For assessment of spatial learning and memory after anti-p40 treatment, *APP23* mice were trained in the Morris water maze to locate a hidden target platform on four consecutive days before being tested in a short-term memory retention test on the 5th day. During the training phase both treatment groups showed normal learning behavior, as the time the mice needed to locate the platform decreased from day to day (Figure 33 a). In the short-term probe trial, the latency to reach the target revealed no difference between anti-p40 and isotype-treated *APP23* mice (Figure 33 b).
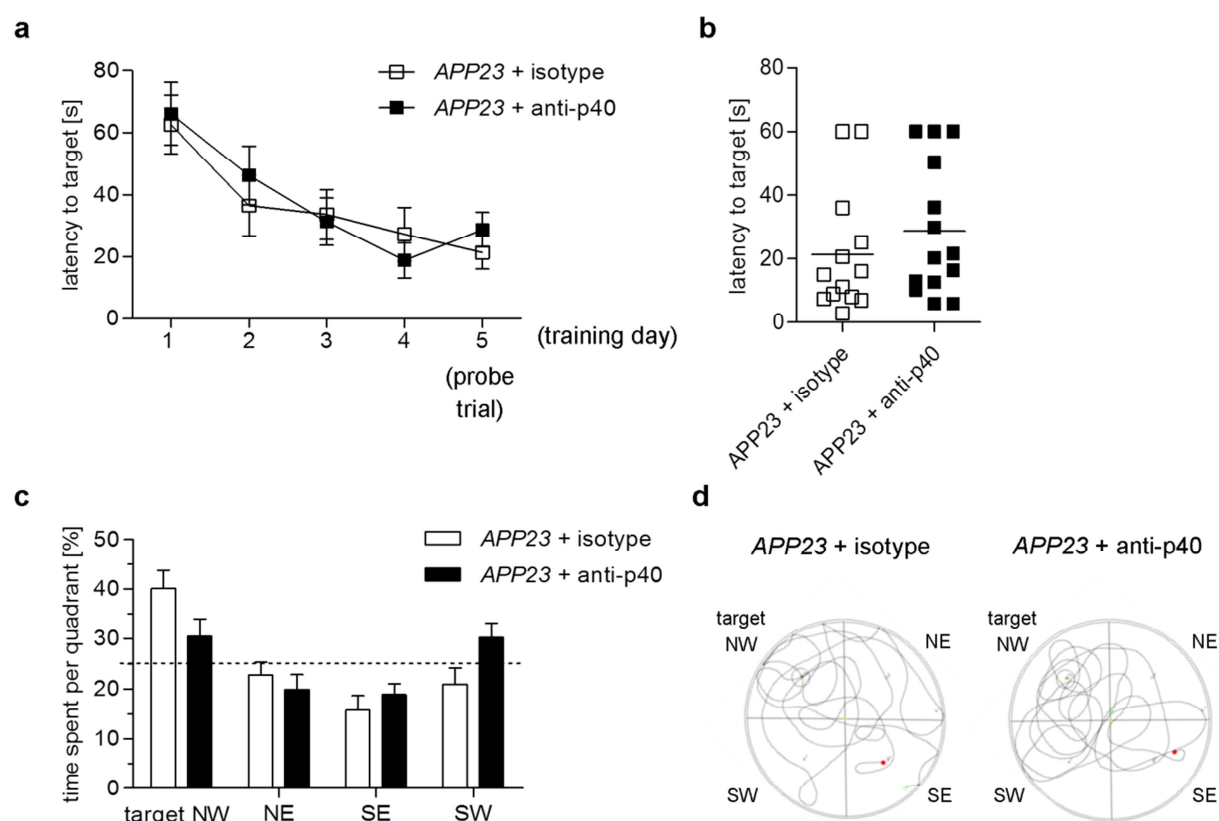

Figure 33: Morris water maze test of aged *APP23* mice after i.p. antibody treatment.
Mice were trained on four consecutive days to locate a target platform in the water maze, followed by a short term probe trial on day 5. (a) Latency to find the target during the training days and probe trial. (b) Latency to target on the short term memory retention probe trial. (c) Percentage of time spent in the target and in each of the other quadrants and (d) representative tracking pathways of isotype and anti-p40 treated mice during short term probe trial. Quadrant description: NW - north west, NE - north east, SE - south east, SW - south west. n = 13 – 14. For statistical analysis student's t-test (b), or two-way ANOVA with Bonferroni's post test were used (c).

Likewise, analysis of the percentage of time the animals spent in each of the four quadrants of the maze during the probe trial did not show any significant differences between both treatment groups (Figure 33 c, d). However, the fact that aged *APP23* mice treated with isotype control antibody showed a clear preference of the target

quadrant and spent on average 40 % of the time in the region of the target during the probe trial, indicates that these mice did not show a substantial impairment in spatial learning and memory at the age they were tested. However, since aged-matched wt littermate controls were lacking in this experiment, a clear conclusion as to whether major cognitive deficits were detectable in *APP23* mice at the time-point they were tested and on a behavioral effect of p40 inhibition cannot be drawn at this point.

4.9.4 Histological analysis of Aβ plaque burden after i.p. anti-p40 treatment

To determine if long-term i.p. application of anti-p40 antibodies influences Aβ plaque burden in aged *APP23* mice, immunohistochemical analysis using the Aβ-specific antibody 4G8 was conducted. Serial brain sections throughout the cortex were stained and the Aβ covered area was quantified using the Stereoinvestigator system. Since we observed that the *APP23* mouse line exhibits strong differences in plaque burden between the genders at the time point they were analyzed, male and female mice were considered separately in the analysis. Histological and quantitative analysis of Aβ plaque burden did not show significant alterations in Aβ plaque burden between the treatment groups in female (Figure 34 a, c) and male (Figure 34 b, d) mice, or when data from both genders were combined (Figure 34 e). However, there could possibly be a slight trend towards reduced Aβ burden in female mice treated with anti-p40 antibody, an effect which might be blurred by the substantial variability of Aβ burden in this AD-like model at the investigated age. Overall, i.p. treatment of aged *APP23* mice with anti-p40 antibodies twice a week over 3 month did not significantly influence Aβ plaque load in the cortex of these mice.
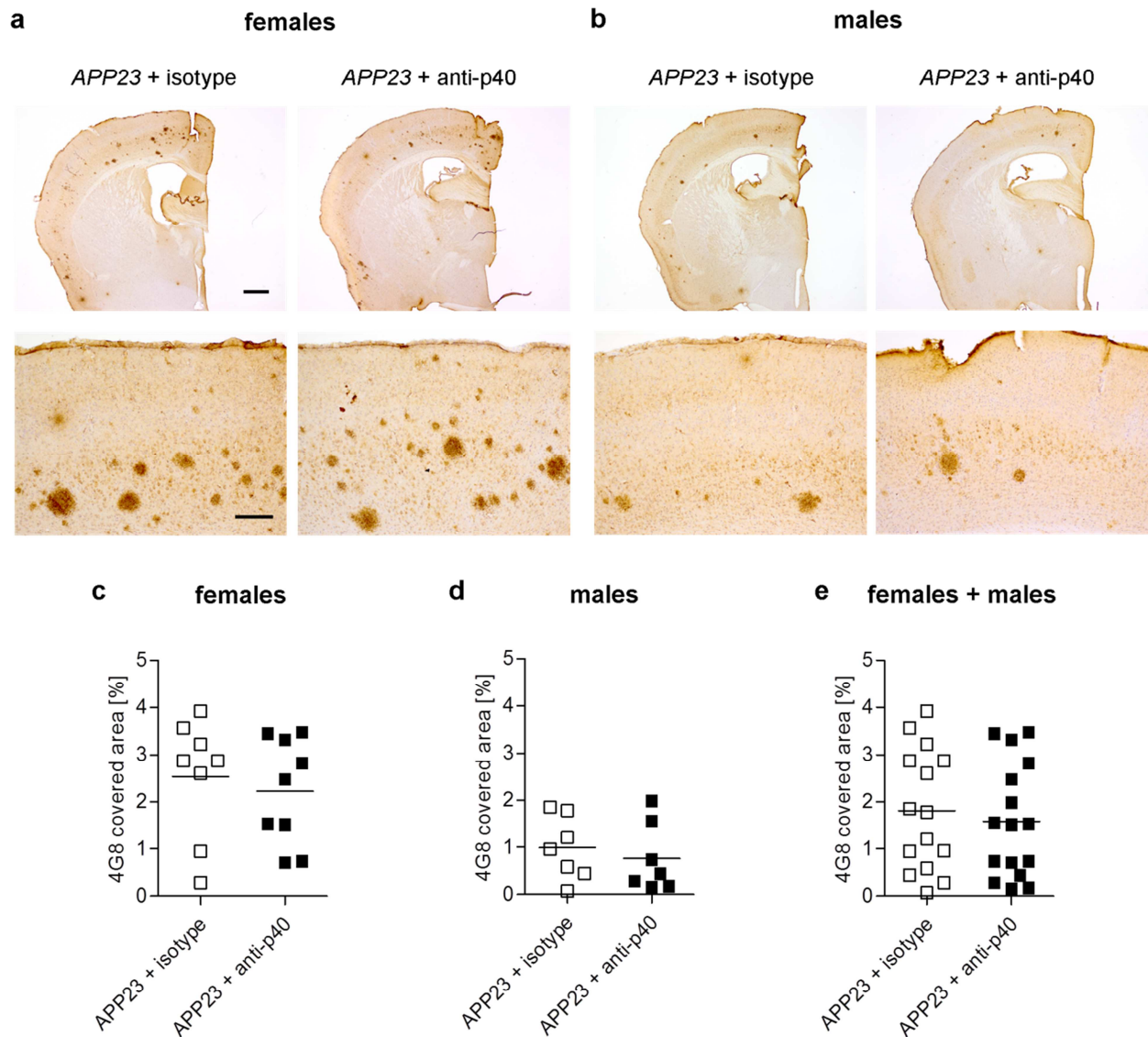
Figure 34: Histological analysis of Aβ plaque burden in *APP23* mice after i.p. antibody delivery. Aβ burden was assessed by immunohistochemical staining using the amyloid-β reactive antibody 4G8 (a, b). Representative images of 4G8 staining in (a) female and (b) male *APP23* mice which received isotype control or anti-p40 antibody at low magnification (upper row, scale bar 500 μm) and higher magnification (lower row, scale bar 200 μm). (c - e) Stereomorphometric quantification of the area covered by 4G8 in (c) female, (d) male and (e) both male and female mice was assessed using the Stereo Investigator system. n = 15 – 16. For statistical analysis the student's t-test was used.

4.9.5 Analysis of Aβ levels in the plasma after i.p. anti-p40 treatment

Anti-p40 applied via i.p. injections resulted in a strong decrease in p40 levels in the plasma (chapter 4.9.1). To find out whether reduced p40 levels in the blood modulated soluble Aβ levels in the plasma, $A\beta_{40}$ and $A\beta_{42}$ concentrations were measured by electrochemiluminescence assay using the MSD 4G8 assay. Steady-state Aβ levels

were not altered in the plasma (Figure 35) of anti-p40 compared to isotype control treated *APP23* mice, indicating no direct effect of reduced p40 levels on Aβ levels in the peripheral blood stream.
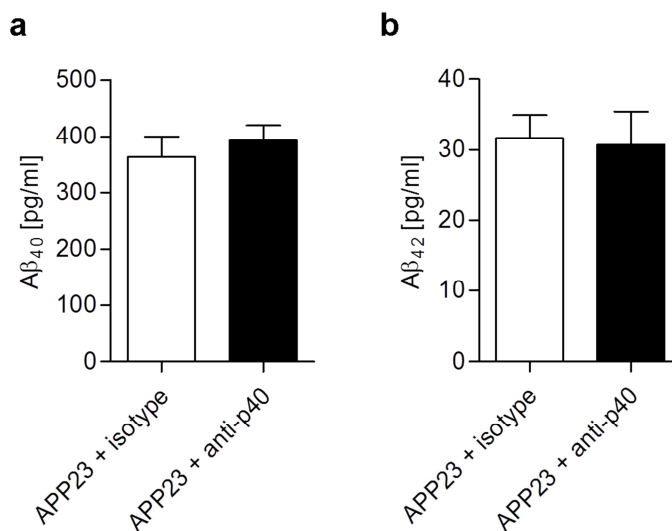

Figure 35: Aβ$_{40}$ and Aβ$_{42}$ levels in the plasma of aged *APP23* mice after i.p. antibody treatment. Aβ$_{40}$ (a) and Aβ$_{42}$ (b) levels were determined in the plasma of anti-p40 and isotype control antibody treated *APP23* mice using the Meso Scale 4G8 Aβ Triplex Assay. n = 15 - 16. For statistical analysis student's t-test was used.

4.9.6 Biochemical analysis of cortical Aβ levels after i.p. anti-p40 treatment

Histological analysis of cortical Aβ plaque burden did not reveal significant changes between anti-p40 and isotype control treated *APP23* mice. To determine whether the amount of soluble and insoluble Aβ species in the brain are modulated by i.p. anti-p40 treatment, frozen brains were homogenized consecutively in TBS-, TX, SDS- and FA buffer and thereby obtained protein fractions were analyzed by electrochemiluminescence assay using the MSD 6E10 assay. No significant differences between anti-p40 and isotype control-treated *APP23* mice could be detected in any of the protein fractions (Figure 36). However, a slight decrease in Aβ$_{40}$ and Aβ$_{42}$ levels in the TBS- and the SDS-extracted protein fractions in the anti-p40 treated animals could be depicted, which is in line with the observed slight trend towards reduced Aβ burden – at least in female *APP23* mice treated with anti-p40 antibody, as shown in Figure 34 c. But overall, i.p. application of anti-p40 into aged *APP23* mice did not lead to a significant reduction in Aβ load in the brain after 3 months of treatment.
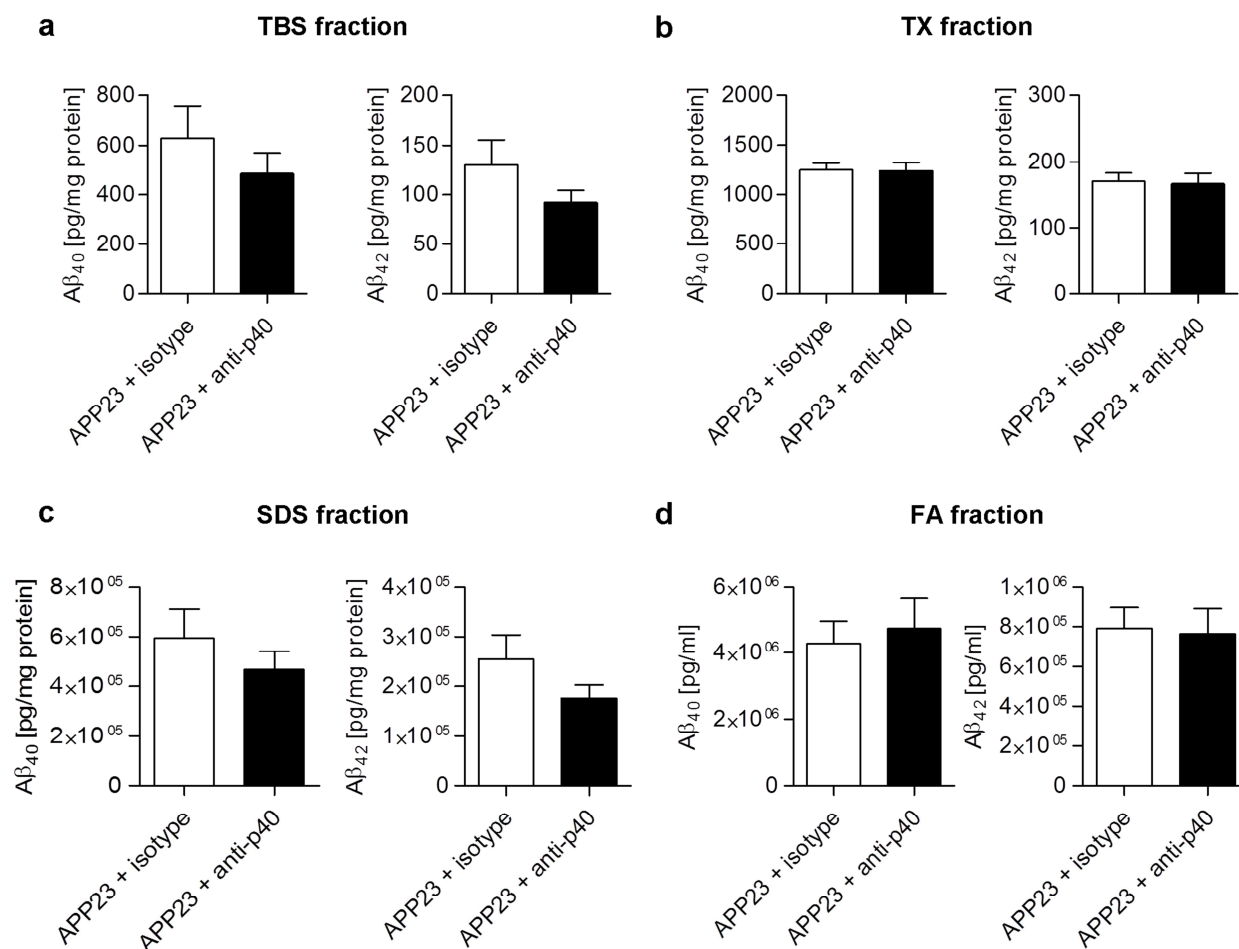
Figure 36: Cerebral Aβ$_{40}$ and Aβ$_{42}$ levels in brain homogenates of aged *APP23* mice after i.p. antibody treatment.
Frozen brain tissue of anti-p40 and isotype control antibody treated *APP23* mice was homogenized consecutively in (a) TBS, (b) TX, (c) SDS and (d) FA buffer and supernatants of each fraction were subjected to Meso Scale analysis using the 6E10 Aβ Triplex Assay. n = 15 - 16. For statistical analysis student's t-test was used.

Even though i.p. anti-p40 treatment to aged *APP23* mice did not significantly reduce Aβ pathology, there is a significant linear correlation between Aβ levels and brain intrinsic p40 levels in *APP23* mice. Aβ$_{40}$ (Figure 37 a) and Aβ$_{42}$ (Figure 37 b) both correlate to p40 levels in the TBS-extracted protein fraction of anti-p40 and isotype control treated animals, suggesting a possible role of the amount of p40 in regulating Aβ levels in the brain.
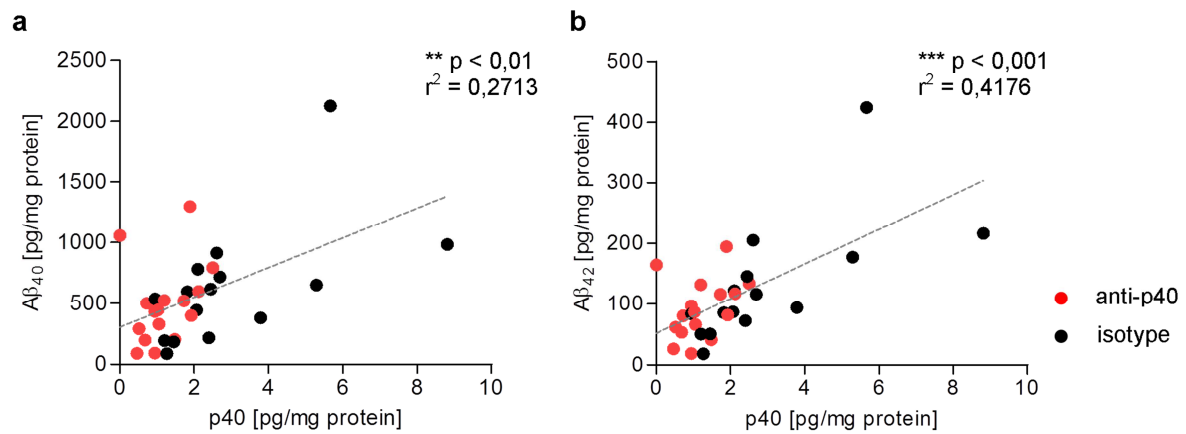
Figure 37: Linear correlation of Aβ$_{40}$ and Aβ$_{42}$ levels with IL-12 / IL-23p40 levels in brain homogenates of *APP23* mice after i.p. antibody treatment.
Aβ$_{40}$ (a) and Aβ$_{42}$ (b) levels in the brain TBS fraction were correlated to IL-12 / IL-23p40 levels in the TBS fraction from anti-p40 and isotype control treated *APP23* mice. n = 15 – 16. Correlation was performed using the linear Pearson correlation.

5. Discussion

In this thesis the influence of the pro-inflammatory cytokines IL-12 and IL-23 on AD associated Aβ pathology was investigated. Previous findings in the laboratory of Prof. Heppner demonstrated an up-regulation of these cytokines in AD-prone *APPPS1* mice and showed that the absence of IL-12 and/or IL-23 resulted in a pronounced reduction of Aβ pathology[121] (chapter 1.4). Innate immunity is considered to be a major contributor to the pathogenic cascade in AD, and a growing number of inflammatory pathways has been implicated in the progression of the disease. However, the exact mechanism by which specific immune mediators such as IL-12 and IL-23 affect disease progression is not clarified. Gaining further insight into mechanistic aspects of immune modulatory pathways involved in AD pathology is necessary especially the light of developing novel treatment strategies to combat AD. Hence, one major aim of this thesis was to investigate different aspects of Aβ modulation that could be affected by the presence or absence of IL-12 and IL-23. To decipher the precise mechanism of IL-12 / IL-23-mediated Aβ modulation, it is a pre-requisite to identify the cell types involved in these pathways. Consequently, another aim was to define cellular players and signaling pathways involved in mediating the observed effects on Aβ pathology. As a third aim, it was sought to establish whether pharmacological reduction of p40 impacts disease pathology, including behavioral deficicts, which would suggest p40 as potential target for interventional treatment.

5.1 Mechanisms of Aβ modulation by IL-12 and IL-23

Aβ accumulation and deposition in senile plaques is thought to be the result of an imbalance between Aβ production and Aβ clearance as well as altered aggregation properties of Aβ. An alteration in any of these aspects leads to changes in the homeostasis of Aβ levels in the brain which results in reduced or increased Aβ accumulation. Since it was shown that the absence of IL-12 and/or IL-23 leads to reduced Aβ accumulation in the brain[121], we hypothesized that the lack of these pro-inflammatory cytokines either reduces Aβ production or increases Aβ clearance mechanisms.

5.1.1 Impact of IL-12 and IL-23 on Aβ production

Aβ is produced through sequential proteolytic cleavage of APP by β-secretase and γ-secretase[19]. Pro-inflammatory cytokines such as TNFα and IFNγ have been shown to increase Aβ production by affecting the activity of APP-cleaving enzymes *in vitro*[151,152]. Hence, we aimed to determine whether IL-12 and IL-23 alter mechanisms of Aβ production. The initial step in the production of Aβ is the processing of APP by β-secretase, which results in the release of the sAPPβ fragment[19]. Levels of sAPPβ can thus be used as a measure of β-secretase activity and amyloidogenic APP processing. Since Aβ burden is decreased upon p40 deficiency, we hypothesized that β-secretase cleavage of APP is reduced in the brain of *APPPS1* mice deficient in p40 compared to control *APPPS1* mice. However, sAPPβ levels were found to be unchanged in brains of *APPPS1* deficient in p40 indicating that APP processing by β-secretase is not affected, at least in young mice before onset of plaque deposition. Further evidence that the function of the APP-processing machinery is unaffected by p40 deficiency is that APP levels, the ratio of α-CTFs to β-CTFs and the ratio of $A\beta_{40}$ to $A\beta_{42}$ were not altered in the absence of p40 signaling in the brain of 120 day old mice[121], which demonstrates unchanged function of β-secretase and γ-secretase upon p40 deficiency *in vivo*.

Differences of Aβ deposition in mice lacking IL-12 and IL-23 are evident at 120 days and 250 days of age[121], time-points when robust Aβ plaque deposition is present in the *APPPS1* mouse model. Analysis of steady state Aβ levels as an indicator of Aβ production *in vivo* can only be reliably performed when Aβ deposition in plaques has not been initiated in the brain to avoid that different aggregation states of Aβ hamper the result of the analysis. At the age of 7 weeks, *APPPS1* mice do not display visible plaque deposition and Aβ pathogenesis is mainly characterized by *de novo* generation of Aβ through processing of APP. Hence, measuring cortical Aβ levels at this early disease stage can provide evidence if the production of Aβ is affected by the absence of p40. The sequential extraction of different protein fractions according to the 4-step extraction protocol[124] allowed to evaluate the amount of soluble Aβ species and more fibrillized Aβ separately. At the early stage of Aβ pathology, we observed no significant differences between *APPPS1* mice with functional p40 signaling and *APPPS1* mice deficient in p40, although a tendency towards higher Aβ levels in all analyzed protein fractions was discovered in *APPPS1xIl12b*^{-/-} mice. The fact that young *APPPS1* mice lacking p40 did

not show a reduction in soluble Aβ levels before onset of plaque deposition indicates that Aβ production is not affected by the lack of p40 in *APPPS1* mice. An alternative explanation for the fact that Aβ levels are not decreased at this early time-point of Aβ pathogenesis is that microglia activation, associated with the up-regulation of inflammatory mediators such as IL-12 and IL-23, might not be observed in young *APPPS1* mice before the formation of plaques. Microglial activation, evident by the presence of hypertrophic microglia clustering around Aβ plaques, appears concomitantly with the appearance of first plaques, and is not observed in pre-depositing *APPPS1* mice[36]. Hence, it might be possible that the Aβ-modulating effect of p40 signaling is not apparent until a later stage of the disease, when innate immune responses are more pronounced.

Taken together, the aforementioned *in vivo* data show no indication for altered APP processing and subsequent Aβ production in the absence of IL-12 and IL-23 signaling.

5.1.2 Microglial phagocytosis as a mechanism of Aβ clearance

Microglia are the brain's intrinsic myeloid cells and, similar to their peripheral counterparts, are capable of phagocytosis. Several studies demonstrated that microglia can take up Aβ *in vivo*[153,134] and *in vitro*[154,155,135], which can then be localized to phagosome-like structures[154] and subsequently be degraded[133,134,156]. However, others have failed to demonstrate a clear association of Aβ within lysosomal compartments *in vivo*[157,158]. Furthermore, it is questionable whether Aβ itself is an appropriate substrate for microglia-mediated phagocytosis, since it is considered to be rather immunologically inert[68]. Hence, it is still a matter of intense debate in the field whether or not microglia are indeed able to phagocytose and degrade Aβ *in vivo*[68,159].

Aβ clearance by microglial phagocytosis in the context of AD seems to be either inefficient or inadequate. In mice with AD-like pathology phagocytosis capacity of microglia has been shown to be impaired and this impairment in microglial function correlated with the grade of Aβ plaque deposition[136]. One possible explanation for this is that Aβ-induced production of pro-inflammatory cytokines decreases the expression of genes involved in Aβ clearance by phagocytosis and thereby causing microglial dysfunction and accumulation of Aβ[120]. Indeed, stimulation of microglia with TNFα *in vitro* decreased expression of Aβ-binding scavenger receptors and reduced Aβ

uptake[120]. Other cytokines have also been shown to influence phagocytic function of microglia. The lack of NLRP3 inflammasome which results in decreased IL-1β levels has been shown to increase microglial phagocytosis activity[80] and the absence of IL-10 has likewise resulted in an increased Aβ clearance by microglia[83]. A similar effect is possible in the absence of IL-12 and IL-23. To determine whether microglial phagocytosis is altered in the absence of IL-12 and IL-23, the general capacity of microglia to take up fluorescent microbeads was analyzed in an *in situ* assay of adult brain slices. In brain slices obtained from non-AD mice the genetic deletion of p40 did not affect microglial phagocytosis, indicating that in the absence of Aβ pathology IL-12 and IL-23 are not sufficient to modulate phagocytosis activity of microglia. In contrast, microglial phagocytosis was increased in brain slices of *APPPS1* mice deficient in p40 compared to *APPPS1* slices used as control. The finding that p40 exerts an effect on phagocytosis only in the context of Aβ pathology points to the fact that pathogenic insults such as Aβ deposition are a pre-requisite to induce p40 expression and subsequent modulatory effects of p40 on microglial phagocytosis. This is in accordance with previous data showing that p40 is expressed at low levels under normal, physiological conditions and up-regulated in the AD-diseased brain[121]. However, we cannot conclude that p40 directly affects microglial phagocytosis, due to the observation that Aβ plaque burden in the mice that were used in this assay is significantly decreased upon p40 deficiency. Since Aβ plaque burden correlates with phagocytosis capacity of microglia[136], the observed increase of phagocytic cells in the absence of p40 could possibly be a consequence of the differential amount of plaque deposition in these mice and not necessarily a direct effect of p40 on phagocytosis. The lack of p40 in *APPPS1* mice may lead to Aβ reduction by other mechanisms than phagocytosis which then, as a secondary effect due to decreased plaque burden, influences microglia phagocytosis activity.

To address whether p40 directly influences microglial phagocytosis, primary neonatal microglia were incubated with IL-12 before assessment of phagocytic activity. In consideration of the fact that astrocytes might mediate p40-induced downstream effects (chapters 4.6, 4.7), microglia phagocytosis was also analyzed in the presence of primary astrocytes, to allow a putative paracrine signaling between the two cell types. The observation that p40 deficiency leads to increased phagocytosis activity of microglia in adult brain slices indicated that p40 negatively affects microglial

phagocytosis, and thus we hypothesized that stimulation of primary glia cultures with IL-12 would reduce phagocytic capacity of microglia. However, neither in single nor in co-cultures stimulation with IL-12 exerted any effect on microglial uptake of fluorescent microbeads, which demonstrates no direct effect of IL-12 on general phagocytosis capacity of primary microglia *in vitro*. In contrast, control stimulation with LPS increased phagocytic activity of microglia, which is in accordance with previous studies that showed the same effect of LPS stimulation[160–162] and demonstrates that the phagocytosis activity of microglia in the cultures *per se* can be altered upon pro-inflammatory stimulation. In the microglia/astrocyte co-cultures phagocytosis of microglia was significantly increased regardless of the treatment, suggesting that the presence of astrocytes influences phagocytosis capacity of microglia. Previous reports demonstrate contrary effects of the presence of astrocytes on microglial phagocytosis[163,164], which is likely due to differences in experimental setups regarding cell density, proportions and purity of microglia/astrocytes in the cultures and substrates used for assessing phagocytosis.

The capability of astrocytes to participate in phagocytosis is rarely studied. However it was reported that adult astrocytes are able to take up and degrade Aβ *in vitro*[165], and that transplanted adult and neonatal astrocytes in brains of *APP*-transgenic mice internalized deposited Aβ[166]. Although a recent study showed an efficient uptake of fluorescent microbeads by neonatal astrocytes *in vitro*[167], we did not observe an uptake of beads by astrocytes in our cultures. However, it would be of interest to further investigate the potential phagocytosis activity of astrocytes in the context of AD and regarding the effect of IL-12 and/or IL-23, since astrocytes appear to be the main target cells of p40 signaling (chapters 4.6, 4.7) and downstream effects could modulate the function of these cells.

Taken together, we observed an improvement of microglial phagocytosis of fluorescent microbeads in acute brain slices of *APPPS1* mice deficient in p40 compared to control *APPPS1* mice, which suggests a negative effect of IL-12 and IL-23 on microglial phagocytosis during AD pathology that could lead to the observed effect of decreased Aβ plaque burden in the absence of these cytokines. However, the observed effect of altered microglial phagocytosis in the absence of p40 may be an indirect result of the reduced plaque burden present in *APPPS1* mice upon p40 deficiency and not

necessarily a direct cause of reduced Aβ levels. The fact that we did not observe a direct effect of IL-12 on microglial phagocytosis *in vitro* speaks for either an indirect effect of p40 on phagocytosis capacity during Aβ pathology, or might be explained by the lack of the specific microenvironment present in the Aβ-prone brain which cannot be reproduced in the *in vitro* setting, or by the fact that primary neonatal glia cells used in this assay do not reflect functional properties of mature microglia and/or astrocytes present in the adult brain. Furthermore, it is inevitable to mention that the here described assays using fluorescent microbeads as substrates for assessing microglial phagocytosis do not necessarily reflect microglial reaction towards Aβ. Phagocytosis of microbeads is an often used approach to assess general phagocytosis capacity of microglia *in vitro*, however, phagocytosis of microbeads probably requires a different mechanism to the phagocytosis of Aβ. Hence, it is possible that microglial phagocytosis of specific peptides like Aβ, which may also be rather immunologically inert, could be affected by the presence or absence of p40¸ a possibility which should be tested in the future.

5.1.3 Effect of IL-12 and IL-23 on the inflammatory profile in the AD brain

Cerebral Aβ plaque deposition is associated with increased levels of pro-inflammatory mediators, such as TNF-α, IL-1β, IL-6 and GM-CSF[60]. Recent studies focusing on the effect of specific immune pathways on Aβ pathology have demonstrated that manipulating inflammatory mediators influenced the gene expression profile and the activation state of microglia, which can provide hints towards differential function of brain-intrinsic immune cells. Genetic deficiency of the NLRP3 inflammasome resulted in a decrease of pro-inflammatory markers and increased expression of anti-inflammatory genes, which are associated with an altered microglial phenotype and beneficial Aβ clearance function[80]. Another recent example is that the deficiency of IL-10 leads to the selective modulation of innate immune genes that drive innate immune response in favor of Aβ phagocytosis by microglia[83]. To investigate whether the absence of IL-12 and IL-23 influences the inflammatory gene expression profile of microglia and/or other brain cells, we selectively analyzed mediators associated with pro- and anti-inflammatory responses during Aβ pathology in *APPPS1* mice deficient in p40 compared to *APPPS1* as control. We hypothesized that the lack of pro-inflammatory mediators IL-12 and IL-23 might reduce pro-inflammatory cytokine expression in favor

of anti-inflammatory markers, which could in turn render microglia more able to phagocytose. At 90 days of age, the time-point gene expression was analyzed, *APPPS1* mice that lack p40 show decreased Aβ plaque burden and an improvement in microglial phagocytosis (chapter 4.3.1). Although the effect on the AD-associated pathology is evident in these mice upon p40 deficiency, no differential expression of the analyzed genes were observed, neither in microglia cells, nor in the CD11b-negative brain cell population, indicating that the inflammatory milieu in the brain is not altered by the absence of p40 at this time-point. In addition, gene expression changes of markers associated with phagocytosis, namely *msr-1*, *cd36* and *trem-2*, were not observed by microglia. Since only a small number of genes were analyzed in this assay, it might be more beneficial to look at global gene expression changes using exome sequencing or other whole genome-wide arrays. Furthermore, since we examined the whole CD11b-negative population and did not separate specific CD11b-negative cell types it would be of great interest to investigate gene expression changes specifically in astrocytes which we assume to be the direct target cells of p40 signaling (chapters 4.6, 4.7). In addition, protein expression of different pro- and anti-inflammatory markers were not found to be affected by the absence of p40 or IL12Rβ1 as assessed using whole brain lysates of 120 and 250 day old *APPPS1* mice. These time-points mark different stages of plaque deposition in this mouse line and the lack of p40 resulted in a significant decrease in plaque burden at both time-points[121]. The fact that differences in the analyzed inflammatory markers were not detected does not necessarily exclude that changes in the inflammatory profile are present, but could be due to the use of whole brain lysates, in which subtle changes in lowly expressed cytokines cannot be reliably depicted. Analyzing inflammatory factors in distinct cell populations, such as isolated astrocytes and microglia, and as mentioned above, using a broader panel of markers, is required to evaluate the inflammatory profile in a more precise manner.

Taken together, the here presented data do not provide evidence for an altered expression profile of inflammatory markers upon p40 deficiency in *APPPS1* mice, at least at the investigated time-points of Aβ pathology and of the specific genes and factors analyzed.

5.2   Cellular localization of IL-12 and IL-23 components in the AD context

The observation of reduced Aβ plaque deposition in the brain of p40-deficient *APPPS1* mice indicated a major role of IL-12 and IL-23 during Aβ pathogenesis. IL-12 and IL-23 typically exert their effect in cell-mediated immunity by binding to their respective receptors, which are mainly localized on lymphocytes[168]. However, a CNS invasion of blood-derived leukocytes of the adaptive immune system, like T and B lymphocytes, is considered to be limited in neurodegenerative diseases[59,60,169], suggesting that AD is primarily driven by CNS-resident and/or blood-derived innate immune cells[59]. Additionally, experiments using bone-marrow chimeric mice clarified that genetic deletion of p40 in resident brain cells is sufficient to induce Aβ reduction and that this effect is not mediated by peripheral immune cells[121] (chapter 1.4). In order to determine whether genetic deletion of the IL-12 and IL-23 receptor is sufficient to induce Aβ reduction similar to that observed upon p40 deficiency, *APPPS1* mice were crossed to mice that lack *Il12rb1*, the common receptor subunit of both IL-12 and IL-23. At 120 days of age, a time-point when *APPPS1* mice show robust plaque deposition[36], Aβ plaque load was significantly decreased upon *Il12rb1*-deficiency compared to control *APPPS1* mice. In addition, the number of Iba-1-positive microglia was likewise reduced, similar to mice deficient in p40[121]. The finding that *APPPS1* mice lacking the receptor subunit IL12Rβ1 show a similar phenotype to mice lacking p40 strongly suggests that receptor-mediated downstream effects of IL-12 and IL-23 by p40-binding target cells are responsible for the modulation of Aβ pathology. This result emphasizes the necessity to identify the downstream target cells of p40 signaling as the cell type mediating Aβ-modulating effects.

Vom Berg et.al. reported an up-regulation of IL-12 and IL-23 related subunits in the context of AD[121]. While p40, the common essential subunit of both IL-12 and IL-23, was up-regulated by brain-intrinsic microglia in brains of *APPPS1* mice, the shared receptor subunit appeared to be mainly increased in non-myeloid cells, indicating that the main target and effector cells of p40 signaling are CNS-resident brain cells other than microglia. Since the non-myeloid cell population expressed high levels of *gfap*[121], we hypothesized that astrocytes are the primary target of p40 signaling in the brain. To investigate whether this is the case, the expression of a prominent downstream mediator of both IL-12 and IL-23 signaling, namely STAT4, was investigated. IL-12

typically activates STAT4 in T cells and NK cells[104]. IL-23 has also been shown to activate STAT4, although to a lower degree than IL-12[107]. Due to the fact that STAT4 is a common downstream mediator of IL-12 and IL-23, cell-specific localization of STAT4 in the brain could elucidate potential target cells of p40. Although its expression in lymphoid organs and peripheral immune cells is well-established, no data exists regarding STAT4 expression by brain-intrinsic cells, apart from some studies demonstrating STAT4 expression in the cerebellum[170,171]. The finding that STAT4 expression is increased in the cortex of *APPPS1* mice compared to wildtype controls further emphasizes the role of IL-12 and IL-23 signaling during AD pathogenesis. While in wildtype mice STAT4 is exclusively expressed by GFAP-positive cells close to the lateral ventricle, in *APPPS1* mice STAT4 was additionally observed in GFAP-positive astrocytes in the cortex, where it was found to be localized to cells surrounding Aβ plaques. The observation that STAT4 is expressed by astrocytes in amyloidosis-prone *APPPS1* mice further supports the hypothesis that these cells are the primary target of p40 signaling during AD pathogenesis. The localization of STAT4 in astrocytes in close proximity to Aβ lesions further indicates that up-regulation of STAT4 is a specific response towards Aβ deposition. However, further data is required to ultimately prove that IL-12 and/or IL-23 produced by microglia in the AD context is/are able to activate STAT4 in astrocytes by inducing its phosphorylation.

Moreover, STAT4 might not be the only mediator of IL-12 / IL-23 downstream effects. IL-12 and IL-23 have also been shown to activate STAT1, STAT3 and STAT5 in peripheral immune cells, and specifically IL-23 was proposed to mediate its effect via inducing a STAT3 / STAT4 heterodimer[172,107]. With regard to previous reports which showed that the STAT1 and STAT3 pathways are abnormally regulated in the context of AD[173–176], it would be of interest to investigate whether there is a possible link to up-regulated IL-12 / IL-23 signaling observed in AD pathology.

Gene expression analysis of IL-12 receptor subunits in different brain cell populations[121] and immunohistochemical detection of STAT4 suggest that astrocytes are the direct target cells of microglia-produced p40 in AD. To further confirm this, the expression pattern of IL-12 and IL-12 receptor subunits in primary neonatal microglia and astrocytes were analyzed *in vitro*. After pro-inflammatory stimulation with LPS and IFNγ, microglia showed a strong up-regulation of IL-12 subunits which resulted in p40 secretion. This is in accordance with previous reports which showed an increase in IL-

12 subunits in human or murine microglia after stimulation[99,101,102]. The fact that primary microglia respond to pro-inflammatory stimulation by increasing the expression of IL-12 subunits and secreting p40 protein, confirms microglia as the main cellular source of these cytokines *in vitro*. The aforementioned studies also described an up-regulation of *Il12rb1* mRNA in microglia after stimulation, which we likewise observed. However, *Il12rb1* was up-regulated to a higher extent in primary astrocytes than in microglia. Moreover, an up-regulation of *Il12rb2* mRNA was exclusively observed by astrocytes, not by microglia. Since the co-expression of both receptor subunits is required for the generation of a functional receptor[104,107], the increased expression of both IL-12 receptor subunits upon pro-inflammatory stimulation by primary astrocytes indicates their exclusive ability to respond to IL-12.

Astrocytes are typically found in a reactive state in close proximity to Aβ plaques[61] and are known to participate in inflammatory reactions expressing pro-inflammatory molecules, such as cytokines and chemokines[177]. In response to Aβ it was shown that astrocytes activate the transcriptional nuclear factor-κB (NF-κB) and up-regulate inflammatory mediators, namely TNFα, IL-1β and COX-2[178], which are factors that are critically involved in AD pathology. Astrocytes have been thus also considered as "conductors of the Alzheimer disease neuroinflammatory symphony"[179]. Regarding inflammatory processes, a constant cross-talk between microglia and astrocytes has been proposed, with both cell types influencing their mutual activation or inhibition[180]. Molecules contributing to their intercommunication include IL-1, adenosine triphosphate (ATP) and TGF-β[180]. A similar scenario is conceivable regarding IL-12 and IL-23 signaling during Aβ pathogenesis, with microglia as the cellular source of p40 and astrocytes responding to this pathway. It is possible that astrocytes then directly facilitate the observed modulation of Aβ pathology, for instance by Aβ uptake and subsequent degradation or transport via the blood brain barrier to the peripheral circulation. However, in *APPPS1* mice lacking p40 or AD-like mice after anti-p40 treatment, plasma Aβ levels as an indicator for altered Aβ transport across the blood brain barrier were not changed, which does not support this theory. Another possible scenario includes paracrine signaling back to microglia, which then promote further downstream effects like for example phagocytosis and degradation of Aβ.

The aforementioned data strongly suggest astrocytes as the direct target and effector cells of IL-12 and IL-23 in the brain of *APPPS1* mice. However, definite proof is needed

to validate this, for example by detecting phosphorylated STAT4 or gene expression changes downstream of STAT4 exclusively in astrocytes, or by detection of the IL-12 and/or IL-23 receptor on astrocytes *in vivo*. Although *Il12rb1* has been previously described to be expressed in microglia[181,99] and neurons[103], the data presented here point towards astrocytes being the main cell type mediating IL-12 / IL-23 downstream effects in the context of AD.

5.3 Pharmacological reduction of p40 as a therapeutic strategy in AD

The finding that the manipulation of IL-12 and IL-23 signaling influences Aβ plaque pathology suggests these pathways as novel targets for interventional treatment approaches. Indeed, monoclonal antibodies that neutralize p40 and thereby inhibit the formation of functional IL-12 and IL-23 exist, and have been used in clinical trials for treatment of other primarily inflammatory diseases such as Psoriasis, Crohn's disease and Multiple sclerosis[182]. Recently, it was shown that peripheral administration of anti-p40 antibodies to young *APPPS1* mice over the course of 3 months resulted in a significant decrease of Aβ plaque deposition[121], indicating a beneficial effect of p40 neutralizing antibodies on AD pathology. Furthermore, reducing p40 levels using non-viral small interfering RNA (siRNA) or anti-p40 antibodies in a mouse model of accelerated aging (senescence-accelerated prone 8 (SAMP8)) resulted in decreased cerebral amyloidosis and improved cognitive function[183]. To evaluate whether anti-p40 antibody treatment also affects cognitive abilities in AD-prone mice, a pre-requisite for the initiation of clinical trials, behavioral performance was assessed after the treatment in two different mouse models of amyloidosis. In *APPPS1* mice, intracerebroventricular (icv) application of anti-p40 antibodies resulted in a pronounced improvement of spatial learning and memory abilities assessed in the Barnes maze test, as well as improved object recognition skills compared to *APPPS1* mice treated with isotype control, which showed clear deficits in these cognitive tasks. This demonstrates that reducing p40 levels in the brain by icv infusion of anti-p40 antibodies leads to a beneficial effect on cognitive symptoms present in *APPPS1* mice. Notably, the fact that the treatment was effective when initiated during an established disease pathology also speaks for the relevance of anti-p40 antibodies for therapeutic intervention. Although the amount of Aβ plaque deposition in the brain of anti-p40 antibody-treated mice did not differ from

control-treated animals, we observed a significant reduction of soluble Aβ species in the brain upon anti-p40 antibody treatment. Several studies proposed that soluble, oligomeric Aβ species are more toxic to neurons than Aβ plaques, by inhibiting long-term potentiation and impairing synaptic plasticity which leads to neuritic degeneration and memory deficits[22,23,145,184]. In contrast to Aβ deposition, the amount of soluble Aβ in human AD brains shows a strong inverse correlation with the grade of synaptic damage[25]. Moreover, soluble oligomers of Aβ rather than fibrillar Aβ have been implicated in inducing potentially harmful inflammatory responses in microglia as well as astrocytes[185,186], which lead to disturbed microglial phagocytosis and clearance of Aβ fibrils[185]. The exact mechanism by which the reduction of p40 by anti-p40 antibody treatment leads to a decrease in soluble Aβ is not clarified, but the fact that levels of these soluble Aβ species are decreased could explain the beneficial effect on behavior observed after anti-p40 treatment. Icv anti-p40 treatment was not efficient in reducing Aβ plaque burden in aged *APPPS1* mice, in contrast to previous results showing a substantial decrease in plaque deposition after intraperitoneal treatment of young *APPPS1* mice[121]. This could be due to the different mode of application or the initiation of treatment during different stages of Aβ pathogenesis. While in the previous treatment paradigm, treatment was initiated early, before onset of plaque deposition, the here described icv treatment started much later during the disease course, at a time-point when the *APPPS1* mouse model shows a robust plaque burden. Even though *APPPS1* mice exhibit an early and fast disease progression, cognitive deficits develop rather late and are not detectable before the age of 8 months[36]. Hence, icv treatment was initiated when mice already possessed a high degree of plaque deposition. The finding that anti-p40 treatment influenced Aβ plaque formation in young animals but did not affect plaque maintenance in older mice could be due to the fact that the treatment period of 2 months was too short to exert an effect on Aβ plaque maintenance in this AD-like mouse model with fast disease progression. However, the efficiency of anti-p40 treatment in reducing soluble Aβ species and ameliorating cognitive abilities at late stages of Aβ pathology, together with previous data showing an effect on plaque formation when treatment was initiated early during the disease, strongly suggests reducing p40 levels as a potential disease-modifying therapeutic to target AD pathology. The fact that p40 levels in CSF of human MCI and AD cases inversely correlate with cognitive function[121], together with the finding that plasma p40 levels are strongly

associated with abnormal cognition[187], emphasizes the relevance of the results in AD-like mice for human subjects.

APP23 mice display properties and kinetics of Aβ plaque deposition distinct from the *APPPS1* mouse model. Cerebral amyloidosis in *APP23* mice is mainly driven by elevated $A\beta_{40}$ production which leads to the formation of dense-core plaques in the parenchyma[37]. We asked whether the effects of anti-p40 treatment on behavior and Aβ pathology observed in *APPPS1* mice can be reproduced using the *APP23* mouse model. Based on the observation that intraperitoneal treatment with anti-p40 is effective in reducing Aβ pathology, aged *APP23* mice were treated according to the previously conducted i.p. protocol[121]. After 3 months of i.p. treatment with anti-p40 antibodies, *APP23* mice did not show significant differences in the behavioral paradigms that were analyzed compared to control-treated *APP23*. Mice of both treatment groups showed no preference of novel object exploration and no statistical significant differences could be detected in spatial learning abilities as assessed in the Morris water maze. Notably, *APP23* mice demonstrated pronounced learning behavior during the training phase and a clear preference of the target quadrant in the probe trial, which indicates that mice did not show distinctive learning and memory impairments at the investigated age. Previous studies reported deficits in spatial learning in *APP23* mice at the age of 22 months[188], 18 months[147], 15 months[146] or even 3 months[189]. The fact that we did not detect spatial memory impairment in 15 month old mice could be due to methodological differences in the Morris water maze setup or the use of mixed genders in the experiment. The lack of distinct cognitive dysfunction in *APP23* mice precludes making a statement regarding the effectiveness of anti-p40 treatment on cognition in this context. However, comparison of cognitive function to antibody-treated wt littermate controls would have been necessary to ultimately prove the absence of cognitive deficits in the *APP23* mice. Histological analysis of cerebral plaque burden revealed no significant differences between anti-p40 and control-treated *APP23* mice. There was possibly a slight trend towards lower Aβ burden in anti-p40-treated female *APP23* mice, which, however, showed a strong variability in Aβ plaque load thus blurring the results. Likewise, biochemical analysis demonstrated no significant effect of i.p. anti-p40 treatment on Aβ levels in the different protein fractions, even though, again, a slight trend towards reduced Aβ levels in the TBS- and SDS fractions upon anti-p40 treatment could be observed. Notably, anti-p40 antibody was detected at high levels in the plasma and at

lower levels in the brain, which demonstrates that minor amounts of the antibody crossed the blood brain barrier and reached the brain after i.p. treatment. Furthermore, anti-p40 treatment resulted in a pronounced decrease of p40 levels in the plasma, while brain endogenous p40 levels were also decreased although to a lower extent than in the plasma. Even though levels of anti-p40 antibody detectable in the brain were low, they were efficient in reducing p40 levels by approximately 60 %. However, it is possible that the achieved reduction of p40 levels is not sufficient to cause a major effect on Aβ pathology or that the *APP23* mouse model, which, in contrast to the *APPPS1* model, is rather Aβ$_{40}$-driven, may be less sensitive to anti-p40 treatment. Furthermore, in light of the slow plaque pathology of the *APP23* model, the duration of the treatment might have been too short to elicit any major effects on Aβ pathology or the time-point of antibody application was simply too late. However, while Aβ levels in the brain were not statistically altered in the brain after i.p. treatment, we observed a significant linear correlation between p40- and Aβ$_{40}$ / Aβ$_{42}$ levels in the brain, indicating a direct correlation of the amount of p40 and Aβ homeostasis. Hence, further clarification is needed to determine if IL-12 and IL-23 impact Aβ pathogenesis in the *APP23* mouse model. Studying Aβ pathology in *APP23* mice that constitutively lack p40 would help to decipher whether these cytokines play a major role in Aβ deposition in this mouse model.

5.4   Conclusion & outlook

This thesis provides further evidence for the importance of the IL-12 and IL-23 pathway in mouse models of AD-like pathology. In accordance with this, the pathogenic role of IL-12 and IL-23 pathways has recently been demonstrated in a model of accelerated aging, which showed decreased cerebral amyloidosis and improved cognitive function after p40 reduction using anti-p40 antibodies (identical to those used in this study) or non-viral small interfering RNA (siRNA)[183]. Further evidence for the deleterious role of the IL-23 pathway in AD comes from a case-control association study showing that IL-23R genetic polymorphisms are associated with AD in a Northern Han Chinese population[190]. The role of p40 in AD is further highlighted by a recent plasma multianalyte profiling study in mild cognitive impairment and AD subjects demonstrating an association of plasma p40 levels with abnormal cognition[187]. Further research should

focus on dissecting whether rather IL-12 or IL-23 or both pathways are the main contributors to AD-associated pathology. While a reduction of Aβ pathology was observed when either of the two pathways was genetically deleted, the effect appeared to be most pronounced when both pathways were disrupted[121]. Evaluating the influence of each pathway during Aβ pathogenesis and their specific downstream effects on brain-intrinsic cell types would strongly contribute to clarifying mechanistic aspects of IL-12 and IL-23-mediated Aβ modulation. Although we demonstrated that microglial phagocytosis capacity is affected by the lack of IL-12 and IL-23 signaling, we did not observe alterations in the activation state or the expression of markers implicated in phagocytosis by microglia, hence, the precise mechanisms leading to altered phagocytosis activity need to be determined. The finding that the IL-12 / IL-23 downstream signaling mediator STAT4 is expressed by astrocytes in AD-like brains *in vivo* and that these cells are able to produce IL-12 receptor components *in vitro* proposes astrocytes as the direct target of p40 signaling in the brain, which mediate p40 downstream effects. A specific focus on these brain cells regarding gene expression changes and functional properties would be extremely useful to further elucidate mechanistic aspects of IL-12 and IL-23-mediated Aβ modulation. Moreover, the finding that pharmacological inhibition of p40 by p40 neutralizing antibodies positively affected Aβ pathology and cognitive performance in *APPPS1* mice suggests that pharmacological blockade of IL-12 and IL-23 pathways can be used to alter the disease course. Especially regarding the development of new treatment strategies to fight AD, components of the IL-12 and IL-23 pathway appear to be promising targets. The fact that p40 neutralizing antibodies have been previously used in clinical trials for psoriasis[114,191–194], Crohn's disease[112,195], and multiple sclerosis[113] and thus, FDA approval and data concerning safety and tolerance in humans exist, recommends the use of anti-p40 antibodies in initial prevention or treatment trials in the context of AD.

6. Bibliography

1. Querfurth, H. W. & Laferla, F. M. Alzheimer's Disease. *N. Engl. J. Med.* **362,** 329–344 (2010).

2. Hebert, L. E., Weuve, J., Scherr, P. A. & Evans, D. A. Alzheimer disease in the United States (2010-2050) estimated using the 2010 census. *Neurology* **80,** 1778–83 (2013).

3. Ferri, C. P. *et al.* Global prevalence of dementia: a Delphi consensus study. *Lancet* **366,** 2112–7 (2005).

4. Association, A. 2014 Alzheimer's disease facts and figures. *Alzheimer's Dement.* **10,** e47–e92 (2014).

5. Blennow, K., de Leon, M. J. & Zetterberg, H. Alzheimer's disease. *Lancet* **368,** 387–403 (2006).

6. Waldemar, G. *et al.* Recommendations for the diagnosis and management of Alzheimer's disease and other disorders associated with dementia: EFNS guideline. *Eur. J. Neurol.* **14,** e1–26 (2007).

7. Herholz, K. *et al.* Discrimination between Alzheimer dementia and controls by automated analysis of multicenter FDG PET. *Neuroimage* **17,** 302–16 (2002).

8. Jagust, W. Positron emission tomography and magnetic resonance imaging in the diagnosis and prediction of dementia. *Alzheimers. Dement.* **2,** 36–42 (2006).

9. Ballard, C. *et al.* Alzheimer's disease. *Lancet* **377,** 1019–31 (2011).

10. Mattsson, N. *et al.* CSF biomarkers and incipient Alzheimer disease in patients with mild cognitive impairment. *JAMA* **302,** 385–93 (2009).

11. Hansson, O. *et al.* Association between CSF biomarkers and incipient Alzheimer's disease in patients with mild cognitive impairment: a follow-up study. *Lancet. Neurol.* **5,** 228–34 (2006).

12. Sunderland, T. *et al.* Decreased beta-amyloid1-42 and increased tau levels in cerebrospinal fluid of patients with Alzheimer disease. *JAMA* **289,** 2094–103 (2003).

13. Blennow, K., Zetterberg, H. & Fagan, A. M. Fluid biomarkers in Alzheimer disease. *Cold Spring Harb. Perspect. Med.* **2,** a006221 (2012).

14. Selkoe, D. J. Alzheimer ' s Disease : Genes , Proteins , and Therapy. *Physiol. Rev.* **81,** (2001).

15. Braak, H. & Braak, E. Neuropathological stageing of Alzheimer-related changes. *Acta Neuropathol.* **82,** 239–259 (1991).

16. Serrano-Pozo, A., Frosch, M. P., Masliah, E. & Hyman, B. T. Neuropathological alterations in Alzheimer disease. *Cold Spring Harb. Perspect. Med.* **1,** a006189 (2011).

17. Love, S. Neuropathological investigation of dementia: a guide for neurologists. *J. Neurol. Neurosurg. Psychiatry* **76 Suppl 5,** v8–14 (2005).

18. Haass, C. & Steiner, H. Alzheimer disease gamma-secretase: a complex story of GxGD-type presenilin proteases. *Trends Cell Biol.* **12,** 556–62 (2002).

19. De Strooper, B., Vassar, R. & Golde, T. The secretases: enzymes with therapeutic potential in Alzheimer disease. *Nat. Rev. Neurol.* **6,** 99–107 (2010).

20. Seubert, P. *et al.* Isolation and quantification of soluble Alzheimer's beta-peptide from biological fluids. *Nature* **359,** 325–7 (1992).

21. Mawuenyega, K. G. *et al.* Decreased clearance of CNS beta-amyloid in Alzheimer's disease. *Science* **330,** 1774 (2010).

22. Walsh, D. M. *et al.* Naturally secreted oligomers of amyloid beta protein potently inhibit hippocampal long-term potentiation in vivo. *Nature* **416,** 535–9 (2002).

23. Shankar, G. M. *et al.* Amyloid-beta protein dimers isolated directly from Alzheimer's brains impair synaptic plasticity and memory. *Nat. Med.* **14,** 837–42 (2008).

24.   Jin, M. *et al.* Soluble amyloid beta-protein dimers isolated from Alzheimer cortex directly induce Tau hyperphosphorylation and neuritic degeneration. *Proc. Natl. Acad. Sci. U. S. A.* **108,** 5819–24 (2011).

25.   Lue, L. F. *et al.* Soluble amyloid beta peptide concentration as a predictor of synaptic change in Alzheimer's disease. *Am. J. Pathol.* **155,** 853–62 (1999).

26.   Hardy, J. & Selkoe, D. J. The amyloid hypothesis of Alzheimer's disease: progress and problems on the road to therapeutics. *Science* **297,** 353–6 (2002).

27.   Jack, C. R. *et al.* Hypothetical model of dynamic biomarkers of the Alzheimer's pathological cascade. *Lancet Neurol.* **9,** 119–28 (2010).

28.   Tanzi, R. E. & Bertram, L. Twenty years of the Alzheimer's disease amyloid hypothesis: a genetic perspective. *Cell* **120,** 545–55 (2005).

29.   Strittmatter, W. J. *et al.* Apolipoprotein E: high-avidity binding to beta-amyloid and increased frequency of type 4 allele in late-onset familial Alzheimer disease. *Proc. Natl. Acad. Sci. U. S. A.* **90,** 1977–81 (1993).

30.   Corder, E. H. *et al.* Protective effect of apolipoprotein E type 2 allele for late onset Alzheimer disease. *Nat. Genet.* **7,** 180–4 (1994).

31.   Holtzman, D. M. Role of apoe/Abeta interactions in the pathogenesis of Alzheimer's disease and cerebral amyloid angiopathy. *J. Mol. Neurosci.* **17,** 147–55 (2001).

32.   Tanzi, R. E. The genetics of Alzheimer disease. *Cold Spring Harb. Perspect. Med.* **2,** 1–10 (2012).

33.   Götz, J. *et al.* A decade of tau transgenic animal models and beyond. *Brain Pathol.* **17,** 91–103 (2007).

34.   LaFerla, F. M. & Green, K. N. Animal models of Alzheimer disease. *Cold Spring Harb. Perspect. Med.* **2,** a006320– (2012).

35.   Findeis, M. A. The role of amyloid beta peptide 42 in Alzheimer's disease. *Pharmacol. Ther.* **116,** 266–86 (2007).

36.   Radde, R. *et al.* Abeta42-driven cerebral amyloidosis in transgenic mice reveals early and robust pathology. *EMBO Rep.* **7,** 940–6 (2006).

37.   Sturchler-Pierrat, C. *et al.* Two amyloid precursor protein transgenic mouse models with Alzheimer disease-like pathology. *Proc. Natl. Acad. Sci. U. S. A.* **94,** 13287–13292 (1997).

38.   Oddo, S. *et al.* Triple-transgenic model of Alzheimer's disease with plaques and tangles: intracellular Abeta and synaptic dysfunction. *Neuron* **39,** 409–21 (2003).

39.   Radde, R., Duma, C., Goedert, M. & Jucker, M. The value of incomplete mouse models of Alzheimer's disease. *Eur. J. Nucl. Med. Mol. Imaging* **35 Suppl 1,** S70–4 (2008).

40.   Yiannopoulou, K. G. & Papageorgiou, S. G. Current and future treatments for Alzheimer's disease. *Ther. Adv. Neurol. Disord.* **6,** 19–33 (2013).

41.   Birks, J. Cholinesterase inhibitors for Alzheimer's disease. *Cochrane database Syst. Rev.* CD005593 (2006). doi:10.1002/14651858.CD005593

42.   Schenk, D. *et al.* Immunization with amyloid-beta attenuates Alzheimer-disease-like pathology in the PDAPP mouse. *Nature* **400,** 173–7 (1999).

43.   Bard, F. *et al.* Peripherally administered antibodies against amyloid beta-peptide enter the central nervous system and reduce pathology in a mouse model of Alzheimer disease. *Nat. Med.* **6,** 916–9 (2000).

44.   Orgogozo, J.-M. *et al.* Subacute meningoencephalitis in a subset of patients with AD after Abeta42 immunization. *Neurology* **61,** 46–54 (2003).

45.   Wisniewski, T. & Goñi, F. Immunotherapeutic Approaches for Alzheimer's Disease. *Neuron* **85,** 1162–1176 (2015).

46.   Winblad, B. *et al.* Safety , tolerability , and antibody response of active Aβ immunotherapy with CAD106 in patients with Alzheimer ' s disease : randomised , double-blind , placebo-controlled , fi rst-in-human study. *Lancet Neurol.* **11,** 597–604 (2012).

47. Hickman, D. T. *et al.* Sequence-independent control of peptide conformation in liposomal vaccines for targeting protein misfolding diseases. *J. Biol. Chem.* **286,** 13966–13976 (2011).

48. Muhs, A. *et al.* Liposomal vaccines with conformation-specific amyloid peptide antigens define immune response and efficacy in APP transgenic mice. *Proc. Natl. Acad. Sci. U. S. A.* **104,** 9810–9815 (2007).

49. Spencer, B. & Masliah, E. Immunotherapy for Alzheimer's disease: past, present and future. *Front. Aging Neurosci.* **6,** 114 (2014).

50. Moulder, K. L. *et al.* Dominantly Inherited Alzheimer Network: facilitating research and clinical trials. *Alzheimers. Res. Ther.* **5,** 48 (2013).

51. Schenk, D., Basi, G. S. & Pangalos, M. N. Treatment strategies targeting amyloid β-protein. *Cold Spring Harb. Perspect. Med.* **2,** a006387 (2012).

52. Aisen PS, Gauthier S, Vellas B, Briand R, Saumier D, Laurin J, G. D. Alzhemed: A Potential Treatment for Alzheimers Disease | BenthamScience. *Curr. Alzheimer Res.* 473 – 478 (2007). at <http://www.eurekaselect.com/78814/article>

53. Ritchie, C. W. *et al.* Metal-protein attenuation with iodochlorhydroxyquin (clioquinol) targeting Abeta amyloid deposition and toxicity in Alzheimer disease: a pilot phase 2 clinical trial. *Arch. Neurol.* **60,** 1685–91 (2003).

54. Fenili, D., Brown, M., Rappaport, R. & McLaurin, J. Properties of scyllo-inositol as a therapeutic treatment of AD-like pathology. *J. Mol. Med. (Berl).* **85,** 603–11 (2007).

55. Forlenza, O. V *et al.* Disease-modifying properties of long-term lithium treatment for amnestic mild cognitive impairment: randomised controlled trial. *Br. J. Psychiatry* **198,** 351–6 (2011).

56. Wischik, C. & Staff, R. Challenges in the conduct of disease-modifying trials in AD: practical experience from a phase 2 trial of Tau-aggregation inhibitor therapy. *J. Nutr. Health Aging* **13,** 367–9 (2009).

57. Fernández, P. L., Britton, G. B. & Rao, K. S. Potential immunotargets for Alzheimer's disease treatment strategies. *J. Alzheimers. Dis.* **33,** 297–312 (2013).

58. Griffin, W. S. T. Perispinal etanercept : Potential as an Alzheimer therapeutic. *J. Neuroinflammation* **3,** 3–5 (2008).

59. Heppner, F. L., Ransohoff, R. M. & Becher, B. Immune attack: the role of inflammation in Alzheimer disease. *Nat. Rev. Neurosci.* **16,** 358–372 (2015).

60. Akiyama, H., Barger, S., Barnum, S. & Bradt, B. Inflammation and Alzheimer's disease. *Neurobiol. …* **21,** 383–421 (2000).

61. Sofroniew, M. V. & Vinters, H. V. Astrocytes: Biology and pathology. *Acta Neuropathol.* **119,** 7–35 (2010).

62. Nimmerjahn, A., Kirchhoff, F. & Helmchen, F. Resting Microglial Cells Are Highly Dynamic Surveillants of Brain Parenchyma in Vivo. *Science (80-.).* **308,** 1314–1319 (2005).

63. Kettenmann, H., Hanisch, U., Noda, M. & Verkhratsky, A. Physiology of microglia. *Physiol. Rev.* **91,** 461–553 (2011).

64. McGeer, P. L., Itagaki, S., Tago, H. & McGeer, E. G. Reactive microglia in patients with senile dementia of the Alzheimer type are positive for the histocompatibility glycoprotein HLA-DR. *Neurosci. Lett.* **79,** 195–200 (1987).

65. Lue, L. F. *et al.* Inflammatory repertoire of Alzheimer's disease and nondemented elderly microglia in vitro. *Glia* **35,** 72–79 (2001).

66. Meda, L. *et al.* Proinflammatory profile of cytokine production by human monocytes and murine microglia stimulated with ??-amyloid[25-35]. *J. Neuroimmunol.* **93,** 45–52 (1999).

67. Wyss-Coray, T. Inflammation in Alzheimer disease: driving force, bystander or beneficial response? *Nat. Med.* **12,** 1005–15 (2006).

68. Prokop, S., Miller, K. R. & Heppner, F. L. Microglia actions in Alzheimer's disease. *Acta Neuropathol.* **2,** (2013).

69. Miller, K. R. & Streit, W. J. The effects of aging, injury and disease on microglial function: a case for cellular senescence. *Neuron Glia Biol.* **3,** 245–53 (2007).

70. Jonsson T1, Stefansson H, Steinberg S, Jonsdottir I, Jonsson PV, Snaedal J, Bjornsson S, Huttenlocher J, Levey AI, Lah JJ, Rujescu D, Hampel H, Giegling I, Andreassen OA, Engedal K, Ulstein I, Djurovic S, Ibrahim-Verbaas C, Hofman A, Ikram MA, van Duijn C, S. K. Variant of TREM2 Associated with the Risk of Alzheimer's Disease. *N. Engl. J. Med.* **368,** 107–116 (2013).

71. Guerreiro R, Wojtas A, Bras J, Carrasquillo M, Rogaeva E, Majounie E, Cruchaga C, Sassi C, Kauwe JS, Younkin S, Hazrati L, Collinge J, Pocock J, Lashley T, Williams J, Lambert JC, Amouyel P, Goate A, Rademakers R, Morgan K, Powell J, St George-Hyslop P, H. J. A. G. A. G. TREM2 Variants in Alzheimer's Disease. *N. Engl. J. Med.* **368,** 117 – 127 (2013).

72. Zhang, B. *et al.* Integrated systems approach identifies genetic nodes and networks in late-onset Alzheimer's disease. *Cell* **153,** 707–20 (2013).

73. Naj, A. C. *et al.* Common variants at MS4A4/MS4A6E, CD2AP, CD33 and EPHA1 are associated with late-onset Alzheimer's disease. *Nat. Genet.* **43,** 436–41 (2011).

74. Griciuc, A. *et al.* Alzheimer's Disease Risk Gene CD33 Inhibits Microglial Uptake of Amyloid Beta. *Neuron* **78,** 631–643 (2013).

75. Rich, J. B. *et al.* Nonsteroidal anti-inflammatory drugs in Alzheimer's disease. *Neurology* **45,** 51–5 (1995).

76. McGeer, P. L., Schulzer, M. & McGeer, E. G. Arthritis and anti-inflammatory agents as possible protective factors for Alzheimer's disease: a review of 17 epidemiologic studies. *Neurology* **47,** 425–32 (1996).

77. Aisen, P. S. *et al.* Effects of rofecoxib or naproxen vs placebo on Alzheimer disease progression: a randomized controlled trial. *JAMA* **289,** 2819–26 (2003).

78. Lyketsos, C. G. *et al.* Naproxen and celecoxib do not prevent AD in early results from a randomized controlled trial. *Neurology* **68,** 1800–8 (2007).

79. Breitner, J. C. *et al.* Extended results of the Alzheimer's disease anti-inflammatory prevention trial. *Alzheimers. Dement.* **7,** 402–11 (2011).

80. Heneka, M. T. *et al.* NLRP3 is activated in Alzheimer's disease and contributes to pathology in APP/PS1 mice. *Nature* **493,** 674–8 (2013).

81. He, P. *et al.* Deletion of tumor necrosis factor death receptor inhibits amyloid beta generation and prevents learning and memory deficits in Alzheimer's mice. *J. Cell Biol.* **178,** 829–41 (2007).

82. Chakrabarty, P. *et al.* IL-10 Alters Immunoproteostasis in APP Mice, Increasing Plaque Burden and Worsening Cognitive Behavior. *Neuron* **85,** 519–533 (2015).

83. Guillot-Sestier, M.-V. *et al.* Il10 Deficiency Rebalances Innate Immunity to Mitigate Alzheimer-Like Pathology. *Neuron* **85,** 1–15 (2015).

84. Ma, X. & Trinchieri, G. Regulation of interleukin-12 production in antigen-presenting cells. *Adv. Immunol.* **79,** 55–92 (2001).

85. Arase, H., Mocarski, E. S., Campbell, A. E., Hill, A. B. & Lanier, L. L. Direct recognition of cytomegalovirus by activating and inhibitory NK cell receptors. *Science* **296,** 1323–6 (2002).

86. Kastelein, R. a, Hunter, C. a & Cua, D. J. Discovery and biology of IL-23 and IL-27: related but functionally distinct regulators of inflammation. *Annu. Rev. Immunol.* **25,** 221–42 (2007).

87. Hunter, C. a. New IL-12-family members: IL-23 and IL-27, cytokines with divergent functions. *Nat. Rev. Immunol.* **5,** 521–31 (2005).

88. Kobayashi, M. *et al.* Identification and purification of natural killer cell stimulatory factor (NKSF), a cytokine with multiple biologic effects on human lymphocytes. *J. Exp. Med.* **170,** 827–845 (1989).

89. Hsieh, C. S. *et al.* Development of TH1 CD4+ T cells through IL-12 produced by Listeria-induced macrophages. *Science* **260,** 547–549 (1993).

90. Manetti, B. R. *et al.* Natural killer cell stimulatory factor (Interleukin 12 [IL-12] induces T helper type 1 (Th1)-specific immune responses and inhibits the development of IL-4-producing Th cells. *J. Exp. Med.* **177,** 1199–1204 (1993).

91. Ma, B. X., Chow, J. M., Gri, G. & Carra, G. The interleukin 12 p40 gene promoter is primed by interferon gamma in monocytic cells. *J. Exp. Med.* **183,** (1996).

92. Grohmann, U. *et al.* IL-12 acts directly on DC to promote nuclear localization of NF-kB and primes DC for IL-12 production. *Immunity* **9,** 315–323 (1998).

93. Watford, W. T., Moriguchi, M., Morinobu, A. & O'Shea, J. J. The biology of IL-12: coordinating innate and adaptive immune responses. *Cytokine Growth Factor Rev.* **14,** 361–368 (2003).

94. Oppmann, B. *et al.* Novel p19 protein engages IL-12p40 to form a cytokine, IL-23, with biological activities similar as well as distinct from IL-12. *Immunity* **13,** 715–725 (2000).

95. Aggarwal, S., Ghilardi, N., Xie, M.-H., de Sauvage, F. J. & Gurney, A. L. Interleukin-23 promotes a distinct CD4 T cell activation state characterized by the production of interleukin-17. *J. Biol. Chem.* **278,** 1910–4 (2003).

96. Bettelli, E. *et al.* Reciprocal developmental pathways for the generation of pathogenic effector TH17 and regulatory T cells. *Nature* **441,** 235–8 (2006).

97. Gyülvészi, G., Haak, S. & Becher, B. IL-23-driven encephalo-tropism and Th17 polarization during CNS-inflammation in vivo. *Eur. J. Immunol.* **39,** 1864–1869 (2009).

98. Teng, M. W. L. *et al.* IL-12 and IL-23 cytokines: from discovery to targeted therapies for immune-mediated inflammatory diseases. *Nat. Med.* **21,** 719–729 (2015).

99. Taoufik, Y. *et al.* Human microglial cells express a functional IL-12 receptor and produce IL-12 following IL-12 stimulation. *Eur. J. Immunol.* **31,** 3228–39 (2001).

100. Sonobe, Y. *et al.* Microglia express a functional receptor for interleukin-23. *Biochem. Biophys. Res. Commun.* **370,** 129–33 (2008).

101. Li, J. *et al.* Differential expression and regulation of IL-23 and IL-12 subunits and receptors in adult mouse microglia. *J. Neurol. Sci.* **215,** 95–103 (2003).

102. Suzumura, a, Sawada, M. & Takayanagi, T. Production of interleukin-12 and expression of its receptors by murine microglia. *Brain Res.* **787,** 139–42 (1998).

103. Ireland, D. D. C. & Reiss, C. S. Expression of IL-12 receptor by neurons. *Viral Immunol.* **17,** 411–22 (2004).

104. Trinchieri, G. Interleukin-12 and the regulation of innate resistance and adaptive immunity. *Nat. Rev. Immunol.* **3,** 133–46 (2003).

105. Thierfelder, W. E. *et al.* Requirement for Stat4 in interleukin-12-mediated responses of natural killer and T cells. *Nature* **382,** 171–174 (1996).

106. Kaplan, M. H., Sun, Y. L., Hoey, T. & Grusby, M. J. Impaired IL-12 responses and enhanced development of Th2 cells in Stat4-deficient mice. *Nature* **382,** 174–177 (1996).

107. Parham, C. *et al.* A Receptor for the Heterodimeric Cytokine IL-23 Is Composed of IL-12R 1 and a Novel Cytokine Receptor Subunit, IL-23R. *J. Immunol.* **168,** 5699–5708 (2002).

108. Trinchieri, G., Pflanz, S. & Kastelein, R. A. The IL-12 family of heterodimeric cytokines: New players in the regulation of T cell responses. *Immunity* **19,** 641–644 (2003).

109. Zaba, L. C. *et al.* Psoriasis is characterized by accumulation of immunostimulatory and Th1/Th17 cell-polarizing myeloid dendritic cells. *J. Invest. Dermatol.* **129,** 79–88 (2009).

110. Parronchi, P. *et al.* Type 1 T-helper cell predominance and interleukin-12 expression in the gut of patients with Crohn's disease. *Am. J. Pathol.* **150,** 823–832 (1997).

111. Adorini, L. Interleukin-12, a key cytokine in Th1-mediated autoimmune diseases. *Cell. Mol. Life Sci.* **55,** 1610–1625 (1999).

112. Mannon, P. J. *et al.* Anti-interleukin-12 antibody for active Crohn's disease. *N. Engl. J. Med.* **351,** 2069–2079 (2004).

113. Segal, B. M. *et al.* Repeated subcutaneous injections of IL12/23 p40 neutralising antibody, ustekinumab, in patients with relapsing-remitting multiple sclerosis: a phase II, double-blind, placebo-controlled, randomised, dose-ranging study. *Lancet Neurol.* **7,** 796–804 (2008).

114. Gottlieb, A. B. *et al.* A phase 1, double-blind, placebo-controlled study evaluating single subcutaneous administrations of a human interleukin-12/23 monoclonal antibody in subjects with plaque psoriasis. *Curr. Med. Res. Opin.* **23,** 1081–1092 (2007).

115. Papp, K. a. *et al.* Efficacy and safety of ustekinumab, a human interleukin-12/23 monoclonal antibody, in patients with psoriasis: 52-week results from a randomised, double-blind, placebo-controlled trial (PHOENIX 2). *Lancet* **371,** 1675–1684 (2008).

116. Becher, B., Durell, B. G. & Noelle, R. J. Experimental autoimmune encephalitis and inflammation in the absence of interleukin-12. *J. Clin. Invest.* **110,** 493–497 (2002).

117. Di Cesare, A., Di Meglio, P. & Nestle, F. O. The IL-23/Th17 axis in the immunopathogenesis of psoriasis. *J. Invest. Dermatol.* **129,** 1339–1350 (2009).

118. Croxford, A. L., Kulig, P. & Becher, B. IL-12-and IL-23 in health and disease. *Cytokine Growth Factor Rev.* **25,** 415–21 (2014).

119. Streit, W. J., Mrak, R. E. & Griffin, W. S. T. Microglia and neuroinflammation: a pathological perspective. *J. Neuroinflammation* **1,** 14 (2004).

120. Hickman, S. E., Allison, E. K. & Khoury, J. El. Microglial dysfunction and defective β-amyloid clearance pathways in aging Alzheimer's disease mice. *Immunology* **28,** 8354–8360 (2009).

121. Vom Berg, J. *et al.* Inhibition of IL-12/IL-23 signaling reduces Alzheimer's disease-like pathology and cognitive decline. *Nat. Med.* **18,** 1812–9 (2012).

122. Magram, J. *et al.* IL-12-deficient mice are defective in IFN gamma production and type 1 cytokine responses. *Immunity* **4,** 471–81 (1996).

123. Wu, C., Ferrante, J., Gately, M. K. & Magram, J. Characterization of IL-12 receptor beta1 chain (IL-12Rbeta1)-deficient mice: IL-12Rbeta1 is an essential component of the functional mouse IL-12 receptor. *J. Immunol.* **159,** 1658–1665 (1997).

124. Kawarabayashi, T. *et al.* Age-dependent changes in brain, CSF, and plasma amyloid (beta) protein in the Tg2576 transgenic mouse model of Alzheimer's disease. *J. Neurosci.* **21,** 372–381 (2001).

125. Krabbe, G. *et al.* Activation of serotonin receptors promotes microglial injury-induced motility but attenuates phagocytic activity. *Brain. Behav. Immun.* **26,** 419–28 (2012).

126. Chen, S.-H. *et al.* Microglial regulation of immunological and neuroprotective functions of astroglia. *Glia* **00,** 1–14 (2014).

127. Losciuto, S. *et al.* An efficient method to limit microglia-dependent effects in astroglial cultures. *J. Neurosci. Methods* **207,** 59–71 (2012).

128. Nalivaeva, N. N., Belyaev, N. D., Kerridge, C. & Turner, A. J. Amyloid-clearing proteins and their epigenetic regulation as a therapeutic target in Alzheimer's disease. *Front. Aging Neurosci.* **6,** 235 (2014).

129. Zlokovic, B. V. Clearing amyloid through the blood-brain barrier. *J. Neurochem.* **89,** 807–11 (2004).

130. Hartz, A. M. S., Miller, D. S. & Bauer, B. Restoring blood-brain barrier P-glycoprotein reduces brain amyloid-beta in a mouse model of Alzheimer's disease. *Mol. Pharmacol.* **77,** 715–23 (2010).

131. Sagare, A. *et al.* Clearance of amyloid-beta by circulating lipoprotein receptors. *Nat. Med.* **13,** 1029–31 (2007).

132. Sagare, A. P. *et al.* A lipoprotein receptor cluster IV mutant preferentially binds amyloid-β and regulates its clearance from the mouse brain. *J. Biol. Chem.* **288,** 15154–66 (2013).

133. Frautschy, S. A., Cole, G. M. & Baird, A. Phagocytosis and deposition of vascular beta-amyloid in rat brains injected with Alzheimer beta-amyloid. *Am. J. Pathol.* **140,** 1389–1399 (1992).

134. Weldon, D. T. *et al.* Fibrillar beta-amyloid induces microglial phagocytosis, expression of inducible nitric oxide synthase, and loss of a select population of neurons in the rat CNS in vivo. *J. Neurosci.* **18,** 2161–73 (1998).

135. Frackowiak, J. *et al.* Ultrastructure of the microglia that phagocytose amyloid and the microglia that produce beta-amyloid fibrils. *Acta Neuropathol.* **84,** 225–33 (1992).

136. Krabbe, G. *et al.* Functional impairment of microglia coincides with Beta-amyloid deposition in mice with Alzheimer-like pathology. *PLoS One* **8,** e60921 (2013).

137. Neher, J. J. *et al.* Inhibition of microglial phagocytosis is sufficient to prevent inflammatory neuronal death. *J. Immunol.* **186,** 4973–4983 (2011).

138. Holtzman, D. M., Herz, J. & Bu, G. Apolipoprotein E and apolipoprotein E receptors: normal biology and roles in Alzheimer disease. *Cold Spring Harb. Perspect. Med.* **2,** a006312 (2012).

139. Deane, R. *et al.* apoE isoform – specific disruption of amyloid β peptide clearance from mouse brain. *J. Clin. Invest.* **118,** 4002–4013 (2008).

140. Sheedy, F. J. *et al.* CD36 coordinates NLRP3 inflammasome activation by facilitating intracellular nucleation of soluble ligands into particulate ligands in sterile inflammation. *Nat. Immunol.* **14,** 812–20 (2013).

141. Frenkel, D. *et al.* Scara1 deficiency impairs clearance of soluble amyloid-b by mononuclear phagocytes and accelerates Alzheimer's-like disease progression. *Nat. Commun.* **4,** 1–9 (2013).

142. Presky, D. H. *et al.* A functional interleukin 12 receptor complex is composed of two beta-type cytokine receptor subunits. *Proc. Natl. Acad. Sci. U. S. A.* **93,** 14002–7 (1996).

143. Wu, C., Ferrante, J., Gately, M. K. & Magram, J. Characterization of IL-12 receptor beta1 chain (IL-12Rbeta1)-deficient mice: IL-12Rbeta1 is an essential component of the functional mouse IL-12 receptor. *J. Immunol.* **159,** 1658–1665 (1997).

144. Saura, J. Microglial cells in astroglial cultures: a cautionary note. *J. Neuroinflammation* **4,** 26 (2007).

145. Hu, N.-W., Smith, I. M., Walsh, D. M. & Rowan, M. J. Soluble amyloid-beta peptides potently disrupt hippocampal synaptic plasticity in the absence of cerebrovascular dysfunction in vivo. *Brain* **131,** 2414–24 (2008).

146. Terwel, D. *et al.* Critical role of astroglial apolipoprotein E and liver X receptor-α expression for microglial Aβ phagocytosis. *J. Neurosci.* **31,** 7049–59 (2011).

147. Kelly, P. H. *et al.* Progressive age-related impairment of cognitive behavior in APP23 transgenic mice. *Neurobiol. Aging* **24,** 365–78 (2003).

148. Krstic, D. *et al.* Systemic immune challenges trigger and drive Alzheimer-like neuropathology in mice. *J. Neuroinflammation* **9,** 151 (2012).

149. Cunningham, C. Microglia and neurodegeneration: The role of systemic inflammation. *Glia* **61,** 71–90 (2013).

150. Kitazawa, M. *et al.* Blocking IL-1 signaling rescues cognition, attenuates tau pathology, and restores neuronal β-catenin pathway function in an Alzheimer's disease model. *J. Immunol.* **187,** 6539–49 (2011).

151. Liao, Y.-F., Wang, B.-J., Cheng, H.-T., Kuo, L.-H. & Wolfe, M. S. Tumor necrosis factor-alpha, interleukin-1beta, and interferon-gamma stimulate gamma-secretase-mediated cleavage of amyloid precursor protein through a JNK-dependent MAPK pathway. *J. Biol. Chem.* **279,** 49523–32 (2004).

152. Blasko, I., Marx, F., Steiner, E., Hartmann, T. & Grubeck-Loebenstein, B. TNF{alpha} plus IFN{gamma} induce the production of Alzheimer ß-amyloid peptides and decrease the secretion of APPs. *FASEB J* **13,** 63–68 (1999).

153. Frautschy, S. A., Cole, G. M. & Baird, A. Phagocytosis and deposition of vascular beta-amyloid in rat brains injected with Alzheimer beta-amyloid. *Am. J. Pathol.* **140,** 1389–99 (1992).

154. Ard, M. D., Cole, G. M., Wei, J., Mehrle, A. P. & Fratkin, J. D. Scavenging of Alzheimer's amyloid beta-protein by microglia in culture. *J. Neurosci. Res.* **43,** 190–202 (1996).

155. Paresce, D., Ghosh, R. & Maxfield, F. Microglial cells internalize aggregates of the Alzheimer's disease amyloid beta-protein via a scavenger receptor. *Neuron* **17,** 553–565 (1996).

156. Rogers, J., Strohmeyer, R., Kovelowski, C. J. & Li, R. Microglia and inflammatory mechanisms in the clearance of amyloid beta peptide. *Glia* **40,** 260–9 (2002).

157. Wisniewski, H. M., Barcikowska, M. & Kida, E. Phagocytosis of β/A4 amyloid fibrils of the neuritic neocortical plaques. *Acta Neuropathol.* **81,** 588–590 (1991).

158. Stalder, M. 3D-Reconstruction of microglia and amyloid in APP23 transgenic mice: no evidence of intracellular amyloid. *Neurobiol. Aging* **22,** 427–434 (2001).

159. Jucker, M. & Heppner, F. L. Cerebral and peripheral amyloid phagocytes--an old liaison with a new twist. *Neuron* **59,** 8–10 (2008).

160. Ferreira, R. *et al.* Neuropeptide Y inhibits interleukin-1β-induced phagocytosis by microglial cells. *J. Neuroinflammation* **8,** 169 (2011).

161. Otani, Y. *et al.* PLD4 is involved in phagocytosis of microglia: expression and localization changes of PLD4 are correlated with activation state of microglia. *PLoS One* **6,** e27544 (2011).

162. Mairuae, N., Connor, J. R. & Cheepsunthorn, P. Increased cellular iron levels affect matrix metalloproteinase expression and phagocytosis in activated microglia. *Neurosci. Lett.* **500,** 36–40 (2011).

163. DeWitt, D. A., Perry, G., Cohen, M., Doller, C. & Silver, J. Astrocytes regulate microglial phagocytosis of senile plaque cores of Alzheimer's disease. *Exp. Neurol.* **149,** 329–40 (1998).

164. Smith, M. E. & Hoerner, M. T. Astrocytes modulate macrophage phagocytosis of myelin in vitro. *J. Neuroimmunol.* **102,** 154–162 (2000).

165. Wyss-Coray, T. *et al.* Adult mouse astrocytes degrade amyloid-beta in vitro and in situ. *Nat. Med.* **9,** 453–7 (2003).

166. Pihlaja, R. *et al.* Transplanted astrocytes internalize deposited beta-amyloid peptides in a transgenic mouse model of Alzheimer's disease. *Glia* **56,** 154–63 (2008).

167. Jones, R. S., Minogue, A. M., Connor, T. J. & Lynch, M. a. Amyloid-β-Induced Astrocytic Phagocytosis is Mediated by CD36, CD47 and RAGE. *J. Neuroimmune Pharmacol.* **8,** 301–11 (2013).

168. Vignali, D. a a & Kuchroo, V. K. IL-12 family cytokines: immunological playmakers. *Nat. Immunol.* **13,** 722–8 (2012).

169. Stalder, A. K. *et al.* Invasion of hematopoietic cells into the brain of amyloid precursor protein transgenic mice. *J. Neurosci.* **25,** 11125–11132 (2005).

170. Krauthausen, M. *et al.* Opposing roles for CXCR3 signaling in central nervous system versus ocular inflammation mediated by the astrocyte-targeted production of IL-12. *Am. J. Pathol.* **179,** 2346–59 (2011).

171. Wang, J., Pham-Mitchell, N., Schindler, C. & Campbell, I. L. Dysregulated Sonic hedgehog signaling and medulloblastoma consequent to IFN-alpha-stimulated STAT2-independent production of IFN-gamma in the brain. *J. Clin. Invest.* **112,** 535–43 (2003).

172. Watford, W. T. *et al.* Signaling by IL-12 and IL-23 and the immunoregulatory roles of STAT4. *Immunol. Rev.* **202,** 139–156 (2004).

173. Cho, H. J. *et al.* IFN-gamma-induced BACE1 expression is mediated by activation of JAK2 and ERK1/2 signaling pathways and direct binding of STAT1 to BACE1 promoter in astrocytes. *Glia* **55,** 253–62 (2007).

174. Wan, J. *et al.* Tyk2/STAT3 signaling mediates beta-amyloid-induced neuronal cell death: implications in Alzheimer's disease. *J. Neurosci.* **30,** 6873–81 (2010).

175. Chiba, T. *et al.* Amyloid-beta causes memory impairment by disturbing the JAK2/STAT3 axis in hippocampal neurons. *Mol. Psychiatry* **14,** 206–22 (2009).

176. Ben Haim, L. *et al.* The JAK/STAT3 Pathway Is a Common Inducer of Astrocyte Reactivity in Alzheimer's and Huntington's Diseases. *J. Neurosci.* **35,** 2817–2829 (2015).

177. Farina, C., Aloisi, F. & Meinl, E. Astrocytes are active players in cerebral innate immunity. *Trends Immunol.* **28,** 138–45 (2007).

178. Carrero, I. *et al.* Oligomers of β-amyloid protein (Aβ1-42) induce the activation of cyclooxygenase-2 in astrocytes via an interaction with interleukin-1β, tumour necrosis factor-α, and a nuclear factor κ-B mechanism in the rat brain. *Exp. Neurol.* **236,** 215–27 (2012).

179. Medeiros, R. & LaFerla, F. M. Astrocytes: conductors of the Alzheimer disease neuroinflammatory symphony. *Exp. Neurol.* **239,** 133–8 (2013).

180. Liu, W., Tang, Y. & Feng, J. Cross talk between activation of microglia and astrocytes in pathological conditions in the central nervous system. *Life Sci.* **89,** 141–6 (2011).

181. Lein, E. S. *et al.* Genome-wide atlas of gene expression in the adult mouse brain. *Nature* **445,** 168–76 (2007).

182. Koutruba, N., Emer, J. & Lebwohl, M. Review of ustekinumab, an interleukin-12 and interleukin-23 inhibitor used for the treatment of plaque psoriasis. *Ther. Clin. Risk Manag.* **6,** 123–41 (2010).

183. Tan, M.-S. *et al.* IL12/23 p40 inhibition ameliorates Alzheimer's disease-associated neuropathology and spatial memory in SAMP8 mice. *J. Alzheimers. Dis.* **38,** 633–46 (2014).

184. Selkoe, D. J. Soluble oligomers of the amyloid beta-protein impair synaptic plasticity and behavior. *Behav. Brain Res.* **192,** 106–13 (2008).

185. Pan, X.-D. *et al.* Microglial phagocytosis induced by fibrillar β-amyloid is attenuated by oligomeric β-amyloid: implications for Alzheimer's disease. *Mol. Neurodegener.* **6,** 45 (2011).

186. White, J. a, Manelli, A. M., Holmberg, K. H., Van Eldik, L. J. & Ladu, M. J. Differential effects of oligomeric and fibrillar amyloid-beta 1-42 on astrocyte-mediated inflammation. *Neurobiol. Dis.* **18,** 459–65 (2005).

187. Hu, W. T. *et al.* Plasma multianalyte profiling in mild cognitive impairment and Alzheimer disease. *Neurology* **79,** 897–905 (2012).

188. Lefterov, I. *et al.* Memory deficits in APP23/Abca1+/- mice correlate with the level of Aβ oligomers. *ASN Neuro* **1,** 65–76 (2009).

189. CNS Spectrums: APP23 Mice as a Model of Alzheimer's Disease: An Example of a Transgenic Approach to Modeling a CNS Disorder. at <http://www.cnsspectrums.com/aspx/articledetail.aspx?articleid=282>

190. Liu, Y. *et al.* Interleukin-23 receptor polymorphisms are associated with Alzheimer's disease in Han Chinese. *J. Neuroimmunol.* **271,** 43–48 (2014).

191. Kauffman, C. L. *et al.* A phase I study evaluating the safety, pharmacokinetics, and clinical response of a human IL-12 p40 antibody in subjects with plaque psoriasis. *J. Invest. Dermatol.* **123,** 1037–44 (2004).

192. Krueger, G. G. *et al.* A human interleukin-12/23 monoclonal antibody for the treatment of psoriasis. *N. Engl. J. Med.* **356,** 580–92 (2007).

193. Leonardi, C. L. *et al.* Efficacy and safety of ustekinumab, a human interleukin-12/23 monoclonal antibody, in patients with psoriasis: 76-week results from a randomised, double-blind, placebo-controlled trial (PHOENIX 1). *Lancet* **371,** 1665–74 (2008).

194. Strober, B. E., Crowley, J. J., Yamauchi, P. S., Olds, M. & Williams, D. A. Efficacy and safety results from a phase III, randomized controlled trial comparing the safety and efficacy of briakinumab with etanercept and placebo in patients with moderate to severe chronic plaque psoriasis. *Br. J. Dermatol.* **165,** 661–8 (2011).

195. Sandborn, W. J. *et al.* A randomized trial of Ustekinumab, a human interleukin-12/23 monoclonal antibody, in patients with moderate-to-severe Crohn's disease. *Gastroenterology* **135,** 1130–41 (2008).

7.   Appendix

7.1   Abbreviations

(P)	Papain
°C	Degree Celsius
ABC	ATP-binding cassette
aCSF	Artificial cerebrospinal fluid
AD	Alzheimer's disease
APC	Allophycocyanin
ApoE	Apolipoprotein E
APP	Amyloid precursor protein
APPPS1	Tg(Thy1-APPKM670/671NL, Thy1-PS1L166P)21
APP23	Tg(Thy1-APPKM670/671NL)23
ATP	Adenosine triphosphate
Aβ	Amyloid β
BACE-1	β-site APP cleaving enzyme 1
BCA	Bicinchoninsäure
BIN1	bridging integrator 1
BSA	Bovine serum albumine
CAA	Cerebral amyloid angiopathy
CD	Cluster of differentiation
CLU	Clusterin
CNS	Central nervous system
CO_2	Carbon dioxide
COX2	Cyclooxygenase 2
CR1	Complement receptor 1
C_t	Cycle threshold
CT	Computed tomography
CTF	C-terminal fragment
d	Day
DAB	3,3'-Diaminobenzidin
DAPI	4',6-Diamidino-2-phenylindol
DMEM	Dulbecco's modified eagle medium
DNA	Desoxyribonucleic acid
dNTP	Desoxyribonucleoside triphosphate
EDTA	Ethylenediaminetetraacetic acid
ELISA	Enzyme linked immunosorbent assay
EPHA1	ephrin type-A receptor 1
FA	70 % formic acid in ddH2O
FACS	Fluorescence-activated cell sorter
FAD	Familial Alzheimer's disease
FCS	Fetal calf serum
FDA	Food and Drug Administration
FDG	Fluorodeoxyglucose

g	Gram
GFAP	Glial fibrillary acidic protein
GLAST-1	GLutamate ASpartate Transporter 1
GWAS	Genome-wide association study
h	hour
H_2O	Water
HBSS	Hanks balanced salt solution w Ca2+ Mg2+
Iba-1	Ioniced calcium binding protein 1
Icv	Intracerebroventricular
IFN	Interferon
IL	Interleukin
i.p.	intraperitoneal
JAK	Janus kinase
kDa	Kilo dalton
KCL	Potassium chloride
$KHCO_3$	Potassium hydrogen carbonate
K_2HPO_4	Dipotassium hydrogen orthophosphate
LOAD	Late-onset Alzheimer's disease
LPS	Lipopolysaccharide
LRP	Lipoprotein receptor-related protein
M	Molar
mA	Milliampere
MACS	Magnetic associated cell sorting
MRI	Magnetic resonance imaging
MCI	Mild cognitive impairment
MCP	macrophage chemotactic protein
M-CSF	Macrophage-colony stimulating factor
MHC	major histocompatibility complex
MSD	Meso Scale Discovery
min	minute
MIP	macrophage inflammatory protein
ml	Milliliter
mm	Millimeter
MMSE	Mini-mental state examination
mRNA	messenger RNA
mV	Millivolt
NaCl	Sodium chloride
$NaHCO_3$	Sodium hydrogen carbonate
NaOH	Sodium hydroxide
NeuN	Neuronal nuclei
NFT	Neurofibrillary tangles
NGS	normal goat serum
NH_4Cl	Ammonium chloride
NK-cells	Natural killer cells
NLRP3	NOD-like receptor family, pyrin domain containing 3
nm	Nanometer
NMDA	N-methyl-D-aspartate
NSAID	Non-steroidal anti-inflammatory drugs
p	phosphorylated

PBS	Phosphate buffer saline
PCR	Polymerase chain reaction
PE	Phycoerythrin
PET	Positron emission tomography
PFA	Paraformaldehyde
PI	Propidium iodide
PIB	Pittsburgh compound B
PICALM	phosphatidylinositol binding clathrin assembly protein
PS	presinilin
qRT-PCR	quantitative real time PCR
RNA	Ribonucleic acid
RT	Room temperature
RT-PCR	reverse transcription polymerase chain reaction
sAPPβ	Soluble ectodomain fragment
SDS	Sodium dodecylsulphate
SNP	Single nucleotide polymorphism
SPECT	Single-photon emission CT
STAT	Signal Transducer and Activator of Transcription
TAE	Tris-Acetat-EDTA-elektrophoresis buffer
TBS	Tris buffered saline
Tg	Transgene
TGF-β	Transforming growth factor β
Th	T helper
TNFα	Tumor necrosis factor α
TREM-2	Triggering receptor expressed on myeloid cells 2
Tris	tris(hydroxymethyl)aminomethane
TX	TBS buffer containing 1 % Triton X-100
wt	Wildtype
µg	Microgram
µL	Microliter

7.2   Figures

7.3   Tables

8. Affidavit

I, Juliane Obst, certify under penalty of perjury by my own signature that I have submitted the thesis on the topic "Influence of IL-12 / IL-23 signaling on Alzheimer's disease β-amyloid pathology". I wrote this thesis independently and without assistance from third parties, I used no other aids than the listed sources and resources.

All points based literally or in spirit on publications or presentations of other authors are, as such, in proper citations (see "uniform requirements for manuscripts (URM)" the ICMJE www.icmje.org) indicated. The sections on methodology (in particular practical work, laboratory requirements, statistical processing) and results (in particular images, graphics and tables) correspond to the URM (s.o.) and are answered by me. My interest in any publications to this dissertation correspond to those that are specified in the following joint declaration with the responsible person and supervisor. All publications resulting from this thesis and which I am author correspond to the URM (see above) and I am solely responsible.

The importance of this affidavit and the criminal consequences of a false affidavit (section 156,161 of the Criminal Code) are known to me and I understand the rights and responsibilities stated therein.

Date   Signature

Declaration of any eventual publications

I, Juliane Obst, had the following share in the following publications:

Publication:

> Vom Berg J, Prokop S, Miller KR, Obst J, Kälin RE, Lopategui-Cabezas I, Wegner A, Mair F, Schipke CG, Peters O, Winter Y, Becher B, Heppner FL. "Inhibition of IL-12/ IL-23 signaling reduces Alzheimer's disease-like pathology and cognitive decline" Nature Medicine 18, 1812–9 (2012). doi: 10.1038/nm.2965

Contribution in detail (please briefly explain):

> I, Juliane Obst, performed intracerebroventricular (icv) treatment of wildtype and *APPPS1* mice, behaviour experiments of icv-treated wildtype and *APPPS1* mice (depicted in Figure 5, Suppl. Figure 7), histological and biochemical analysis of icv-treated *APPPS1* mice (depicted in Suppl. Figure 8) and histological analysis of IL12Rβ1-deficient *APPPS1* mice (depicted in Suppl. Figure 5)

Signature of the doctoral candidate

_____

9.   Curriculum vitae

Mein Lebenslauf wird aus datenschutzrechtlichen Gründen in der elektronischen Version meiner Arbeit nicht veröffentlicht.

10. Publications

Vom Berg J, Prokop S, Miller KR, <u>Obst J</u>, Kälin RE, Lopategui-Cabezas I, Wegner A, Mair F, Schipke CG, Peters O, Winter Y, Becher B, Heppner FL. *"Inhibition of IL-12/ IL-23 signaling reduces Alzheimer's disease-like pathology and cognitive decline"* Nature Medicine 18, 1812–9 (2012). doi: 10.1038/nm.2965

11. Acknowledgements

First of all, I would like to express my sincere gratitude to Prof. Dr. Frank Heppner who gave me the great opportunity to pursue my PhD thesis in his institute and for his guidance throughout the years.

A special thank you goes to Dr. Stefan Prokop for his valuable scientific advice and ideas concerning this project, his constant support and for his constructive comments on this thesis.

My sincere thanks also go to our collaboration partner Prof. Dr. Burkhard Becher, who provided resources and advice, as well as Prof. Dr. Matthias Endres and Prof. Dr. York Winter for providing access to the behavior facilities.

I wish to thank the NeuroCure–Cluster of Excellence for granting me a fellowship during the first part of my PhD and funding the attendance of an international conference and laboratory consumables.

Furthermore, thank you to Dr. Kelly Miller for providing help and support with the behavioral experiments.

I would like to thank all other members of the Neuropathology lab, the senior scientists, the technical assistants and my fellow graduate students for their support and the great working atmosphere. Thank you, especially Lisa, Natalia, Caroline, Claudia, Pascale and Judith for the fun time!

Last but not least I would like to thank my great family and friends who have always supported me through the ups and downs of pursuing this thesis. Thank you for always lending me an ear, motivating me and cheering me up when I needed it!